

Carboxypeptidase Z
an extracellular protein in zebrafish development

Maurijn Y. Kessels

Thesis committee

Promotors

Prof. Dr S.C. de Vries
Professor of Biochemistry
Wageningen University

Prof. Dr Ir J.L. van Leeuwen
Professor of Experimental Zoology
Wageningen University

Co-promotors

Prof. Dr S. Schulte-Merker
Professor of Cardiovascular Organogenesis and Regeneration
Westfälische Wilhelms-Universität, Münster

Dr Ir S. Kranenbarg
Assistant Professor at Experimental Zoology
Wageningen University

Other members

Prof. Dr Ir H.F.J. Savelkoul, Wageningen University
Prof. Dr A. Huysseune, Ghent University
Prof. Dr G. Flik, Radboud University Nijmegen
Dr Ir K.A. Hettinga, Wageningen University

This research was conducted under the auspices of the Graduate School VLAG (Advanced studies in Food Technology, Agrobiotechnology, Nutrition and Health Sciences).

Carboxypeptidase Z

an extracellular protein in zebrafish development

Maurijn Y. Kessels

Thesis

submitted in fulfillment of the requirements for the degree of doctor
at Wageningen University
by the authority of the Rector Magnificus
Prof. Dr Ir A.P.J. Mol,
in the presence of the
Thesis Committee appointed by the Academic Board
to be defended in public
on Friday 6 November 2015
at 1:30 pm in the Aula

Maurijn Y. Kessels
Carboxypeptidase Z, an extracellular protein in zebrafish development
136 pages

PhD thesis, Wageningen University, Wageningen, NL (2015)
With references, with summaries in Dutch and English

ISBN 978-94-6257-567-7

Voor pap en mam

Contents

Chapter 1	General Introduction	9
Chapter 2	Proteomics analysis of the zebrafish skeletal extracellular matrix	25
Chapter 3	Expression of the zebrafish <i>cpz</i> gene suggests a role in Wnt4a and Wnt4b initiated signaling	47
Chapter 4	Loss of Cpz affects calcium signaling during zebrafish development	69
Chapter 5	Effect of thyroid hormone on bone development of early stage zebrafish larvae	85
Chapter 6	General Discussion	95
References		105
Summary		123
Samenvatting		125
Acknowledgements		127
Personalia		131

Chapter 1

General Introduction

Zebrafish have attracted increasing attention as a genetic model system to study developmental pathways leading to bone formation and bone homeostasis. Despite the popularity as an experimental model in vertebrate development, especially in functional genomics, the composition of the zebrafish skeleton received less attention. To contribute to a better understanding of developmental changes in the skeleton, I examined the skeletal extracellular matrix at the protein level in three subsequent developmental stages. The expectation at the onset of this analysis was that besides the known abundant structural proteins such as collagens and aggrecan, also less abundant proteins potentially involved in the extracellular formation of the matrix would be encountered. This proteomics analysis indeed provided several candidate proteins with a potential regulatory role in the formation of the skeleton. From this category, the metallopeptidase carboxypeptidase Z (Cpz) was selected for follow-up studies due to its reported role in trimming the C-terminal basic amino acid from the Wnt signaling peptide in rat (Wang et al., 2009). Gene expression analysis and loss-of-function mutants were examined showing the importance of this protein in early developmental stages of zebrafish. Phenotypical analysis of these mutants provided strong evidence for a role of this peptidase in the zebrafish Wnt signaling pathway. While the role of thyroid hormone in vertebrate bone development is well-documented (Wojcicka et al., 2013), evidence in zebrafish was lacking. I therefore set out to study the role of thyroid hormone on early bone formation in zebrafish embryos and showed enhanced ossification early in zebrafish development as a result of thyroid hormone application.

Before I present the details of my studies in the next chapters, I like to introduce vertebrate embryonic development as the broader context of my work. This is followed by the introduction of zebrafish as a model system, and more specifically cartilage and bone formation. Due to its reported complexity and activity in various developmental pathways, the Wnt signaling pathway receives special attention, as this is required to provide a framework for interpreting my Cpz results.

EMBRYONIC DEVELOPMENT OF VERTEBRATES

Embryonic development is a dynamic process that transforms a single undifferentiated cell into a highly organized individual with differentiated tissues and organs. Embryology emerged as a separate science around 1800, with the main focus on morphological changes during embryonic development and interspecies comparisons (Pelegrì, 2011). It was not until the late 1880's that the field shifted from comparative evolutionary embryology towards a more developmental point of view, studying cellular and genetic processes in developing vertebrate species (Pelegrì, 2011). The developmental program used by vertebrates differs between species, but despite these differences, all vertebrate embryos employ common processes during their development. These processes are fertilization, cleavage, gastrulation and organogenesis (Gilbert, 2014).

The life of an embryo starts with fertilization. Fertilization results in the fusion of the male and female gametes and activates the egg's metabolism and development (Sawada et al., 2014). The first stage immediately following fertilization is called the cleavage or cell division stage. During cleavage, a single-cell zygote undergoes a series of rapid synchronous cell

divisions. During these divisions the number of cells increases without increase of the overall mass leading to progressively smaller cells. Once a certain number of cells is reached, the embryo is called a blastula. The blastula enters the next major stage in embryonic development, called gastrulation (Wang and Steinbeisser, 2009).

During gastrulation extensive movements and rearrangements of embryonic cells produce three germ layers; the ectoderm, mesoderm and endoderm. Vertebrate gastrulation involves four evolutionary conserved morphogenetic movements i.e. epiboly, internalization, convergence and extension (Fig. 1.1A), that are for a large part coordinated through planar cell polarity (Box1). Epiboly movements spread and thin the blastoderm during gastrulation through radial intercalation of cells, while simultaneously convergence and extension movements narrow it in a mediolateral fashion (mediolateral intercalation), and elongate the embryo along its anterior-posterior axis (Fig. 1.1A-B). Internalization brings cells of the prospective mesoderm and endoderm beneath the future ectoderm via an opening in the blastula (blastopore), known as blastoderm margin in fish, the blastopore lip in amphibians and the primitive streak in amniotes.

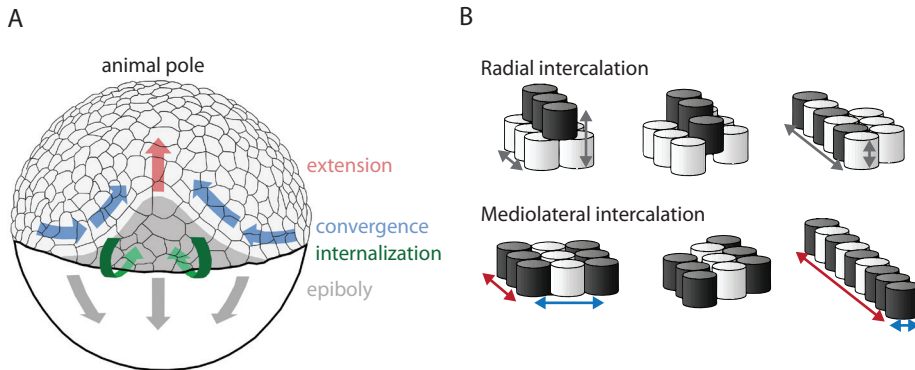
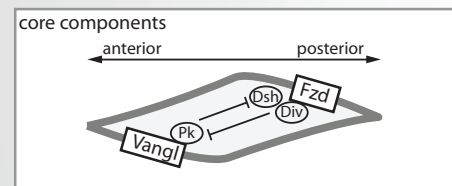
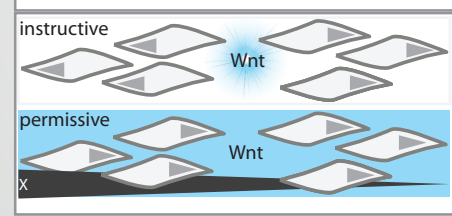


Figure 1.1. Cell movements during zebrafish gastrulation. (A) Dorsal view of the cell movements during zebrafish gastrulation. Epiboly spreads the blastoderm over the surface of the yolk. When the blastoderm cells have covered about half the yolk, a thickening occurs at the future dorsal portion of the embryo. This thickening (shield) is formed by internalization of cells, resulting in a two-layered system with a superficial layer (epiblast) and an inner layer (hypoblast). Convergence and extension of the hypoblast cells converge and extend the cells anteriorly, with a simultaneous narrowing along the midline of the hypoblast. (B) During epiboly, cells undergo radial intercalation. Cells enter the lower plane directly intercalating and extending the orthogonal axis. During convergence and extension movements that shape the anterior-posterior axis, mediolateral intercalation occurs within the same plane, resulting in the extension in the orthogonal-planar axis. Figures adapted from (Gilbert, 2000) and (Yin et al., 2008).

Gastrulation is preceded and accompanied by inductive processes that specify and pattern the germ layers. The control of these inductive processes is for a large part regulated by the organizer, the key embryonic signaling center, which is located in the dorsal or axial aspect of the blastopore (Spemann, 1938). It is clear that mechanisms of cell fate specification are conserved between vertebrate species (Grunz, 2004). However, it is uncertain whether this conservation also extends to the morphogenetic processes of gastrulation. After completion of gastrulation, embryonic development continues with organogenesis. During organogenesis, the cells from the different germ layers start to differentiate and interact, forming different cell types, tissues, organs and organ systems. In vertebrates, one of the primary steps

Box 1. Vertebrate planar cell polarity; the role of Wnt signaling.

Planar cell polarity (PCP) refers to the polarization of a field of cells within the plane of a cell sheet. Originally identified in insects, the first genetic evidence was gathered in *Drosophila melanogaster*, leading to the discovery of a set of core planar cell polarity (PCP) genes, the products of which were found localized asymmetrically within cells. The genes that control PCP in *Drosophila* are conserved in vertebrates and regulate polarized cell movements that shapes the vertebrate body plan (Goodrich and Strutt, 2011; Wang and Nathans, 2007). One of the core components in establishing PCP is Frizzled (Fzd). Fzd recruits Diversin which promotes the downstream activation of Dishevelled (Dsh) effectors. A second core component, Van Gogh-like protein (Vangl), recruits Prickle (Pk). These proteins are asymmetrically localized opposite to Fzd and Dsh and counteract Dsh activation. In the absence of known ligands for Vangl, part of the control of PCP is likely regulated through Fzd, a receptor for Wnt proteins. This notion is supported by several zebrafish PCP mutants in which loss-of-function of Wnt signaling components result in PCP defects. These loss-of-function mutations in β -catenin independent Wnt proteins as well as several other Wnt signaling associated genes, result in defects which lead to phenotypes similar to those induced in other core PCP genes.

	core components	zebrafish PCP mutant	phenotype	reference
		<i>pipetail/wnt5b</i>	CE movement defects	Kilian et al., 2003
		<i>silberblick/wnt11</i>	CE movement defects	Heisenberg et al., 2000
		<i>knypek/gpc4</i>	CE movement defects	Topczewski et al., 2001
		<i>ptk7</i>	CE movement defects neural tube defects	Golubkov et al., 2010
		<i>ryk</i>	impaired Ca ²⁺ dynamics defective directional cell movement	Andre et al., 2012
		<i>ror2</i>	CE movement defects	Gao et al., 2011

To generate polarity across a plane, two working models have been proposed for PCP establishment in which Wnt signals regulate PCP through either instructive or permissive signaling. In the first, directionality is created by a Wnt gradient resulting in different responses within a plane depending on the relative position of the cell compared to the release site of the cue. In the latter model, Wnt would be responsible for polarizing the entire plane but the cell response depends on a gradient of a yet-to-be-identified factor (factor x) (Heisenberg et al., 2000; Kilian et al., 2003).

during organogenesis is the formation of the neural system. The ectoderm which forms epithelial cells and tissues, also forms the neural tissues (Wilson and Hemmati-Brivanlou, 1997). During the formation of the neural system, part of the ectoderm forms the neural plate (neural keel in teleosts) which in turn forms the neural tube (Blader and Strahle, 2000; Greene and Copp, 2009). The mesoderm will develop into the various connective tissues. During neurulation, the mesoderm can be divided into five different regions. The first region is the chordamesoderm which forms the notochord. The notochord plays a major inductive function in the formation of the neural tube as well as in establishing the anterior-posterior body axis. The second region is the paraxial mesoderm which give rise to the somites. The somites produce many of the connective tissues including bone, muscle, cartilage and dermis

(Baggiolini et al., 2015; Simoes-Costa and Bronner, 2013). The intermediate mesoderm is the third region and is responsible for the formation of the urogenital system. The lateral plate mesoderm gives rise to the heart and blood vessels. Finally, the head mesenchyme is a major contributor to the connective tissues and musculature of the face. The third germ layer, the endoderm, forms most of the internal organs, including the digestive tube, liver, pancreas, the thyroid gland and most of the respiratory system (Zorn and Wells, 2009). Vertebrate embryos display a conserved body plan with an elongated axis, a dorsally and anteroposteriorly positioned nervous system located above the notochord, which is flanked by bilateral somites. After the process of organogenesis most embryos are either born or hatch.

The substantial similarity in major processes and mechanisms during embryonic development allows the study of corresponding processes in various types of organisms, thereby identifying common developmental mechanisms. An example of such a mechanism is the release of calcium ions from internal stores into the cytoplasm which is observed throughout embryonic development (Box2). Specific features differ between species. The choice of an experimental model system depends largely on characteristics of the organism and how these fit with the process that is under investigation. This thesis focuses on the use of the zebrafish (*Danio rerio*) as a model to study the development of the vertebrate embryo. In particular making use of the transparency of the developing embryos facilitates precise microscopic determination of crucial events such as convergence and extension movements.

THE ZEBRAFISH MODEL IN DEVELOPMENTAL BIOLOGY

The zebrafish, *Danio rerio*, is a small fresh water teleost found in shallow, slow-flowing waters of the Indian subcontinent (e.g. India, Nepal and Pakistan) (Engeszer et al., 2007; Spence et al., 2008). In recent years, zebrafish have received increasing attention as a model for studying vertebrate developmental processes, due to several advantageous properties over traditional model organisms such as mice. Adult zebrafish have a total body length of 3–4 cm and reach maturity at 3 months from which time point they start to reproduce (Fig. 1.2). Female zebrafish can produce 100–200 eggs weekly, which allows for appropriate numbers for large scale experiments. Eggs are fertilized externally and embryos develop at a fast rate *ex utero*, overcoming mammalian limitations in which *in utero* development interferes with studying embryogenesis. Most importantly, the transparency of developing embryos allows for direct visualization of early developmental processes which can be tracked in real-time. In addition, the aquatic environment in which zebrafish develop makes it an ideal system for carrying out toxicological and chemical studies (Lieschke and Currie, 2007). In contrast to mice, the large brood sizes of zebrafish allow for faster genetics and higher numbers of accessible mutant embryos.

Another important feature of the zebrafish model is the high conservation in developmental processes compared to other vertebrates. Recently, Howe et al. (Howe et al., 2013) revealed that more than 75% of human genes implicated in disease have counterparts in zebrafish, which provides an opportunity to analyze their roles in this model system. The use of invertebrate genetic models (e.g. *Caenorhabditis elegans* and *Drosophila*

melanogaster) complemented with the use of large-scale forward genetic screens, have elucidated important mechanisms that control developmental pathways (Jorgensen and Mango, 2002; St Johnston, 2002). However, several structures and organ systems such as an endoskeleton, a vascular system or an advanced central nervous system, that are key to vertebrates are lacking in invertebrates with the exception of *Cephalopods*. Currently available forward-genetic screens and random mutagenesis-based reverse genetics in the zebrafish provide an “invertebrate-style” forward genetic platform to analyze vertebrate development (Giacomotto and Segalat, 2010; Lawson and Wolfe, 2011). Together, these characteristics have established the zebrafish as a mainstream model in developmental biology, however, there are still some understudied areas such as development of the intestinal and the osteogenic organ system. The knowledge presently collected using specialized techniques, mutants, and transgenic zebrafish lines gives a good indication of the advances made by studying the formation of the vertebrate skeleton in zebrafish. However, with a primary focus on genetic regulation of skeletal cells, the properties of the zebrafish skeleton based on its composition still remain largely unexplored.

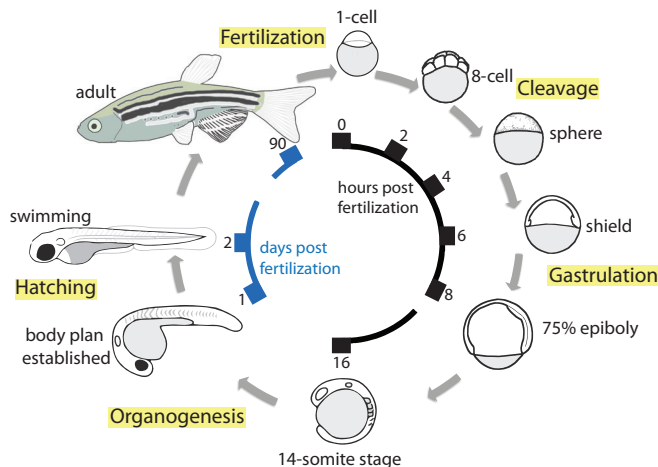


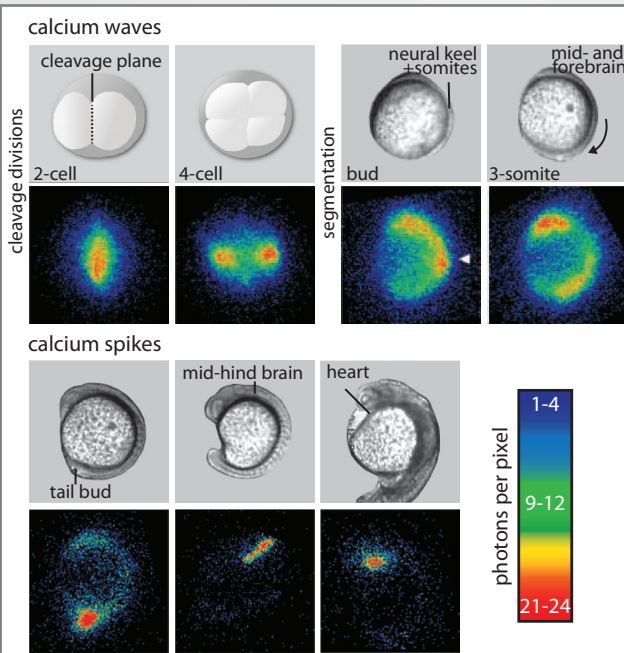
Figure 1.2. Schematic representation of zebrafish life history. Fertilization of the egg activates the segregation of non-yolk cytoplasm at the animal pole. Approximately 30 minutes after fertilization the ooplasm concentrates on top of the yolk and divides through a series of synchronous rapid cell divisions (cleavage). Gastrulation starts approximately 6 hours post fertilization, and after 1 day most of the organ precursors are present. Zebrafish larvae hatch and start swimming after 2 days, and reach sexual maturity around 3 months of age (image modified from (D’Costa and Shepherd, 2009)).

CARTILAGE AND BONE FORMATION IN VERTEBRATE DEVELOPMENT

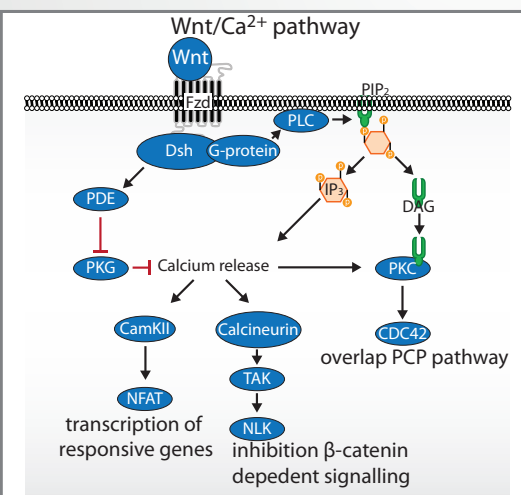
In the past, most studies in the area of skeletogenesis (e.g. bone and cartilage formation) have been performed in mice, chicken and *in vitro* cell culture systems. Fish species such as the zebrafish have long remained underappreciated in studying formation of the vertebrate endoskeleton because of several characteristics that distinguish them from mammals. For instance, fish lack haematopoietic bone marrow tissue. Zebrafish haematopoietic stem cells originate from the kidney marrow, the equivalent of mammalian bone marrow (Goessling and North, 2011). A second major difference originates from their living environment. Fish live in a calcium-rich surrounding which devaluates the need for calcium storage in its

Box 2. Calcium signaling and early embryonic development.

Calcium ions (Ca^{2+}) are used in many physiological contexts as second messengers. The modulated release of calcium from internal stores can be used as a signaling mechanism transferring information across individual or connected cells. The importance of Ca^{2+} during embryonic development is evident from experiments with Ca^{2+} buffer injections in *Xenopus* and zebrafish eggs (Creton et al., 1998; Webb et al., 1997). Calcium release coincides with several important events during embryonic development including the cleavage period, the segmentation period and heart development.



At the onset of cell cleavage divisions, increased Ca^{2+} levels are observed corresponding to the propagation of the cleavage plane functioning in forming and deepening of the furrow (Creton et al., 1998; Golubkov et al., 2010; Topczewski et al., 2001). This increase of Ca^{2+} is essential for the correct formation and orientation of cell divisions during the cleavage stage. In the segmentation period, distinct patterns of Ca^{2+} develop along the antero-posterior axis of the zebrafish embryo. First, Ca^{2+} patterns develop in the presumptive mid- and forebrain regions preceding morphological patterning of the brain (Hsu and Tseng, 2010). In addition, a pronounced slow-moving Ca^{2+} wave is present in the trunk region, moving posteriorly consistent with the formation of the somites and neural keel.



Apart from these Ca^{2+} patterns, high Ca^{2+} levels are also produced in short spikes, which play important functions in their respective areas (Creton et al., 1998). Ca^{2+} spikes are observed in specific regions such as the mid-hind brain region, the tail bud and most pronounced in the region of the developing heart. In the heart region, these Ca^{2+} signals correlate closely with the separation of the heart chambers and looping of the heart. Experiments with Ca^{2+} buffer injections block growth and development of the heart (images adapted with permission of Journal of Cell Science (Creton et al., 1998)).

The majority of intracellular Ca^{2+} release is triggered through inositol 1,4,5-triphosphate (IP3)-sensitive channels (Berridge et al., 2003). A role for Wnt in activation of the phosphatidylinositol (PI) cycle was initially identified in *Xenopus* and zebrafish embryos (Slusarski et al., 1997a). In the case of Wnt/ Ca^{2+} pathway activation, Wnt triggers Frizzled mediated activation of heterotrimeric G proteins. This activates phospholipase C (PLC), which in turn stimulates diacylglycerol (DAG) and IP3 production. The release of Ca^{2+} from intracellular stores is triggered by IP3 and activates effectors such as Ca^{2+} and calmodulin-dependent kinase II (CAMKII), calcineurin and protein kinase C (PKC), which activates the transcriptional regulator nuclear factor associated with T cells (NFAT), inhibit the β -catenin dependent signaling pathway through activation of nemo-like protein (NLK), or activation of CDC42 which role has been implicated in cell movement.

skeleton. Nonetheless, in a low calcium environment, the zebrafish skeleton appears to react in a similar fashion to that of mammals (Glowacki et al., 1986). Another major difference posed by the environment is the difference in the influence of gravity between aquatic and terrestrial animals. Nonetheless, studies of mechanical loading effects on the skeleton have been successful in several aquatic species, including the zebrafish (Fiaz et al., 2012). Despite these differences that have side-lined fish species in studying skeletogenesis, the high level of conservation in skeletogenic processes, including the overlap at the cellular level and genetic level are slowly becoming appreciated. Below, these conserved aspects will be highlighted for the zebrafish and compared to mammalian species.

The vertebrate skeleton consists predominantly of two tissue types; cartilage and bone. Cartilage and bone are produced and shaped by three major cell lineages, chondrocytes, osteoblasts, and osteoclasts. The former two cell types are derived from mesenchymal progenitor cells, whereas osteoclasts are of hematopoietic origin. The skeletal histology in zebrafish is comparable to that of mammalian species and the development of the zebrafish cranial skeleton (Cubbage and Mabee, 1996) and axial skeleton (Bird and Mabee, 2003) have been well-documented. As in mammals, the zebrafish skeleton is produced by cartilage-forming chondrocytes, bone-forming osteoblasts and the resorption of bone is controlled by osteoclasts. In addition, the zebrafish contains cellular bone which means osteoblasts get embedded in the bone matrix as osteocytes (Apschner et al., 2011). The zebrafish skeleton is formed by chondral and intramembranous ossification (Cubbage and Mabee, 1996). The first cartilaginous elements appear already during the second day of development and originate from condensation of mesenchymal cells. Mesenchymal cells subsequently differentiate into chondrocytes that secrete typical cartilage extracellular matrix components or form sheath cells that encapsulate the matrix produced by chondrocytes. During development, much of the cartilaginous skeleton is replaced by bone via so-called chondral ossification. Chondral ossification consists of perichondral and endochondral ossification. In zebrafish, perichondral ossification is the major process during the ossification of the preformed cartilage elements, whereas in mammalian species endochondral ossification plays a dominant role. Two populations of zebrafish osteoblast cells are responsible for chondral ossification (Hammond and Schulte-Merker, 2009). Cells in the encapsulating sheath of cartilage elements first start to display characteristics of osteoblasts and produce a so-called bone collar (Fig. 1.3). In subsequent events, this bone collar grows towards the extremes of the cartilage elements, and endochondral ossification is initiated by cells within the cartilage. These cells, while still possessing chondrocyte morphology, start expressing differentiation markers of osteoblasts and produce bone matrix inside the already formed collar. Other bone elements are formed

via intramembranous (dermal) ossification. In this process, mesenchymal cells directly differentiate into osteoblasts that produce bone matrix *de novo* (Fig. 1.3).

Next to similarities at the tissue and cellular level, high conservation is also observed in the genetic control of skeletal cells (Fig. 1.4). The formation of cartilage in vertebrates starts with differentiation of cells in mesenchymal condensations. This differentiation is accompanied by expression of the transcription factor *SOX9*, a member of the SoxE family of transcription factors containing a high-mobility-group-box DNA binding domain (Bi et al., 1999). Expression of *SOX9* regulates the expression of cartilage matrix molecules including the major matrix protein collagen type II (Bell et al., 1997). As a result of a fish-specific genome duplication, the zebrafish possesses two *sox9* genes, *sox9a* and *sox9b* (Chiang et al., 2001). Both *sox9* genes are expressed during cartilage development, and correlate with the expression of collagen type II genes. Conserved functions have been identified via mutant studies, revealing that zebrafish that are homozygous for a mutation in one or both of the *sox9* genes exhibit craniofacial defects and loss of skeletal elements that are

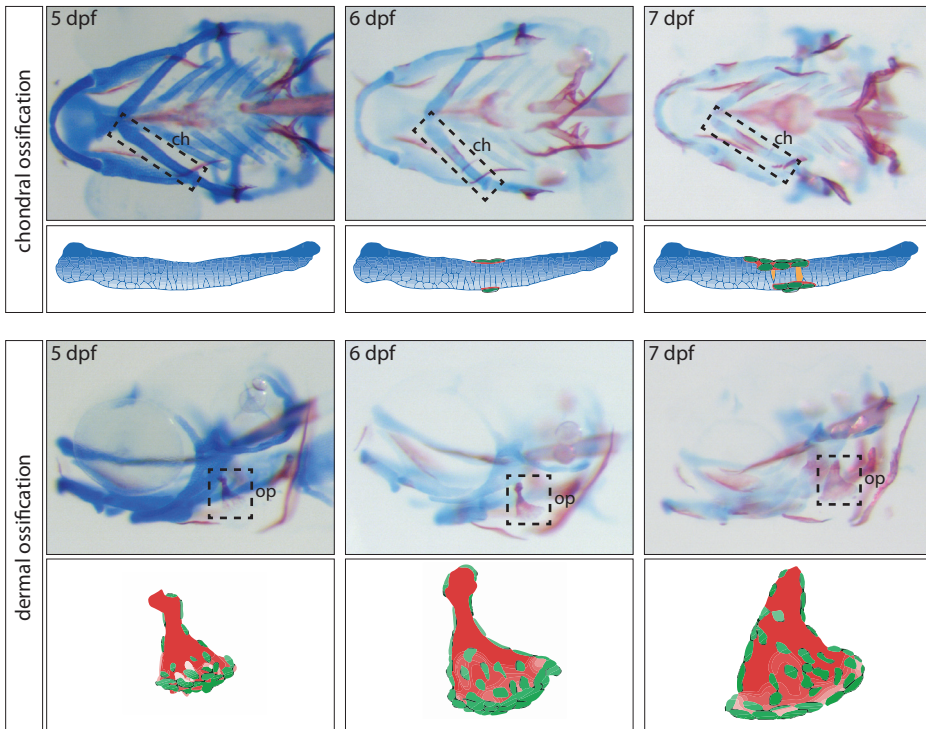


Figure 1.3. Different modes of ossification in zebrafish. Representation of chondral and dermal ossification via bone (red) and cartilage (blue) staining, with illustrations of the ceratohyal (ch) and the opercle (op) of zebrafish at 5-7 days post fertilization (dpf). Top panel: Chondral ossification. Ventral view of the zebrafish head region focusing on the ceratohyal. During chondral ossification, osteoblasts (green) first form a bone collar around cartilage elements which expands during development. Meanwhile chondrocytes within this bone collar start to express osteoblast markers (orange). Bottom panel: Dermal ossification. Lateral view of the zebrafish head region focusing on the opercle. Osteoblast produce bone directly, expanding bone structures during development (Illustrated images are produced using (Hammond and Schulte-Merker, 2009; Kimmel et al., 2010)).

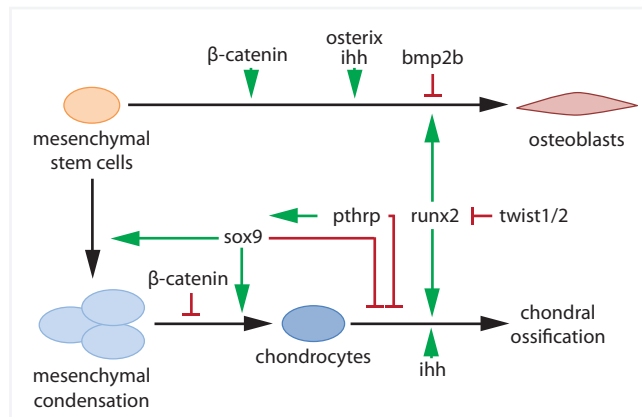


Figure 1.4. Schematic representation of factors that regulate differentiation of chondrocytes and osteoblasts in both mammals and zebrafish. Stimulation (>) or inhibition (I) are indicated in green and red, respectively (image modified from (Renn et al., 2006; Zhang et al., 2009))

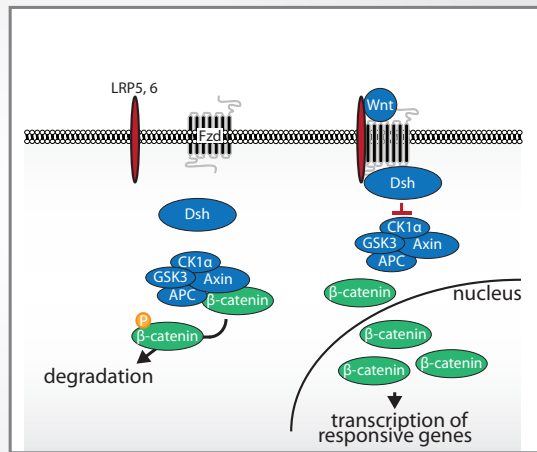
derived from cartilage (Yan et al., 2005). This corresponds to observations made in humans, in which a mutation in a single *SOX9* allele results in severe malformation (campomelic dysplasia) as a consequence of incomplete or underdeveloped cartilage-derived skeletal elements (Houston et al., 1983).

A second important transcription factor in vertebrate skeletogenesis is the runt-related transcription factor 2 (RUNX2). In higher vertebrate species such as mammals, RUNX2 is an important regulator of vertebrate osteoblast differentiation and crucial for initializing dermal and chondral ossification (Komori et al., 1997). The zebrafish homologues of *runx2* (*runx2a* and *runx2b*) are expressed in early osteoblast cells as well (Li et al., 2009; van der Meulen et al., 2005). As in mammals, *runx2* expression in zebrafish is followed by that of osterix and the transcription of bone matrix proteins such as collagen type I, osteocalcin and matrix Gla protein (Li et al., 2009). Expression of vertebrate RUNX2 is in part affected by TWIST1 (Kronenberg, 2004). The *TWIST1* gene encodes a basic helix-loop-helix transcription factor containing a so-called twist-box (Bialek et al., 2004). This functionally important domain is able to inhibit RUNX2 via direct interaction and displays remarkable sequence similarities between zebrafish and mammals (Bialek et al., 2004). Zebrafish Twist1 homologues, Twist1a and Twist1b, appear to function in a similar fashion affecting proper skeletal development by regulation of *runx2b* expression (Yang et al., 2011).

The process of chondral ossification is for a large part regulated by the hedgehog signaling pathway (St-Jacques et al., 1999). Expression of the main hedgehog ligand Indian hedgehog (IHH) by chondrocytes affects both chondrocytes and cells in the cartilage encapsulating sheath. In mice, deletion of *Ihh* leads to reduced chondrocyte proliferation and defects in osteoblast formation in the encapsulating sheath of cartilage elements, which results to dwarfism (Karaplis et al., 1994). A similar role is fulfilled by zebrafish *ihh* homologues (*ihha* and *ihhb*), which are expressed in chondrocytes during chondral ossification (Avaron et al., 2006), a critical process for the differentiation of osteoblasts in chondral bone elements (Felber et al., 2011; Hammond and Schulte-Merker, 2009). The IHH signaling

Box 3. Beta-catenin dependent Wnt signaling.

In the absence of a Wnt ligand, the multifunctional protein β -catenin is targeted to a multimeric protein complex named destruction complex (Barker, 2008). This complex phosphorylates several amino acid residues of β -catenin which is subsequently marked for degradation by the proteasome. In the presence of a Wnt ligand, the destruction complex is disassembled and β -catenin accumulates. β -catenin is imported into the nucleus where it functions as a transcriptional coactivator. Abbreviations: APC, adenomatous polyposis coli; CK1 α , casein kinase 1 α ; Dsh, Dishevelled; Fzd, Frizzled; GSK3, glycogen synthase kinase 3; LRP5/6, low-density lipoprotein receptor-related protein 5/6.



pathway in vertebrates is partly regulated by parathyroid hormone-related protein (PTHrP) (Vortkamp et al., 1996). Expression of *IHH* regulates *PTHrP* expression which in turn forms a negative feedback-loop, maintaining a balance between proliferation and differentiation of chondrocytes (Karp et al., 2000). Loss-of-function mutations in mice and knockdown of zebrafish parathyroid hormone-like protein (Pthlp) both cause premature bone mineralization (Karaplis et al., 1994; Yan et al., 2012), similar to the process of chondrodysplasia which is observed in humans bearing mutations in the PTHrP receptor (Schipani et al., 1995). In turn, *IHH* and *PTHrP* are sensitive to changes in thyroid hormone (T3) status and regulated by local thyroid hormone metabolism and T3 availability (Dentice et al., 2005; Stevens et al., 2000). Thyroid hormones exert widespread and complex actions in almost all tissues during development. The skeleton is an important T3-target tissue, yet understanding of the specific cellular and molecular mechanisms of T3 action in bone and cartilage is far from complete (Williams, 2003).

Apart from specific factors that control skeletogenesis, some multi-functional pathways are also involved in this process by specification of skeletal cells. One of these pathways is the Wnt signaling pathway. The name Wnt results from a fusion of the name of the *Drosophila* segment polarity gene wingless and the name of the vertebrate homolog, integrated or int-1 (Wodarz and Nusse, 1998). Wnt proteins are important signaling molecules that regulate diverse developmental processes. Wnt genes encode for glycoproteins that are approximately 300 amino acids in length and have a conserved pattern of cysteine residues. Initially, Wnt signaling events were described as independent signaling branches which included the 'non-canonical' (β -catenin independent) signaling pathways comprising the above described planar cell polarity pathway (Box1) and Wnt/ Ca^{2+} pathway (Box2), as well as the 'canonical' (β -catenin dependent) signaling pathway (Box3) (Baron and Kneissel, 2013). Many Wnt ligands are expressed during skeletal development and detected already in early mesenchymal condensations, suggesting a regulatory role in the formation of osteoblasts and chondrocytes (Church and Francis-West, 2002). Indeed, a role for β -catenin dependent

Wnt signaling in cartilage and bone differentiation is well-established (Regard et al., 2012). In mice, ectopic Wnt/ β -catenin signaling promotes ossification at the cost of chondrocyte differentiation, while inactivation of β -catenin in mesenchymal progenitor cells results in ectopic chondrocyte formation (Day et al., 2005b). In zebrafish, defective Wnt/ β -catenin signaling has also been associated with impaired osteoblast differentiation and reduced bone mineralization (Zancan et al., 2015).

COMPLEXITY OF THE WNT SIGNALING NETWORK

In the past decade, huge steps have been made towards a better understanding of the Wnt signaling network. The more traditional representation of the three different outputs; e.g. β -catenin dependent transcriptional regulation, calcium release and cell polarity, is slowly being replaced by the view of an interconnected network. The complexity of this Wnt signaling network, containing numerous components, is subjected to multiple regulatory steps as well as cross-talk mechanisms. The latter have been implicated in such a way that inhibition of PCP signaling has a negative effect on β -catenin dependent signaling (Li et al., 2011), while activation of Ca^{2+} signaling seems to inhibit β -catenin dependent signaling (Ishitani et al., 2003).

Activation of intracellular signaling events is achieved through interaction of Wnt proteins with members of the seven transmembrane receptors of the Frizzled family (Dijksterhuis

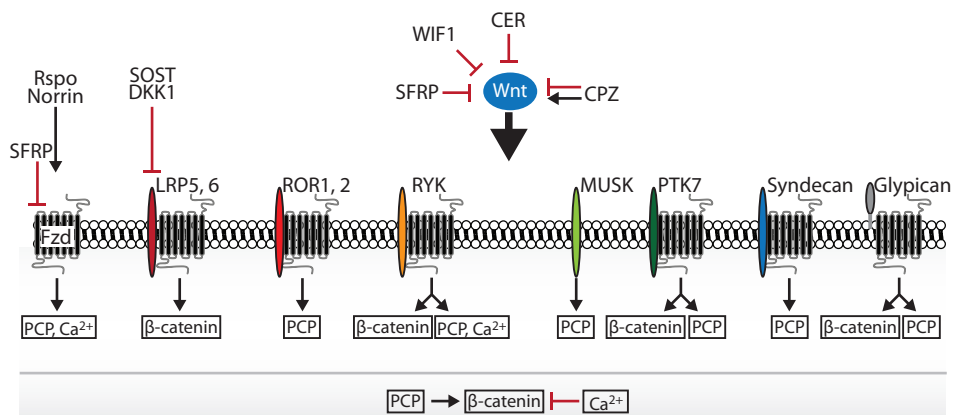


Figure 1.5. Regulation of the Wnt signaling network. Wnt signaling activity is regulated at several levels. First, Wnt ligand availability is regulated by antagonists which prevent interaction of the ligands with their receptors, or process the ligand as is the case upon binding of CPZ. Second, receptor availability is regulated by either blocking of ligand-receptor interactions or the regulation of the number of receptors present on the plasma membrane. Third, different receptor and co-receptor combinations activate different branches of the Wnt signaling network. And finally, the Wnt signaling network is under control of cross-talk mechanisms between the different signaling branches. Stimulation (>) or inhibition (!) are indicated. Abbreviations: β -catenin, β -catenin dependent Wnt signaling; Ca^{2+} , Wnt/ Ca^{2+} signaling; CER, Cerberus; CPZ, Carboxypeptidase Z; DKK1, Dickkopf 1; LRP5/6, low-density lipoprotein receptor-related protein 5/6; MUSK, muscle skeletal receptor Tyr kinase; PCP, planar cell polarity pathway; PTK7, protein Tyr kinase 7; ROR1/2, receptor Tyr kinase-like orphan receptor; Rspo, R-spondin; RYK, receptor Tyr kinase; SFRP, secreted Frizzled-related protein; SOST, Sclerostin; WIF1, Wnt inhibitory factor 1. Figure is adapted from (Niehrs, 2012) and (Cruciat and Niehrs, 2013).

et al., 2014). Here specificity is realized by ligand-receptor combinations, but also via interaction with a growing number of co-receptors that contribute to the output choice (Fig. 1.5) (Mikels and Nusse, 2006). The second layer of complexity is constituted by agonists and antagonist of the Wnt signaling network. For now, the agonist are comprised of R-Spondins (Rspo) and Norrin. The Rspo family is a small growth factor family that is able to induce Wnt signaling activity by inhibiting the targeted degradation of Fzd receptors (Hao et al., 2012). Norrin on the other hand is a high-affinity ligand for the Fzd4 receptor (Xu et al., 2004). Although structurally unrelated, Norrin functions as a Wnt ligand by binding to Fzd4, allowing for binding of the co-receptor low-density lipoprotein receptor-related protein (LRP) 5/6. A completely different mode of action has been described for the carboxypeptidase Z (CPZ). Not only is CPZ able to interact with Wnt proteins, it contains a peptidase domain which is able to remove the C-terminal basic residue from certain Wnt ligands (Wang et al., 2009). By doing so it is able to increase β -catenin dependent signaling in primary pellet cultures of rat growth plate chondrocytes (Wang et al., 2009). The exact mechanism behind this process remains unclear.

Antagonists of Wnt signaling can be separated based on their mode of action. Antagonists that act by sequestering Wnt ligands away from receptor complexes include secreted Frizzled-related proteins (SFRP), Wnt inhibitory factor 1 (WIF1), and Cerberus (CER). The second group includes the Dickkopf (DKK) protein family and Sclerostin (SOST) which affects Wnt signaling activity through their affinity with Wnt receptors or co-receptors. Several members of the DKK family bind to LRP5/6 with high affinity. In addition, DKKs can bind to another class of receptors called Kremen. Formation of a complex with both Kremen and LRP5/6 results in endocytosis and consequently the removal of LRP5/6 from the plasma membrane. The protein SOST antagonizes Wnt signaling by binding to LRP5/6 (Cruciat and Niehrs, 2013).

Box 4. Proteomics as a preferred tool in the study of cartilage and bone formation.

Elucidating the proteome of bone and cartilage is an essential step for understanding the physiology of these tissues and for identifying changes that occur during development and disease. The typical vertebrate skeleton consists of cartilage and bone tissue, which contain extensive amounts of extracellular matrix (ECM). Around 50-70% of the bone mass consist of the inorganic mineral hydroxyapatite. While qualitatively the organic matrix of bone consists of numerous proteins, 90% of this organic fraction is composed of type I collagen. In cartilage, the major fraction of the ECM consists of type II collagen and aggrecans. It is obvious that the high concentration of certain ECM components causes analytical problems in the proteomic analysis of cartilage and bone, similar to those in the analysis of low-abundance proteins present in serum (Georgiou et al., 2001). Given the large dynamic range of protein abundance, the detection of scarcer proteins is a major challenge.

Technical advances made in recent years, ranging from sensitive and high-resolution hybrid mass analyzers, automated coupling of liquid chromatography and introduction of stable isotope labelling techniques, improved mass spectrometry-based proteomics into a high-throughput and extremely accurate and sensitive method (Wasinger et al., 2013). Combining liquid chromatography, MS and label-free quantification presently allows for identification of several hundreds of proteins, even if these differ widely in natural abundance. A second problem results from the massive amounts of carbohydrates present in cartilage proteoglycans, and hydroxyapatite in bone. These characteristics of cartilage and bone severely complicate the extraction of proteins from these tissues. Initially, most bone and cartilage proteomic studies relied on *in vitro* systems in which proteins were extracted from primary cultures or immortalized cell lines allowing for more traditional protein extraction

protocols (Freyria and Becchi, 2004; Tay et al., 2014). However, the absence of the *in vivo* micro-environment and morphology soon revealed the limitations of this system (Zien et al., 2007).

The rise of shotgun proteomics along with the technical improvements in MS allowed for development of new protein extraction techniques. Being less dependent on methods that operate on the protein level (e.g. 2DE proteomics) but rather on a peptide level, the use of for instance strongly acidic conditions to demineralize bones were no longer considered off-limits. Jiang et al. (Jiang et al., 2007) successfully applied such conditions in their complementary sequential extraction protocol in which a large fraction of proteins was identified in this acidic fraction. Also, the protocol avoids a high yield of the abundant structural proteins from bone likely by acidic conversion of collagens to insoluble gelatin.

AIM AND OUTLINE OF THIS THESIS

The aim of this thesis is to analyze the composition of the extracellular matrix in zebrafish and to discuss the role of Cpz as one of its components.

The zebrafish is a relatively new model organism in the field of skeletal development and is used as a powerful model for the identification of novel gene functions during skeletogenesis. Although the biological similarities between the zebrafish and mammalian species at the molecular level are striking, the properties of the skeletal extracellular matrix are largely dependent on, and in part regulated by proteins in the matrix. For now, only a handful of matrix molecules have been characterized in zebrafish and are mainly used as markers for analysis of skeletal cells or to distinguish between different (bone or cartilage) matrices. Therefore, the protein composition of the zebrafish skeleton remains largely unexplored. In order to further our understanding of normal skeletal development in zebrafish and enable the identification of potential key regulatory proteins, it is necessary to identify and characterize the skeletal composition and changes that occur during development. In **chapter 2** we determine the protein content of the zebrafish skeletal ECM and major changes in protein abundance during development from larva to adult, using an MS-based approach. Next to major structural proteins, we show the identification of various components of signaling pathways implicated in skeletogenesis. This first proteomics analysis of the zebrafish skeleton reveals the homology between the zebrafish and the skeleton of other vertebrate species including mammals.

After the identification of potential regulatory proteins in the developing zebrafish skeleton during the MS-based approach, **chapter 3** follows up on one of these proteins, Carboxypeptidase Z (Cpz). This peptidase has previously been implicated in the Wnt signaling pathway and was shown to affect cartilage formation and ossification in several vertebrate species. An analysis of the role of this peptidase in zebrafish was still lacking and therefore we mapped the spatio-temporal expression of *cpz*. We show that expression of *cpz* is localized in and around zebrafish ossified structures that however are produced without a cartilage intermediate. A more thorough analysis showed a complex expression pattern during early developmental stages that predominantly overlaps with that observed in other species. Furthermore, we provide a comparative view of *cpz* expression and the expression of its proposed ligand, Wnt4 (zebrafish Wnt4a and Wnt4b).

In **chapter 4** we explore the role of *cpz* in zebrafish development. The extensive expression analysis of *cpz* and *wnt4a* and *wnt4b* indicates a role for *cpz* during early development. Despite being the topic of studies performed in other vertebrate species, an *in vivo* loss-of-function analysis of *cpz* remained absent. The *ex utero* development of the zebrafish allows for such analysis in early developmental stages and a frame shift mutation was produced via TALEN-mediated mutagenesis. We show that mutant embryos display a variety of phenotypes during early development, most of which copy phenotypical defects in the Wnt/Calcium signaling pathway. These morphologically abnormal phenotypes provide the first evidence for a connection between Cpz and regulation of the β -catenin independent Wnt signaling pathways which places the function of Cpz in a completely new field of focus.

Chapter 5 introduces an alternative approach to study skeletal development which complements the genetic studies. The role of thyroid hormone is well-documented in humans

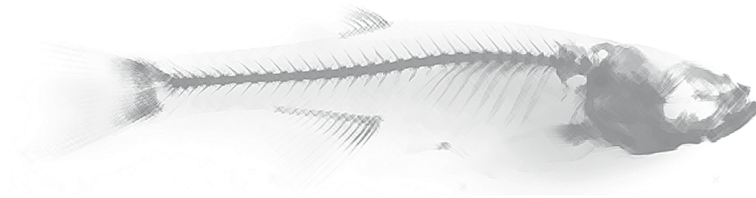
and studied extensively in rodent models. By contrast, the function of thyroid hormone in the development of the zebrafish skeleton has largely been ignored. Therefore, to what extent thyroid hormone affects early bone development in zebrafish remains unclear. Despite the role in vertebrate bone formation, the main focus of thyroid hormone studies in zebrafish have been on development in general and the effect on early cartilage formation. By exposing zebrafish embryos to the thyroid hormone triiodothyronine (T3) or the anti-thyroid drug propylthiouracil (PTU), we show that exposure to T3 accelerates ossification of craniofacial elements including the opercle and ceratohyal. This provides the first histological evidence of increased ossification in zebrafish due to thyroid hormone exposure which can be used as a starting point to explore the mechanism of thyroid hormone on skeletal development at a greater depth.

In the last chapter, **chapter 6**, we discuss the results and observations made in this thesis with respect to observations made in other studies. The results are placed in perspective to the still limited insight into zebrafish osteogenesis. Furthermore, suggestions for future studies are provided which could contribute to the understanding of the proteolytic processing effects of Wnt ligands on Wnt signaling activity.

Chapter 2

Proteomics analysis of the zebrafish skeletal extracellular matrix

Maurijn Y. Kessels^{1,2}, Leonie F. A. Huitema³, Sjef Boeren¹, Sander Kranenbarg², Stefan Schulte-Merker^{2,3}, Johan L. van Leeuwen², Sacco C. de Vries¹.



Plos One, 2014 (3), e90568

¹Laboratory of Biochemistry, Wageningen University, Wageningen, the Netherlands;

²Experimental Zoology Group, Wageningen University, Wageningen, the Netherlands;

³Hubrecht Institute-KNAW and University Medical Centre Utrecht, Utrecht, the Netherlands

ABSTRACT

The extracellular matrix of the immature and mature skeleton is key to the development and function of the skeletal system. Notwithstanding its importance, it has been technically challenging to obtain a comprehensive picture of the changes in skeletal composition throughout the development of bone and cartilage. In this study, we analyzed the extracellular protein composition of the zebrafish skeleton using a mass spectrometry-based approach, resulting in the identification of 262 extracellular proteins, including most of the bone and cartilage specific proteins previously reported in mammalian species. By comparing these extracellular proteins at larval, juvenile, and adult developmental stages, 123 proteins were found that differed significantly in abundance during development. Proteins with a reported function in bone formation increased in abundance during zebrafish development, while analysis of the cartilage matrix revealed major compositional changes during development. The protein list includes ligands and inhibitors of various signaling pathways implicated in skeletogenesis such as the Int/Wingless as well as the insulin-like growth factor signaling pathways. This first proteomic analysis of zebrafish skeletal development reveals that the zebrafish skeleton is comparable with the skeleton of other vertebrate species including mammals. In addition, our study reveals 6 novel proteins that have never been related to vertebrate skeletogenesis and shows a surprisingly large number of differences in the cartilage and bone proteome between the head, axis and caudal fin regions. Our study provides the first systematic assessment of bone and cartilage protein composition in an entire vertebrate at different stages of development.

key words: zebrafish, cartilage, bone, proteomics, skeletogenesis

INTRODUCTION

The vertebrate skeleton is a specialized tissue that provides support and protection for other tissues, enables mechanical functions, and acts as a homeostatic mineral reservoir. The skeleton consists of bone and cartilage that is produced by two distinct cell types called osteoblasts and chondrocytes, respectively. The formation of skeletal elements is realized by two distinct modes called intramembranous (dermal) and chondral ossification. During intramembranous ossification, mesenchymal cells proliferate and differentiate into osteoblasts that produce bone matrix. During chondral ossification, the mesenchymal cells differentiate into chondrocytes that form a cartilage template. This initial cartilage template provides a stable scaffold for bone formation and enables growth of skeletal elements prior to complete ossification (Mackie et al., 2008). Chondrocytes first enter a maturation process, differentiating from small round cells into discoid proliferating chondrocytes that align into columns and regulate the growth of the cartilage element. Chondrocytes then enter a pre-hypertrophic phase during which they expand in volume and form fully differentiated hypertrophic chondrocytes. At this stage the chondrocytes secrete extracellular matrix. These hypertrophic chondrocytes then go into apoptosis, allowing for osteoblast precursors to migrate into the degrading cartilage matrix where they differentiate and deposit the bone matrix (Kronenberg, 2003).

The extracellular matrices (ECMs) of bone and cartilage are mainly composed of a few highly abundant components. The major components of cartilage are the structural proteins of the heterotrophic collagen type II/XI/IX that comprises around 60 % of the dry weight of cartilage (Sophia Fox et al., 2009). The second largest group of structural proteins in cartilage (10-15%) is the proteoglycans. The most abundant proteoglycan is aggrecan that is responsible for the compression resistance of cartilage together with the heterotrophic collagens, and several other proteoglycans. In contrast, bone predominantly consists of a mineral fraction (50-70%) (Weiner and Wagner, 1998). Additional to this mineral phase, the major component of bone is the structural protein collagen type I that comprises approximately 90% of the protein fraction in bone. During bone formation, collagen type I fibrils act as a scaffold for the growing bone minerals (Viguet-Carrin et al., 2006). So-called non-collagenous proteins occupy the remaining 10% of the extracellular bone matrix. These non-collagenous proteins consist mainly of extremely acidic proteins which are believed to play crucial roles in the formation and function of mineralized tissues (Deshpande and Beniash, 2008).

The mechanical properties of the skeleton are largely dependent on the composition of proteins that are secreted into the ECM. This protein diversity cannot be sufficiently derived from mRNA analysis (e.g. microarray techniques) since mRNAs are not inherently part of the ECM, and not all proteins that contribute to the formation of skeletal elements are produced in the vicinity of these elements. In addition, mRNA abundance has been shown to correlate poorly to the protein content (Anderson and Seilhamer, 1997; Hegde et al., 2003; Nunez et al., 2006), and does not take into account the wide variety of post-translational modifications which are critical to protein functions (Karve and Cheema, 2011). This makes proteomics an essential tool for characterizing the composition of the skeletal ECM. Progress in the field of proteomics in both technology and methodology allow for creating large datasets from complex samples with high mass accuracy and sequencing speed (Ahrens et

al., 2010). Mass-spectrometry (MS)-based proteomics is becoming more quantitative, now including protein quantification via label-free and stable isotope labeling technologies (Zhu et al., 2010). Proteomics analysis of bone and cartilage in human, mouse, and rat already provided valuable insights by investigating differential protein expression in bone and joints, articular cartilage, bone cells, and chondrocytes (Lammi et al., 2006).

The zebrafish is an excellent system for proteomics since it is a well-characterized vertebrate model with readily available genetic maps allowing for the identification and characterization of proteins using existing databases. While being a relatively new model organism in the field of skeletal development, zebrafish have been used as a powerful model organism for the identification of novel gene functions during skeletogenesis (Spoorendonk et al., 2010). With key regulatory genes being highly conserved between teleosts and other vertebrate species (Mackay, 2013), zebrafish can provide important complementary information to studies performed in other species (Flores et al., 2004; Li et al., 2009). At the molecular level, the biological similarity between zebrafish and humans is striking and has currently resulted in the identification and analysis of zebrafish genes homologous to human genes associated with disease (Howe et al., 2013). In order to further our understanding of normal skeletal development, it is necessary to identify and characterize changes in skeletal composition, which in turn sheds light on the mechanisms that contribute to the production, functioning, and maintenance of the vertebrate skeleton.

Here, we present the first overview of the zebrafish skeletal proteome during development from larva to adult, using an MS-based approach. With a focus on proteins relevant for skeletal formation, 40 extracellular proteins were identified that are novel in the context of zebrafish skeletogenesis and with an implicated role in the development of the vertebrate skeleton.

MATERIALS AND METHODS

Animal maintenance

Zebrafish wild type strains were reared at the fish facility of Wageningen University at 27.1°C with a 14:10 light dark cycle. All fish were raised in a density of 5 fish/L. For the experiments, matings were set up with two males and three females. Eggs were kept at 28.5°C at the breeding facility, and transferred to the fish facility at 20 days post fertilization (dpf). All fish were fed *ad libitum* three times a day. Zebrafish larvae were fed in-house cultured paramecium from 120 hours post fertilization. Between 10 and 60 dpf the fish were fed both paramecium and artemia, after which the paramecium was exchanged for Tetramin flakes. Zebrafish were kept under standard conditions until they reached 14, 28, or 358 dpf, at which point the fish were euthanized with 0.1% (w/v) tricaine methane sulphonate (TMS, Crescent Research chemicals, USA) buffered with 0.08% (w/v) sodium bicarbonate (Gibco, Paisley, Scotland).

Ethic statement

The experiment was approved by the Wageningen University Animal Experiments Committee (protocol nr. 2011026.a and 2012020.a).

Tissue preparation and extraction

Craniofacial, axial, and caudal fin skeletal elements were isolated from 500 zebrafish of 14 dpf, 100 zebrafish of 28 dpf, and 15 zebrafish of 358 dpf. First, the head region was separated from the axial skeleton between the head and the Weberian vertebrae. The axial skeleton included the Weberian vertebrae, the precaudal, and the caudal vertebrae (Bird and Mabee, 2003). The caudal fin was excised at the start of the caudal fin vertebrae. An overview of skeletal elements exhibited by the 3 developmental stages, obtained by acid-free bone and cartilage staining as described previously (Spoorendonk et al., 2008), is shown in supplemental Fig. S2.1. Skeletal structures were isolated from 14 day old larvae by removal of excess tissue using Accumax solution (Millipore). Larvae were incubated for 1 hour at room temperature while pipetting the sample up and down every 10 minutes using a syringe with a 23G needle. After 1 hour, the skeletal structures were collected using a 70 µm cell strainer (BD Falcon). The bone structures from 28 and 358 dpf zebrafish were excised manually, trimmed free of excess tissue and incubated in Accumax solution for 2 hours at room temperature under vigorous shaking to remove cell remnants.

Protein extraction

For protein extraction the sequential protein extraction method developed by Jiang *et al.* (Jiang et al., 2007) was adapted for optimal protein extraction from the limited sample sizes used here. The main modifications included the removal of the pre-extraction step in 4M guanidine-HCl (GdmCl) to prevent protein loss from the bone structures of zebrafish larvae that were minimal in their degree of ossification as compared to juvenile and adult bone structures. Secondly, the extraction volumes were kept to a minimum so that processing of the extracts could be performed using spin filters (Manza et al., 2005; Wisniewski and Mann, 2009).

Before protein extraction, the isolated material was washed in phosphate buffered saline (PBS) containing a protease inhibitor cocktail (Roche), pH 7.4, for several hours at 4°C. For the protein extraction, the material from the initially separated craniofacial and axial region was used to create triplicates containing 5 mg (wet weight) each. Skeletal material was transferred to 1.5 ml Eppendorf tube containing 6 stainless steel balls (diameter, 3.9 mm), snap frozen in liquid nitrogen, and pulverized using a Retsch mill (Retsch GmbH, Hann, Germany) for 3 times 15 seconds at 30 Hz. Since not enough skeletal material could be isolated from the caudal fin region of zebrafish larva (14 dpf), this sample point was excluded. The isolation from the juvenile (28 dpf) caudal fin region resulted in enough material for one sample only (5 mg), and was therefore extracted as one sample and measured in duplicate. After pulverization the samples were sequentially extracted in order to improve the protein extraction from the mineralized matrix of bone. (I) First, the samples were demineralized by incubation in 1.2 M HCl for 2 hours (larvae), or overnight

(juvenile and adult) at 4°C. The supernatant was collected after centrifugation; the pellet was washed with PBS containing protease inhibitor cocktail (pH 7.4) and also collected after centrifugation. The HCl and PBS fractions were pooled and stored at -80°C. (II) The pelleted skeletal material was incubated in 50 mM Tris-HCl, 4M GdmCl, 0.5 M tetrasodium EDTA (pH 7.4) containing protease inhibitor cocktail, for 72 h at 4°C. The supernatant was collected after centrifugation, and the EDTA was removed by dialysis overnight in Slide-A-Lyzer mini dialysis units (Thermo scientific) against 50 mM Tris-HCl, 4 M GdmCl at 4°C. The dialyzed solution was subsequently stored at -80°C. (III) The remaining pellet was incubated for 24 h at 4°C in 50 mM Tris-HCl, 6 M GdmCl (pH 7.4) containing protease inhibitor cocktail. The solution collected after centrifugation was stored at -80°C.

Filter-aided sample preparation

Filter aided-sample preparation was employed to prevent protein loss during the subsequent precipitation steps. Since two of the extraction steps were performed in high chaotropic salt (GdmCl) concentrations and all extraction steps were performed without a detergent like sodium dodecyl sulfate (SDS), the filter-aided sample preparation method allowed for the use of sample volumes up to 400 µl. To include all the proteins extracted in the first step (HCl extraction), the subsequent extracts of each sample were pooled to obtain a sample containing a high chaotropic salt concentration. Cysteine residues were reduced with 7.5 mM dithiothreitol (DTT) for 30 min at room temperature. 400 µl of the samples was added to a Pall 3K omega filter and centrifuged at 15,871 g for 30 min. The flow-through was discarded and this step was repeated until the complete sample volume was filtered. 400 µl 8 M urea in 100 mM Tris/HCl, pH 8 was added to the filter and centrifuged at 15,871 g for 30 min. Subsequently, 400 µl 0.05 M iodoacetamide/ 8 M urea in 100 mM Tris/HCl, pH 8 was added to the filter, mixed, incubated for 30 min in the dark at RT, and centrifuged at 15,871 g for 30 min. The filter was washed by the addition of 110, 120, and 130 µl 8 M urea in 100 mM Tris/HCl, pH 8 in subsequent steps with a centrifuge step in between each step, 15,871 g for 30 min. 140 µl 0.05 M NH₄HCO₃ (ABC) solution was added to the filter unit and centrifuged at 15,871 g for 30 min. This was then followed by the addition of 100 µl ABC solution containing 0.5 µg trypsin to the filter and incubated overnight at room temperature. A final centrifugation step was then performed at 15,871 g for 30 min and the flow through was acidified using 10% (v/v) trifluoroacetic acid to pH 2-4. The samples were stored at -20°C until the nLC-MS/MS measurement was performed.

Mass spectrometry measurement

The analysis was performed by injecting 18 µl of sample over a 0.10×32mm Prontosil 300-5-C18H (Bischoff, Germany) pre-concentration column (prepared in-house) at a maximum pressure of 270 bar (Thermo Proxeon Easy nLC). The peptides were eluted from the pre-concentration column onto a 0.10×200 mm Prontosil 300-3-C18H analytical column with an acetonitrile gradient at a flow rate of 0.5 µl/min. The gradient that was used here increased the acetonitrile in water percentage from 9 to 21% during 100 min, 21 to 34% in 26 min, 34 to 50% in 3 min and constant at 50% for 5 min. Acetic acid was added to the eluent at 5 ml/l. The column was cleaned by increasing the acetonitrile up to 80% in 3 min. Between

the pre-concentration and analytical column, an electrospray potential of 3.5 kV was applied directly to the eluent via a metal needle electrode fitted into a P777 Upchurch micro cross. Spectra were obtained between m/z 380 and 1400 on an LTQ-Orbitrap XL (Thermo electron, San José, CA, USA). MS/MS scans of the 10 most abundant doubly and triply charged peaks in the FTMS scan were recorded in data-dependent mode in the linear trap (MS/MS threshold= 5000, 60 s exclusion duration).

Data analysis and label-free quantification

MaxQuant software version 1.2.2.5 was used to analyze the raw files from the LTQ-Orbitrap. MS/MS spectra were searched against the Uniprot zebrafish database downloaded from www.uniprot.org (2012), and a contaminant database including frequently observed contaminants such as human keratins and trypsin. For label-free quantification, the MaxQuant settings were kept default (using a 1% false discovery rate (FDR) on both peptide and protein level) except for the following changes. Asparagine or glutamine de-amidation was specified as variable modification. Label-free protein quantification was switched on, together with the “match between runs” option used with a maximal retention time window set to 2 min, and the intensity based absolute quantification (iBAQ) on. Normalized intensity values (LFQ intensity) were used for relative quantification. The MaxQuant results are shown in supplemental Table 2.1. Filtering of the MaxQuant protein groups result file (Supplemental Table 2.1) was performed using the Perseus module (version 1.3.0.4). Reverse hits were removed from the data together with proteins with only 1 identified peptide, no unique peptide, or no unmodified peptide. Database search and quantification results were grouped by combining results for the different injections of the craniofacial, axial, and caudal fin region for each of the developmental stages.

Gene ontology (GO)-terms were specified for each protein using Software Tool for Researching Annotations of Proteins (STRAP) program analysis (Bhatia et al., 2009). For genes with missing zebrafish ontology information, human orthologs were used instead and the same STRAP analysis was performed. Proteins known to be located in the (proteinaceous) extracellular region or matrix were used for further analysis. For quantification purposes, the proteins were additionally filtered and required to be detected in 2 or more out of each triplicate LC-MS/MS runs in at least 2 out of 3 sample points per region. Proteins without enough label-free quantification values were not selected for this procedure. Selected proteins were further analyzed using the Perseus module. Relative protein abundances were compared by performing a pair-wise t-test (both sides), with a permutation-based on FDR, threshold values of 0.05 or 0.01 and $S_0 = 1$, with 250 number of randomizations and $-\log_{10}$ as selected parameters. The obtained protein ratios were used to assess differences in protein abundance between the different regions and developmental stages. Proteins that changed significantly in abundance were subsequently analyzed based on previous identification and/or characterization in the vertebrate skeleton by assessing literature and zebrafish-specific data available at ZFIN (Sprague et al., 2003). Proteins that passed the threshold value of 0.05 were explored by Ingenuity Pathway Analysis (IPA; Ingenuity Systems, Redwood City, CA). Protein abundance ratios (Supplemental Table 2.5) and corresponding t-test values were uploaded into IPA and used to predict biological processes differing in abundance during the complete time course from larvae to adult.

In situ mRNA hybridization

Four of the proteins that differed in abundance (Supplemental Table 2.5) were selected for spatial gene expression analysis with in situ hybridization. Primers were designed using Primer 3 software (Rozen and Skaletsky, 2000) and extended with a T7, or Sp6 transcription initiation sequence on the reverse primer (Supplemental Table 2.6). cDNA obtained from zebrafish of 15 dpf was used to perform a PCR with these primers to generate the specific coding sequences of the genes (0.2–1.0 kb) to use as templates for the DIG labeling reaction. DIG-labeled probes were synthesized according to the manufacturer's instructions (Roche, DIG-labeling) and purified with the Qiagen RNeasy kit (Protocol RNA Cleanup).

Wild type zebrafish (28 dpf) were euthanized as described above and fixed overnight in 4% paraformaldehyde (PFA) in phosphate-buffered saline (PBS) at 4°C. After washing with PBS (2 x 5 min), fish were dehydrated in 100% methanol at RT (room temperature, 2 x 5 min) and stored at -20°C until further use. For sectioning, fish were rehydrated (75%, 50% and 25% methanol/PBS, 1 x 5 min), and washed in PBST (PBS + 0.1% v/v Tween®20, 3 x 5 min). Fish were embedded in 1.5% agar / 5% sucrose and incubated overnight in 30% sucrose at 4°C. Embedded fish were frozen in liquid nitrogen and stored at -80°C. Longitudinal sections of 20 µm were made with the cryostat (Leica CM3050S) and transferred onto polylysine coated slides (Menzel-Gläser, Thermo scientific). Slides were stored in a box with silica gel at -20°C or if used immediately, dried overnight at RT.

In situ hybridization was performed as described in Smith *et al.* (Smith *et al.*, 2008) and Schulte-Merker (Schulte-Merker, 2002) with the following modifications. Probes were diluted to a final concentration of 0.5 ng/µl in hybridization buffer (50% formamide, 5x salt solution; 0.75 M NaCl and 0.075 M sodium citrate pH=7.0, 0.1% v/v Tween®20, 9.2 µM citric acid, 0.5 mg/ml tRNA yeast (Invitrogen), heparin (45 U/ml). Two hundred µl of the probe solution was added to each slide and covered with Nescofilm (Bando Chemical IND., Kobe, Japan). Slides were incubated overnight at 70°C in a humid chamber. Slides were washed in solution A (50% v/v formamide, 1 x salt solution, 0.1% v/v Tween®20, 2 x 30 min, 70°C) and in 1xTBST (0.14 M NaCl, 2.7 mM KCl, 0.025 M Tris HCl, 0.1% v/v Tween®20, pH=7.5), 2 x 30 min, RT. Subsequently, slides were incubated in 2% blocking buffer (Blocking reagent, Roche, Mannheim, Germany) in 1 x TBST for at least 1 hour at RT. The blocking buffer was replaced with 200 µl of a 1:2000 dilution of anti-DIG AP FAB fragments (Roche) in 2% blocking buffer. The slides were covered with Nescofilm and incubated overnight at 4°C. Then, slides were washed with TBST and equilibrated with AP staining buffer (0.1 M Tris, 0.1% v/v Tween®20, 0.1 M NaCl, 0.05 M MgCl₂), 2 x 10 min. Slides were incubated in 400 µl of staining solution (1 ml AP staining buffer, 4.5 µl NBT and 3.5 µl BCIP) in the dark. Staining was monitored regularly and stopped by washing in distilled water (2 x 10 min). After clearing with methanol, washing with PBS and fixation with 4% PFA/PBS (20 min at RT), slides were mounted in Aquatex® (Merck, Darmstadt, Germany) and incubated overnight at RT to dry. Images were taken with an Olympus DP50 digital camera mounted on a Nikon Microphot-FXA microscope and Analysis[®] software (Soft Imaging System GmbH, Germany).

RESULTS

Zebrafish skeletal extracellular proteome

A total of 262 different extracellular proteins (Fig. 2.1A) were identified and quantified in protein extracts of the zebrafish skeleton at three developmental stages of the craniofacial, axial and caudal fin regions (see Fig. 2.2, 2.3 and 2.4 respectively). Extracellular proteins were selected based on available GO information of the zebrafish ($n=126$), and GO information based on human orthologs ($n=136$) as described in the Materials and Methods section. Based on STRAP gene ontology analysis, the extracellular proteins were associated mainly with binding ($n=111$), but also with processes like catalytic activity ($n=40$), structural molecule activity ($n=36$), and enzyme regulatory activity ($n=27$) suggesting that next to major structural proteins, the selected protein set also included proteins with regulatory functions in skeletal development. A large number of proteins ($n=116$) however lacked gene ontology information (Fig. 2.1A). The full list is shown in Supplemental Table 2.1 while an overview of all identified peptides is presented in Supplemental Table 2.2. One hundred and forty-eight cellular proteins were also identified but, together with proteins that could not be properly annotated, these were not further analyzed (Supplemental Table 2.4). As expected, the most abundant proteins within the list of extracellular proteins include major bone (e.g. collagen type I isoforms, extracellular matrix protein 2) and cartilage proteins (e.g. collagen type II, matrilin 1, apolipoprotein A-I, epyphican), previously described in MS based analyses of these tissues/structures in other vertebrate species, including humans (Alves et al., 2011; Onnerfjord et al., 2012; Schreiweis et al., 2007; Wilson et al., 2012). Also the serum-derived protein alpha-2-HS-glycoprotein (Ahsg), reported to bind to the mineral content of bone, was found among the most abundant proteins (Fig. 2.1B) (Ashton et al., 1976; Triffitt et al., 1976).

In addition to these highly abundant proteins, the total protein profile contained multiple other ECM structural constituents among which various types of collagens, as well as several proteins from the small leucine-rich proteoglycan (SLRP) family (e.g. biglycan, opticin, osteoglycin, asporin), growth factors (e.g. bone morphogenic proteins, transforming growth factors, fibroblast growth factors), growth factor regulator proteins (e.g. insulin-like growth factor binding proteins, transforming growth factor binding proteins), various peptidases (e.g. matrix metallopeptidases, serine peptidases, carboxypeptidases), several peptidase inhibitors (e.g. serpin peptidase inhibitors, timp metallopeptidase inhibitors), and serum proteins (e.g. transferrin, thrombin, apolipoproteins, complement factors) (Supplemental Table 2.3).

Analysis of extracellular matrix proteins during skeletal development

The relative contribution of cartilage and bone to the skeletal structures in the craniofacial sections changes rapidly (Fig. 2.2A). To identify extracellular matrix proteins associated with the different skeletal tissues during zebrafish development, relative quantification was performed separately for the craniofacial skeleton, the axial skeleton, and the caudal fin region of three developmental stages; larvae (14 dpf), juveniles (28 dpf) and adult fish (358

dpf). In total, 188 of the proteins identified in the craniofacial skeleton were selected for the relative quantification based analysis. Of these, 127 were found at all three time points (Fig. 2.2B) while limited numbers were found at two or only one time point. Normalized abundance ratios were compared between the three different stages at a threshold of FDR = 0.01. Seventy-four proteins significantly differed in abundance between larval, juvenile and adult stages (Fig. 2.2C-E, Supplemental Table 2.5). Three different analyses are presented, providing a pair-wise comparison between the three developmental stages in terms of protein abundance compared with iBAQ intensity (Schwanhausser et al., 2011). A selection of the proteins that differ most in abundance for the three different stages is given in Fig. 2.2F, and their positions indicated in the diagrams of Fig. 2.2C-E. Among the proteins strongly reduced in abundance upon development between two of the time points, collagen type IV alpha 6 (Col4a6), laminin beta 2-like (Lamb2l), leukocyte cell-derived chemotaxin 1 (Lect1) and serum paraoxonase/arylesterase 2 (Pon2) were found while a strong increase in abundance was noted for osteonectin (Sparc), midkine-related growth factor a (Mdka), midkine-related growth factor b (Mdkb), unique cartilage matrix-associated protein a (Ucmab), secreted phosphoprotein 24 (Spp2) and platelet-derived growth factor receptor-like (Pdgfr1). The entire list of craniofacial extracellular proteins, including the significantly differing proteins, is given in Supplemental Table 2.5.

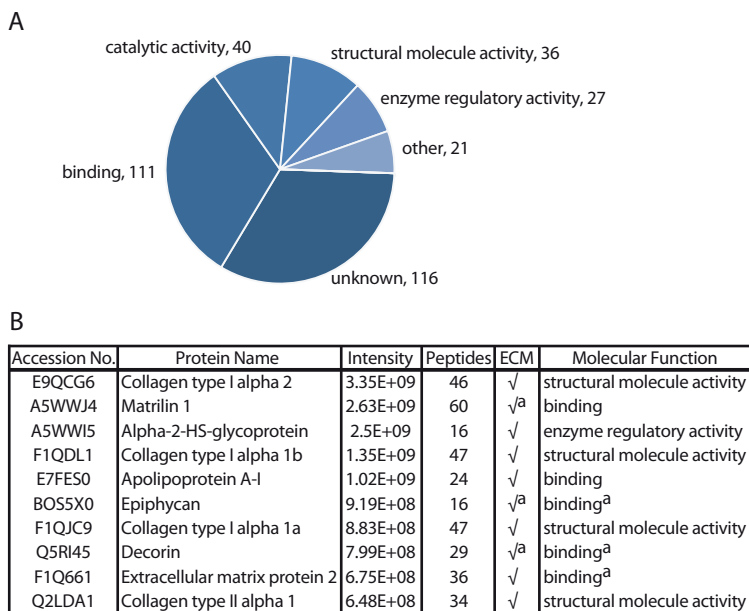


Figure 2.1. Composition of the zebrafish extracellular protein profile. (A) Distribution of molecular functions for the proteins identified as extracellular proteins. ^aGene Ontology information based on the human ortholog of a protein in case this information was absent in the zebrafish database. The diagram contains 351 entries corresponding to 262 different proteins of which some fall into multiple categories (B) Ten most abundant extracellular proteins within the obtained protein profile based on their intensity.

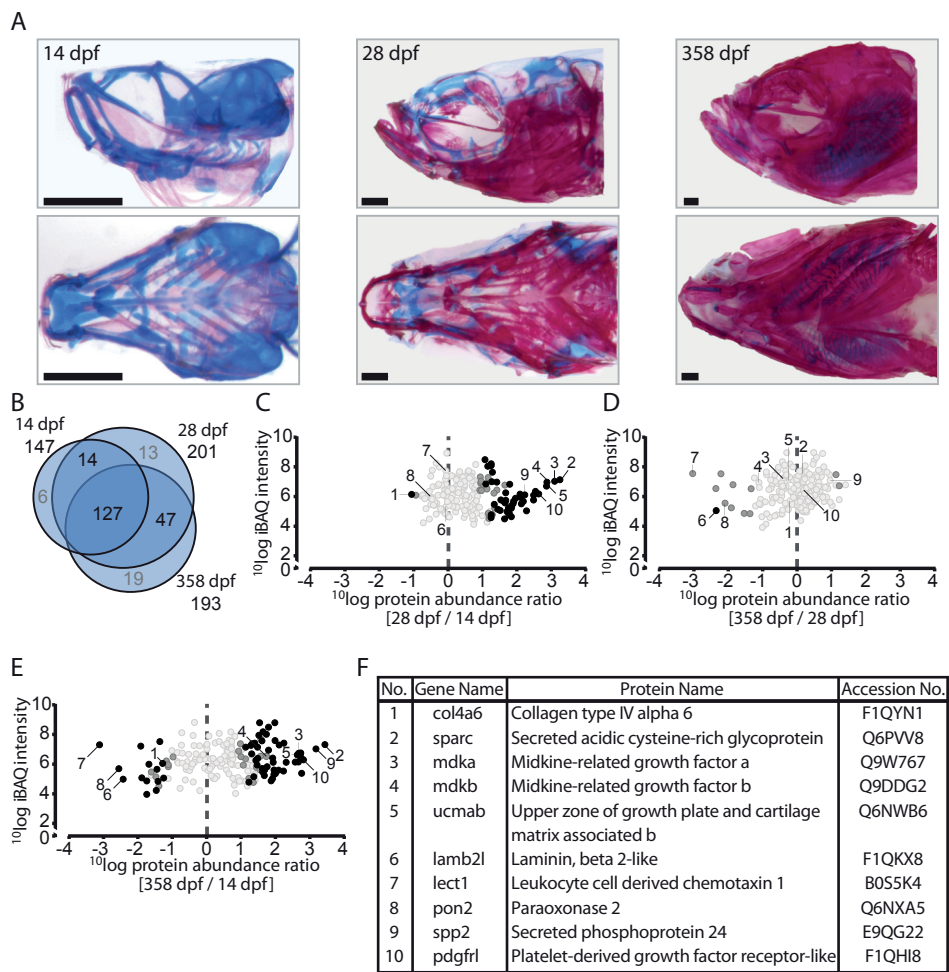


Figure 2.2. Quantitative analysis of the zebrafish craniofacial skeleton by MS-based proteomics. (A) Alcian blue/alizarin red stain of cartilage/bone structures in the craniofacial skeleton. Lateral (top) and ventral (bottom) images of all three time point used for protein extraction (left to right: 14 dpf, 28 dpf, 358 dpf). (B) VENN diagram of proteins selected for label-free quantification, with areas drawn to represent the number of proteins. Total number of proteins as well as distinct and common proteins are indicated for each time point. Proteins that did not qualify for label-free quantification are depicted in grey. (C-E) Ratio abundance plots showing log total iBAQ intensities versus log protein abundance ratio of the 28/14 dpf (C), the 358/28 dpf (D) and the 358/14 dpf (E) craniofacial skeleton ratios of all the proteins that met the strict criteria for label-free quantification (black circles, significantly differential abundant proteins at FDR= 0.01; dark grey circles, significantly differential abundant proteins at FDR= 0.05; light grey circles, no significant change in abundance). The numbers correspond to the proteins listed in 2F. (F) Table containing several of the significant differentially abundant proteins within the cranial skeleton. Specific proteins are discussed in the text.

A similar analysis is presented for the axial region (Fig. 2.3). There, 163 proteins were found to be present at all three time points and again a minority was found to be associated only with one or two time points. In comparing the most significant reduction or increase in protein abundance there are striking differences with the list shown for the head region. For

example the proteins Lamb2l, Nidogen 2 (Nid2), microfibrillar-associated protein 2 (Mfap2), collagen type V alpha 3b (Col5a3b) and collagen type IV alpha 5 (Col4a5) show a reduced 358/14 dpf ratio. Although the analysis is limited to juvenile and adult stages of the caudal fin (Fig. 2.4A), due to the limited yield of skeletal material from the larvae, the list of proteins significantly changed in abundance is again different from the previous two. Of the 8 proteins differing in abundance between the juvenile and adult stages of caudal fin development (Fig. 2.4D), myocilin (Myoc) and prostaglandin D2 synthase b (Ptgdsb) were found to among the proteins that exhibited the highest difference in abundance in the axial protein abundance comparison at the same stages. None of the caudal fin proteins strongly differing in abundance are found in the list of protein abundance comparison of the head region.

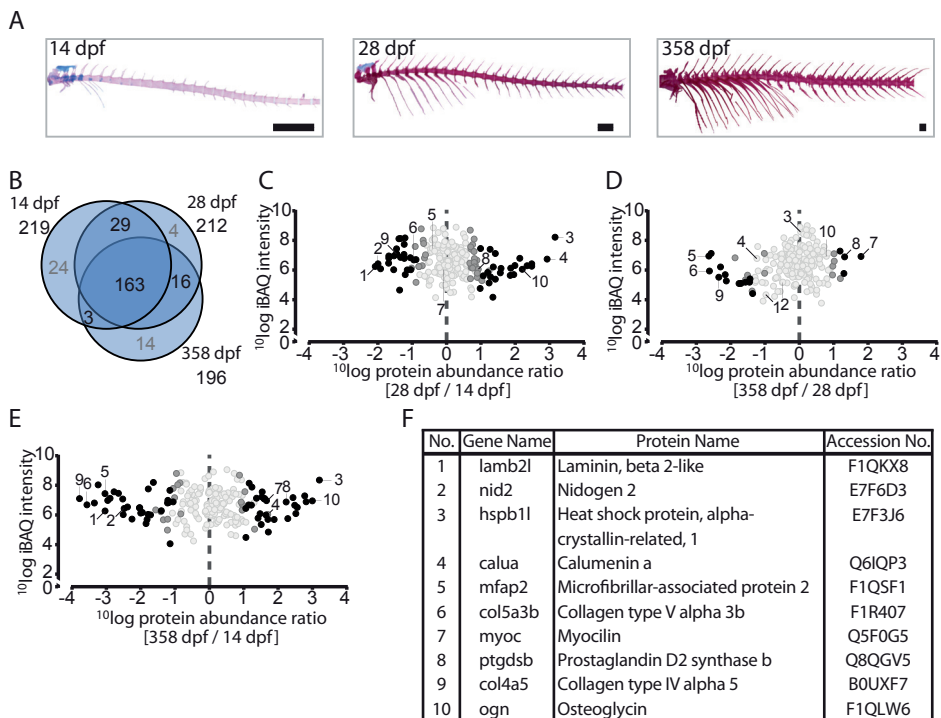


Figure 2.3. Quantitative analysis of the zebrafish axial skeleton by MS-based proteomics. (A) Alcian blue/alizarin red stain of cartilage/bone structures in the axial skeleton. Lateral images of all three time point used for protein extraction (left to right: 14 dpf, 28 dpf, 358 dpf). (B) VENN diagram of proteins selected for label-free quantification, with areas drawn to represent the number of proteins. Total number of proteins as well as distinct and common proteins are indicated for each time point. Proteins that did not qualify for label-free quantification are depicted in grey. (C-E) Ratio abundance plots showing log total iBAQ intensities versus log protein abundance ratio of the 28/14 dpf (C), the 358/28 dpf (D) and the 358/14 dpf (E) axial skeleton ratios of all the proteins that met the strict criteria for label-free quantification (black circles, significantly differential abundant proteins at FDR= 0.01; dark grey circles, significantly differential abundant proteins at FDR= 0.05; light grey circles, no significant change in abundance). The numbers correspond to the proteins listed in 3F. (F) Table containing several of the significant differentially abundant proteins within the axial skeleton. Specific proteins are discussed in the text.

Multiple cartilage matrix proteins, such as Lect1, hyaluronan and proteoglycan link protein 1b (Hapln1b) and optcin (Optc) were found to be reduced in abundance during development. This observation fits with the gradual replacement of cartilage by ossified structures during development. Other proteins including the collagen type IV isoform alpha 6 (Col4a6), Lamb2l, laminin beta 4 (Lamb4), and nidogen 1b (Nid1b) are conventional basement membrane proteins (Quondamatteo, 2002; Timpl et al., 2003). The same proteins are also expressed by chondrocytes and in mice become less abundant during the aging process (Kvist et al., 2008). Other proteins were connected to either mineralization (ectonucleotide pyrophosphatase/ phosphodiesterase family member 1)(Huitema et al., 2012), or remodeling of the bone matrix (annexin A2b) (Takahashi et al., 1994). The extracellular protein slit homolog 3 (Slit3), and otospiralin (Otos) have not previously been associated with vertebrate skeletogenesis.

A number of extracellular proteins are highly abundant in the juvenile skeleton but not in the larval and adult stages, for example several Wnt signaling regulator proteins such as secreted frizzled-related protein 1b (Sfrp1b) and frizzled-related protein (Frzb). Both have a documented role in chondral ossification (Enomoto-Iwamoto et al., 2002; Lu et al., 2013) thereby corresponding with the process of chondral ossification which is most prominent at the juvenile stage, but no longer evident in the adult skeleton. Additional proteins most abundant at the juvenile stage in the head region include the cartilage protein 'upper zone

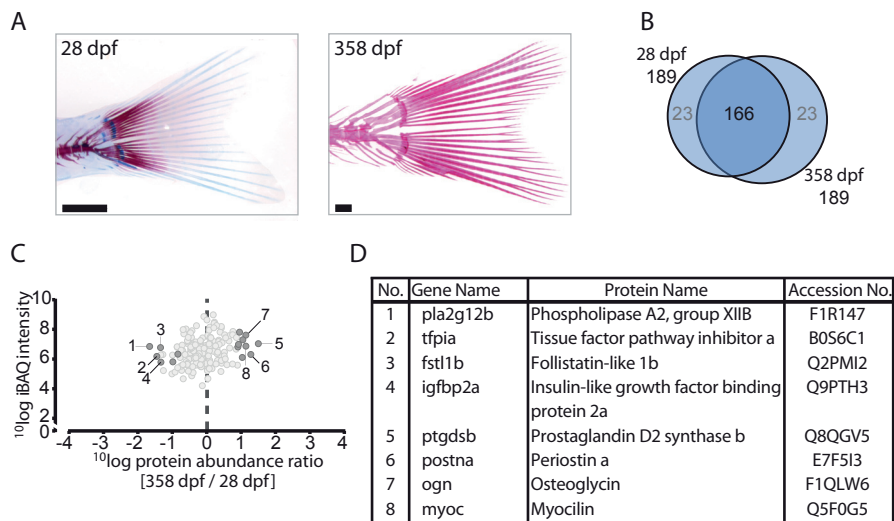


Figure 2.4. Quantitative analysis of the zebrafish caudal fin by MS-based proteomics. (A) Alcian blue/alizarin red stain of cartilage/bone structures in the caudal fin skeleton. Lateral images of two time points used for protein extraction (left to right: 28 dpf, 358 dpf). (B) VENN diagram of proteins selected for label-free quantification, with areas drawn to represent the number of proteins. Total number of proteins as well as distinct and common proteins are indicated for each time point. Proteins that did not qualify for label-free quantification are depicted in grey. (C) Ratio abundance plot showing log total iBAQ intensities versus log protein abundance ratio of the 358/28 dpf caudal fin region ratios of all the proteins that met the strict criteria for label-free quantification (dark grey circles, significantly differential abundant proteins at FDR= 0.05; light grey circles, no significant change in abundance). The numbers correspond to the proteins listed in 4D. (D) Table containing several of the significant differentially abundant proteins within the cranial skeleton. Specific proteins are discussed in the text.

of growth plate and cartilage matrix associated b' (Ucma), as well as lysyl oxidase-like 2b (Loxl2b), and inter-alpha-trypsin inhibitor heavy chain family, member 6 (Itih6) previously identified in cartilage tissues during MS-based approaches (Onnerfjord et al., 2012; Wilson et al., 2012). The protein tissue factor pathway inhibitor a (Tfpi) was the one extracellular protein considered as novel in vertebrate skeletogenesis that showed highest abundance at 28 dpf (Supplemental Table 2.5).

The remaining proteins were shown to increase during the complete developmental sequence analyzed (Supplemental Table 2.5). The list includes proteins with an implicated function in mineralization such as Ahsg and Spp2 (Lee et al., 2009; Sintuu et al., 2008), in bone formation such as osteopontin (Spp1), and Sparc, but also in the process of cartilage maturation, including cartilage intermediate layer protein 2 (Cilp2), and tenascin Xb (Tnxb) (Wilson et al., 2012). Other proteins significantly increased in abundance included growth factor regulators such as fibroblast growth factor-binding protein 2 (Fgfbp2), and Insulin-like growth factor-binding protein 5b (Igfbp5b). This last protein has been implicated to be processed by the proteinase htra serine peptidase 1b (Htra1b) that is able to induce bone formation by regulating transforming growth factor beta (Tgfb) signaling (Graham et al., 2013), but can also regulate IGF signaling by cleaving IGFBP5 (Hou et al., 2005). From the list of 123 extracellular matrix proteins that were significantly differing in abundance ($P=0.01$), 52 were novel in the context of zebrafish skeletal development or have only been studied based on their gene expression pattern by in situ hybridization at stages up to 5 dpf (Table 2.1).

Table 2.1. Extracellular matrix proteins novel in the zebrafish skeleton.

		Craniofacial skeleton			Axial skeleton			Caudal fin region	
Uniprot	Protein name	Ratio 28/14	Ratio 358/28	Ratio 358/14	Ratio 28/14	Ratio 358/28	Ratio 358/14	Ratio 358/28	References
Bone-related proteins									
F1QR30	Bgnb ^a	0.44	0.94	1.38**	0.02	0.51	0.54	0.73	(Alves et al., 2011; Onnerfjord et al., 2012; Wilson et al., 2012)
Q803H7	Itm2ba ^a	1.48**	-0.27	1.21**	0.96*	0.02	0.98	-0.31	(Zhang et al., 2003)
F1R0N0	Lrrc17 ^a	1.72**	0.26	1.98**	0.14	-0.20	-0.06	-0.79	(Kim et al., 2009)
Q6NXA5	Pon2 ^a	-0.47	-2.08*	-2.55**	-0.26	-1.69**	-1.96**	n.s.	(Yamada et al., 2003)
B0S6K5	Tnw ^a	-0.49	0.03	-0.46	-1.23**	-0.55	-1.78**	-0.03	(Brellier et al., 2012)
B0S525	Igfbp5b ^a	2.45**	0.28	2.73**	0.81*	0.15	0.95	-0.38	(Alves et al., 2011; Andress, 2001; Mohan et al., 1995; Schreiwies et al., 2007)
F1RDU8	Fcgrt	0.73	-1.33*	-0.60	0.20	-1.35**	-1.15**	n.s.	(Alves et al., 2011)
E9QG22	Spp2	2.19**	0.96	3.15**	2.13**	0.30	2.43**	0.33	(Sintuu et al., 2008)
F1QXC6	Tgfb2l	1.14*	0.07	1.21*	1.42**	0.28	1.70**	0.01	(Balooch et al., 2005; Erlebacher and Derynck, 1996)
Cartilage-related proteins									
B7SDQ7	Ccdc80 ^a	1.74**	0.15	1.89**	-0.06	0.28	0.21	0.00	(Wilson et al., 2012)
F1Q775	Cilp ^a	0.48	-0.25	0.23	-1.24**	-1.29	-2.53**	n.s.	(Wilson et al., 2012)
F1Q924	Col6a6 ^a	-0.47	-0.51	-0.98*	-1.53**	0.32	-1.21**	0.06	(Fitzgerald et al., 2008)

Table 2.1. Continued.

F1QLW6	Ogn ^a	1.80**	0.86	2.66**	2.20**	0.79	3.00**	1.11*	(Alves et al., 2011; Onnerfjord et al., 2012; Wilson et al., 2012)
F1QKL1	Thbs3a ^a	n.s.	n.s.	n.s.	0.72	0.34	1.06**	-0.93	(Onnerfjord et al., 2012; Wilson et al., 2012)
F1R1P9	Thbs4b ^a	n.s.	n.s.	n.s.	0.56	0.91	1.47**	0.10	(Cerdeja et al., 2002)
E7F6W5	Cmn ^a	n.s.	n.s.	n.s.	-0.10	-2.29**	-2.39**	n.s.	(Onnerfjord et al., 2012; Wilson et al., 2012)
F1RAC0	Aebp1 (2/2)	1.68**	0.53	2.21**	1.85**	0.66	2.51**	0.41	(Bernardo et al., 2011; Wilson et al., 2012)
F1Q5N7	Cilp2	1.16*	0.78	1.94**	0.54	0.60	1.14**	1.01*	(Wilson et al., 2012)
E7FB76	Col21a1	n.s.	n.s.	n.s.	-0.59	-1.26	-1.85**	n.s.	(Onnerfjord et al., 2012)
E7FF99	Fbn2	-0.10	-0.76	-0.86	-0.59	-0.56	-1.15**	-0.57	(Wilson et al., 2012)
F1QLT3	Fgfbp2	1.50**	0.41	1.91**	0.26	-0.22	0.03	n.s.	(Onnerfjord et al., 2012)
F1R5Z2	Fndc1	1.80**	0.05	1.85**	1.24**	-0.48	0.76	-0.55	(James et al., 2005; van Gool et al., 2012)
F1Q5C3	Itih6	1.61**	-0.44	1.16	0.00	-0.55	-0.55	n.s.	(Wilson et al., 2012)
E7F8X0	Srp2	0.82	0.72	1.55*	0.83*	0.39	1.22**	0.88*	(Wilson et al., 2012)
E7F1S4	Thbs2b	0.80	0.11	0.90	1.07**	-0.31	0.75	-0.75	(Wilson et al., 2012)
E7EXE8	Tnxb	2.24**	0.50	2.74**	0.73	0.58	1.31*	0.56	(Wilson et al., 2012)
Bone- and cartilage-related proteins									
Q804H0	Anxa1c ^a	-0.22	-1.52*	-1.74**	n.s.	n.s.	n.s.	n.s.	(Alves et al., 2011; Onnerfjord et al., 2012; Wilson et al., 2012)
Q6IQP3	Calua ^a	n.s.	n.s.	n.s.	2.93**	-1.23	1.69*	-1.35	(Alves et al., 2011; Wilson et al., 2012)
Q5SPR2	Clu ^a	n.s.	n.s.	n.s.	1.58**	1.19**	2.77**	0.35	(Alves et al., 2011; Onnerfjord et al., 2012; Wilson et al., 2012)
Q6AXL0	Cthrc1a ^a	1.92**	0.37	2.29**	n.s.	n.s.	n.s.	n.s.	(Alves et al., 2011; Wilson et al., 2012)
Q6NYE1	Fgb ^a	1.22**	-0.43	0.79	n.s.	n.s.	n.s.	n.s.	(Alves et al., 2011; Onnerfjord et al., 2012; Wilson et al., 2012)
F1QG51	Fmoda ^a	-0.22	-0.32	-0.53	-1.21**	-0.42	-1.63**	-1.29	(Alves et al., 2011; Onnerfjord et al., 2012; Wilson et al., 2012)
F1REI0	Htra3 ^a	0.70	-1.09	-0.40	1.20**	-1.01*	0.19	-0.74	(Tocharus et al., 2004)
Q6GMI5	Bgna ^a	0.92*	0.67	1.59**	0.71*	0.52	1.23**	0.37	(Alves et al., 2011; Onnerfjord et al., 2012; Schreweis et al., 2007)
F1R6R2	Apcs	n.s.	n.s.	n.s.	-1.69**	-0.35	-2.04**	n.s.	(Alves et al., 2011; Onnerfjord et al., 2012)
A9JRB3	Htra1b	1.64**	0.26	1.90**	0.68*	0.28	0.95*	-0.34	(Tiaden et al., 2012) (Tsuchiya et al., 2005)
F1QFZ8	Mmp13b	1.24**	0.07	1.31**	0.88*	0.72	1.61**	0.64	(Inada et al., 2004) (Nakamura et al., 2004)
F1QLH9	Nucb1	0.88	-0.13	0.75	1.36**	-0.93	0.43	-1.00*	(Wilson et al., 2012)
Q29RB4	Olfml3a	0.69	0.60	1.29**	0.81*	0.55	1.37**	0.27	(Alves et al., 2011; Wilson et al., 2012)

Table 2.1. Continued.

B3DJG2	Pcolce (2/2)	1.62*	0.16	1.78**	2.48**	0.33	2.81**	0.32	(Alves et al., 2011; Onnerfjord et al., 2012; Wilson et al., 2012)
Novel proteins									
F1QW52	Habp2	1.62**	0.04	1.67**	-0.22	-0.32	-0.54	-0.31	-
E7F8L7	Otos	0.28	-2.20*	-1.91**	-0.68*	-2.56**	-3.24**	n.s.	-
F1Q9N5	Metrn1	n.s.	n.s.	n.s.	1.28**	-0.34	0.94	-0.62	-
BOUXN0	Qsox1	n.s.	n.s.	n.s.	0.98**	1.30**	2.28**	n.s.	-
F1QK57	Tecta	1.10	0.96	2.07**	n.s.	n.s.	n.s.	n.s.	-
B0S6C1	Tfpia	1.85**	-0.67	1.18	0.92*	-0.86	0.06	-1.46*	-

Of the 123 extracellular proteins that were differentially abundant during zebrafish skeletal development, a subset of 40 proteins was identified as novel proteins in zebrafish skeletal development based on whether they were previously characterized or identified in skeletal tissues of other vertebrate species (mouse, rat, human). In addition, 6 were considered as novel in vertebrate skeletogenesis in general (bottom). a Indicates proteins previously studied based on their gene expression pattern by in situ hybridization in stages up to 5 dpf. Proteins that were not selected for relative quantification based on described criteria (Materials and Methods section) are marked (N.S.). Significantly differential abundant proteins are indicated by a star (*) or a double star (**) based on their significance at a threshold of FDR= 0.05, or FDR= 0.01, respectively.

Finally, a small number of extracellular proteins were found that can be regarded as novel in the context of vertebrate skeletogenesis in general. This list includes tissue factor pathway inhibitor a (Tfpia), hyaluronan binding protein 2 (Habp2), otospiralin (Otos), tectorin alpha (Tecta), meteorin, and glial cell differentiation regulator-like (Metrn1). While there is no clear picture emerging from this small list of proteins in relation to the signaling processes or the structural proteins involved in bone formation, there seem to be a number of proteins acting as growth inhibitors or representing elements of other tissues such as blood vessels

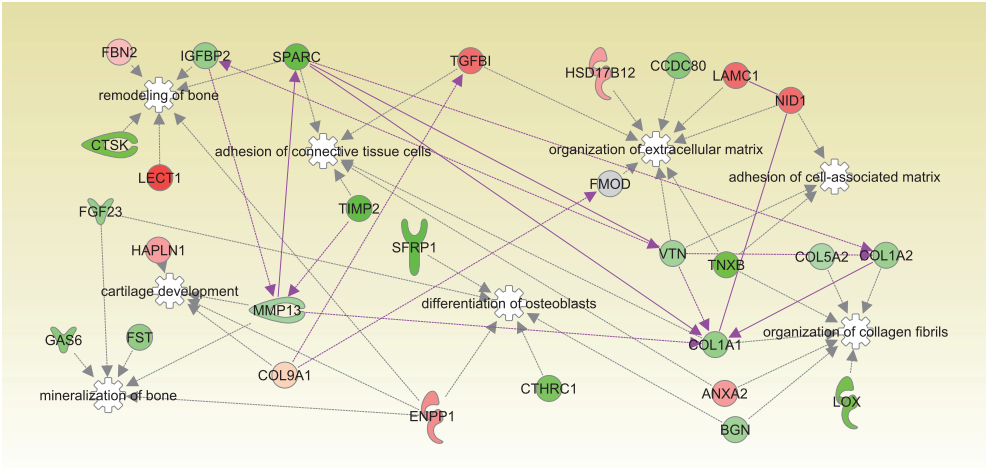


Figure 2.5. Ingenuity Pathway Analysis (IPA). Proteins that differ in abundance are involved in connective tissue, skeletal and muscular development. Green shading indicates an increase in abundance during development whereas red shading indicates a decrease. Increased intensity in colors indicates a higher differential abundance.

or neurons. For instance, the protein *Metrn1* is known to act on glial cell differentiation of mice (Nishino et al., 2004).

The obtained protein abundance ratios were used for analysis using the Ingenuity Pathway Analysis (IPA) tool. As shown in Fig. 2.5, the network consisting of 29 proteins is enriched in proteins linked to processes that contribute to formation of the extracellular matrix, including cell-matrix interactions, organization of collagen type I fibrils, mineralization of bone, and bone remodeling. During development, proteins contributing to the cartilage matrix (e.g. *Hapln1*) decreased in abundance whereas most proteins involved in the formation and remodeling of bone increased.

To determine whether the extracellular proteins as identified here are secreted by either chondrocytes or osteoblasts, in situ mRNA hybridization was employed for the cartilage-related genes *lect1* and *ucmab* and the bone-related genes *bmp6r* and *col1a2* (Fig. 2.6). Sagittal sections of the head region of 28 dpf zebrafish juveniles were used, as both cartilage and bone formation are actively taking place at this stage (cf. Fig. 2.2A). The results show that *lect1* and *ucmab* expression is found in chondrocytes of the parachordal (pch) cartilage (arrows) whereas *bmp6r* is expressed in ossification sites as confirmed by *col1a2* expression. This confirms that these extracellular proteins are deposited close to their respective sites of secretion.

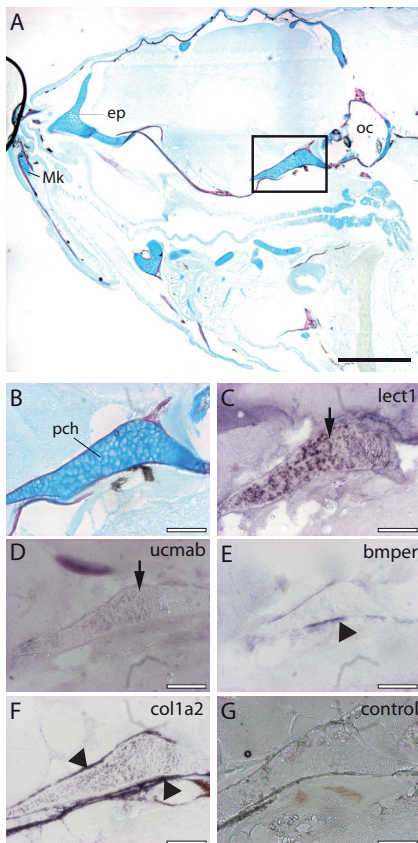


Figure 2.6. In situ mRNA hybridization of genes encoding extracellular proteins implicated in cartilage and bone formation in the head region. Sagittal sections of the head region of 28 dpf zebrafish juveniles stained by acid-free bone (red) and cartilage (blue) staining (A-B), or used for in situ hybridization with an antisense RNA probe corresponding to *lect1* (C), *ucmab* (D), *bmp6r* (E), *col1a2* (F). As a control, hybridization with the *lect1* sense RNA probe is shown (G). (B-G) Magnification of boxed area in A focusing on the parachordal (pch) cartilage. Images are from consecutive sections at the same position. (C-D) Expression of *lect1* and *ucmab* is located in chondrocytes of the parachordal (pch) cartilage (arrows). (E-F) Transcripts of *bmp6r* and *col1a2* were detected in ossification sites surrounding the parachordal chondrocytes (arrow heads). Scale bars indicate 0.5 mm (black), or 100 μ m (white). Abbreviations: ep, ethmoid plate; Mk, Meckel's cartilage; oc, otic capsule; pch, parachordal.

DISCUSSION

In order to obtain a more comprehensive understanding of the factors that are pivotal during osteogenesis and in bone function, it is important to determine the protein composition of the osteoid matrix during earlier and more mature stages of bone formation. This is technically challenging, and a systematic analysis of proteins at different stages of osteogenesis has for this reason not yet been carried out previously. In this study, we present an overview of the extracellular proteins present in zebrafish bone and cartilage elements at three different stages, as determined by LC-MS/MS.

As expected, major bone and cartilage constituents such as collagen type I and collagen type II were among the most abundant proteins. Less abundant proteins, including most of the described non-collagenous proteins in bone (e.g. Spp1, Sparc), multiple proteoglycans including almost the complete small leucine-rich protein family (e.g. decorin, biglycan), and even serum proteins described to bind to the bone mineral content (e.g. Fetub, Ahsg) were detected (Ashton et al., 1976; Lee et al., 2009; Triffitt et al., 1976). Our results indicate that most of the intracellular proteins were significantly reduced and this supports the validity of the procedures that have been employed for tissue purification and protein extraction. In comparison to the previous study describing 417 proteins in zebrafish caudal fins (Singh et al., 2011), few correspondences were found. Out of the 19 proteins found corresponding with the previous study, only 3 (Anxa1b, Col12a1 and Col6a1) were isoforms of the ones in our list of proteins novel to zebrafish bone and cartilage formation (Table 2.1). This apparent lack of correspondence is most likely due to the inclusion of the full set of intracellular proteins in the previous study (Singh et al., 2011).

To obtain an overview of major differences in skeletal composition during development, 262 extracellular proteins were detected and compared at three different stages of development; larval, juvenile, and adult. 123 differentially abundant proteins were identified, among which were well-established components of the vertebrate skeleton. Among these, 40 extracellular proteins were considered as not previously connected to zebrafish skeletogenesis. Based on functional analysis in other vertebrate species, most of the new entries corresponded with major stage-specific differences such as the initial growth of cartilage elements followed by the ossification of most of these elements, and the increase of bone matrix by a growing number of bone structures together with an overall increase in the degree of mineralization. An unexpected finding was that the largest changes in protein abundance were highly dissimilar in the head, axis and caudal fin regions. This may be the result of underlying temporal or spatial differences in skeletal organization between the three regions and underscores the necessity to incorporate detailed localization studies in a proteomics approach such as performed here.

One of the here identified novel proteins in zebrafish skeletogenesis was the protein Cilp2. This protein is believed to be a component of permanent cartilages in mice, since it is not observed in replacement cartilage (Bernardo et al., 2011). In the zebrafish, the ossification of elements in the skull is completed around 70 dpf. In this study, the protein Cilp2 was significantly increased in the adult skeleton, at which point replacement cartilages are no longer present in the zebrafish skeleton. Permanent cartilages in the zebrafish are mainly observed in later stages of development in the skull in which cartilage bands connect

several bones, and between the individual vertebrae (LeClair et al., 2009). The absence of replacement cartilage in the adult zebrafish, and the here observed up-regulation of Cilp2 in the adult skeleton therefore suggests that in zebrafish, Cilp2 also contributes to permanent cartilages.

Another interesting finding was the significant up-regulation of the Wnt signaling pathway antagonists, Frzb and Sfrp1b at the juvenile stage during zebrafish skeletal development. In mice, FRZB is implicated in skeletal development by modulating chondrocyte maturation and preventing chondrocytes from entering the hypertrophic phase during perichondral ossification (Enomoto-Iwamoto et al., 2002). Since perichondral ossification in the zebrafish is observed in the larval and juvenile craniofacial skeleton, but is no longer evident in the adult, the up-regulation of Frzb at the juvenile stage is correlating with this process. The endogenous Wnt signaling antagonist SFRP1 is also implicated in this process by regulating the Wnt/ β -catenin signaling pathway, affecting chondrocyte maturation and ossification events in the cranial base of mice (Nagayama et al., 2008). The involvement of the Wnt signaling pathway in zebrafish cartilage morphogenesis has already been shown (Topczewski et al., 2001). Together with the fact that Wnt proteins are often highly conserved across species (Nusse and Varmus, 2012), the zebrafish could well be used as a model to elucidate the signaling pathways contributing to the formation of skeletal elements.

The effects of the insulin-like growth factor system on skeletal development and maintenance has already been subjected to intensive studies (Bikle and Wang, 2012; Tahimic et al., 2013). Insulin-like growth factor inhibitors, like the here identified Igfbp5b have been implicated in either maintaining osteoblasts in an immature status, or promoting osteoclastogenesis and subsequent bone resorption (Peruzzi et al., 2012). In line with this, increase in human IGFBP5 has been linked to age-related bone loss via an increased rate of bone-resorption (Mohan et al., 1995). Here we identified a significant increase in Igfbp5b abundance in the adult zebrafish skeleton, when compared to younger stages. The combined significant increase in Igfbp5b and collagenase 3 (Mmp13b) emphasizes the possible increase in osteoclastogenesis. Mmp13b is involved in bone resorption but also in the differentiation of osteoclasts (Nakamura et al., 2004; Stickens et al., 2004). The increase of both Igfbp5b, and Mmp13b implicates an increase in osteoclast differentiation and/or activity in adult zebrafish compared to younger developmental stages. The use of transgenic lines that allow visualization of osteoclasts *in vivo* will be a tremendous tool to correlate protein distribution with osteoclast activity in the future (Chatani et al., 2011).

The formation of bone is a gradual process during which proteins such as Sparc are embedded during development (Rotllant et al., 2008). In this study, most bone related proteins were found to increase during the developmental analysis of the ECM proteins. Only one extracellular protein with a function in mineralization was significant decreased in abundance during development. This protein, ectonucleotide pyrophosphatase/ phosphodiesterase family member 1 (Enpp1) is a known regulator of phosphate/pyrophosphate homeostasis *in vivo* (Huitema et al., 2012). Since pyrophosphate is a strong chemical inhibitor of bone mineral formation, the decrease of Enpp1 during development correlates with the progression of ossification observed during the formation of the zebrafish skeleton.

In summary, this study demonstrates that the secreted proteome reflects all major processes taking place during skeletal development of the zebrafish. Processes including cartilage proliferation and morphogenesis, gradual ossification, and even several signaling pathways based on secreted growth factors and growth factor regulators were identified. The substantial number of extracellular zebrafish proteins identified here, which have a mammalian ortholog previously associated with osteogenesis, underscores the validity of our MS-based approach, and we demonstrate that the composition of the zebrafish extracellular matrix has striking similarities to that of other vertebrate species, including mammals. Significantly, we furthermore also identify a number of proteins that have not been connected to osteogenesis previously. These proteins warrant further analysis, and will serve as a very useful reference for future studies not only in zebrafish, but also in other vertebrate species.

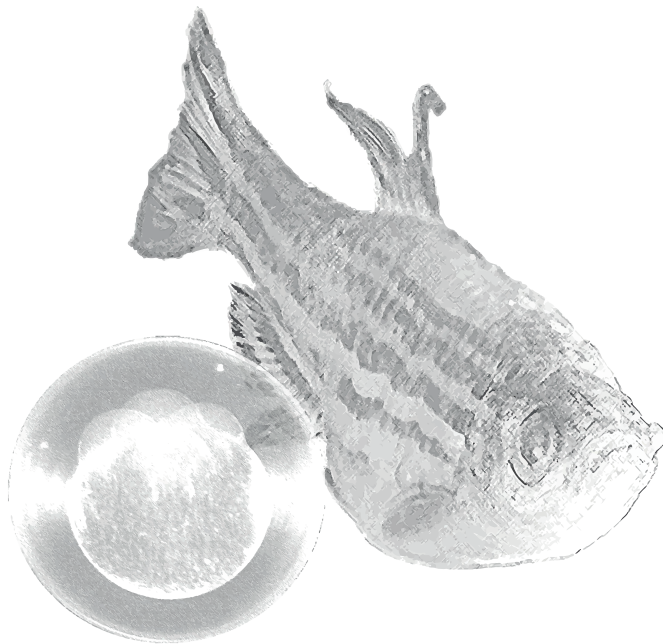
ACKNOWLEDGEMENTS

We wish to thank the members of the Zebrafish Facility at Wageningen University for providing help and taking care of the zebrafish. We thank Barae Jomaa for critical reading of the manuscript and Peter van Baarlen for his assistance with the Ingenuity analysis.

Chapter 3

Expression of the zebrafish cpz gene suggests a role in Wnt4a and Wnt4b initiated signaling

Maurijn Y. Kessels^{1,2}, Karen M. Léon-Kloosterziel², Taslima Nahar², Sander Kranenbarg², Stefan Schulte-Merker^{2,3}, Sacco C. de Vries¹, Johan L. van Leeuwen²



¹Laboratory of Biochemistry, Wageningen University, Wageningen, the Netherlands;

²Experimental Zoology Group, Wageningen University, Wageningen, the Netherlands;

³Hubrecht Institute-KNAW and University Medical Centre Utrecht, Utrecht, the Netherlands

ABSTRACT

Carboxypeptidase Z is an endopeptidase with implicated functions in Wnt signaling. Several studies in mammalian species have proposed a modulatory role for CPZ through proteolytic processing the C-terminus of Wnt proteins. The identification of this protein together with several other Wnt signaling components (Kessels et al., 2014) prompted the expression analysis of this peptidase. Expression detected by whole-mount in situ hybridization revealed *cpz* expression in and around ossified structures of juvenile zebrafish. This, and previous reports on the interactions with the Wnt4 protein in the mammalian skeleton, encouraged a more thorough inquiry of the developmental dynamics of zebrafish *cpz* expression, combined with analysis of two zebrafish *wnt4* orthologues (*wnt4a* and *wnt4b*). Temporal expression mapping traced *cpz* expression back to early zebrafish developmental stages and two *cpz* splice variants were identified of which one was maternally expressed. Spatial expression patterns showed a transient pattern during early development, becoming more restricted to different developmental structures after 14 hours of development. Expression of *cpz* partially coincided with *wnt4a* and *wnt4b* expression in structures such as the ventral fin fold, the developing brain and axial structures including the notochord and neural tube. During development, three different transient expression patterns were found in which (1) expression of *cpz* coincided with that of *wnt4*, (2) expression was observed in adjacent structures, (3) or the expression of *cpz* did not overlap with *wnt4*. Expression of zebrafish *cpz* is strikingly transient, expressed in multiple developing structures throughout development. The function of zebrafish Cpz remains to be identified, however based on these observations, we propose that zebrafish Cpz exerts a function in Wnt signaling in which proteolytic modification of Wnt proteins affects activation of the Wnt signaling pathway.

INTRODUCTION

The Wnt family of secreted signaling molecules has been shown to modulate cell proliferation, fate, and behavior, contributing to specify position and shape of cells in a variety of tissues and structures in both vertebrates and invertebrates (Cadigan and Nusse, 1997; Peifer and Polakis, 2000). In a previous publication we profiled the protein component of the extracellular matrix (ECM) of zebrafish bone and cartilage tissues during development (Kessels et al., 2014). Along with some of the main ECM components, this resulted in the identification of 9 proteins with an implicated function in the Wnt signaling network which is well established in cartilage and bone formation (Day et al., 2005a). The majority of identified Wnt pathway components consisted of antagonists of Wnt signaling, including the Dickkopf 1 protein and several members of the secreted Frizzled-related proteins. One of the secreted proteins however was previously described as an actively modifying enzyme of Wnt signaling proteins as employed in the β -dependent Wnt signaling pathway (Moeller et al., 2003; Wang et al., 2009). This protein, carboxypeptidase Z (Cpz), is the most recently discovered member of the metallo-carboxypeptidase family, a group of 13 zinc-containing exopeptidases that function by catalyzing the removal of C-terminal amino acids from proteins and peptides (Reznik and Fricker, 2001; Song and Fricker, 1997). Cpz is produced as an active enzyme and depends on its substrate specificity and site of secretion to prevent the cleavage of inappropriate substrates. Cpz is a unique member of the metallo-carboxypeptidase family in that it contains a cysteine-rich domain (CRD) N-terminal to the catalytic domain. With 20-30% sequence homology to the CRD present in the frizzled family of Wnt receptors, Cpz has been implicated as a modulator of Wnt signaling by cleaving the C-terminus of Wnt proteins with a clear preference for a C-terminal arginine (Novikova et al., 2001; Reznik and Fricker, 2001).

In vitro testing for potential substrates of CPZ using different Wnt proteins (i.e. WNT1, WNT3a and WNT4), showed a response only for WNT4, the only substrate used containing a C-terminal arginine (Moeller et al., 2003). The physical interactions between WNT4 and CPZ were also confirmed in the respective chicken as well as rat orthologues (Moeller et al., 2003; Wang et al., 2009). Additional experiments with CPZ in rat showed its ability to remove the C-terminal arginine from WNT4, inducing an increase in β -catenin dependent Wnt signal activation in chondrocytes. The Wnt4 protein is officially classified as a β -catenin independent ('non-canonical') protein but activation of the β -catenin dependent ('canonical') signaling pathways has also been shown. An example is the importance of Wnt4 in osteogenic differentiation in which it acts on the β -catenin independent signaling pathway (Chang et al., 2007), while during gonadal development Wnt4 is found activating β -catenin dependent Wnt signaling (Chassot et al., 2014; Li et al., 2013). In addition to these pathways, evidence also suggests that the translocation of β -catenin to the cell membrane is controlled by Wnt4, in which Wnt4 contributes to cell-cell interactions rather than the β -catenin dependent Wnt signaling pathway (Bernard et al., 2008). The cellular context seems essential for the output that is generated, in which combinations of ligand and receptor/co-receptor affects the activation of the different Wnt signaling branches (Grumolato et al., 2010; Mikels and Nusse, 2006).

Due to duplication of the *wnt4* gene during the teleost-specific whole-genome duplication (Nicol et al., 2012), the zebrafish possesses two *wnt4* paralogs; *wnt4a* and *wnt4b*. The

zebrafish Wnt4a protein is most closely related to that of mammalian Wnt4 based on amino acid composition. Wnt4a has a profound role during zebrafish development by partly controlling convergence and extension (CE) movements during gastrulation (Matsui et al., 2005), by rearranging epithelial cells via affecting cell-cell junctional adherence molecules (Choe et al., 2013) and during neuromuscular synapse formation (Strochlic et al., 2012) via β -catenin independent Wnt signaling. The Wnt4b protein is less well studied in zebrafish, though expression appears to be altered in the floor plate of several zebrafish mutants including *cyclops* (*cyc*), *floating head* (*flh*), *you-too* (*yot*), and *sonic you* (*syu*) (Liu et al., 2000). The actual function of Wnt4b in zebrafish remains unexplored. In Medaka, however, Wnt4b is described as essential in the segmental patterning of the vertebral column (Inohaya et al., 2010).

To date the *cpz* gene has not been described in zebrafish development. Therefore an extensive analysis of *cpz* expression was performed and compared to expression of the zebrafish orthologues of *wnt4*, *wnt4a* and *wnt4b*. The results show a complex expression pattern in which *cpz* overlapped predominantly with *wnt4a* during development in structures such as the brain region, the heart, the notochord and in the myosepta. Expression of *cpz* was observed in cell groups adjacent to *wnt4* expressing tissues (floor plate and neural tube), and in cell groups (cleithrum and pharyngeal teeth) without any detectable *wnt4* expression. *cpz* and *wnt4b* expression mainly coincided later in development in parts of the central nervous system (brain and neural tube).

MATERIALS AND METHODS

Ethic statement

Experiments were approved by the Wageningen University Animal Experiments Committee (protocol nr. 2012020.a and 2014125.c).

Animal maintenance

Zebrafish strains were reared at the fish facility of Wageningen at 27.1°C with a 14:10 light dark cycle. All fish were raised in a density of 5 fish/L. For the experiments, matings were set up with two males and three females. Eggs were kept at 28.5°C at the breeding facility, and transferred to the fish facility at 20 days post fertilization (dpf). All fish were fed *ad libitum* three times a day. Zebrafish larvae were fed in-house cultured *Paramecium* from 120 hours post fertilization (hpf). Between 10 and 60 dpf the fish were fed both *Paramecium* and *Artemia*, after which the *Paramecium* was exchanged for Tetramin flakes. Zebrafish were kept under standard conditions. For experiments the fish were euthanized with 0.1% (w/v) tricaine methane sulphonate (TMS, Crescent Research chemicals, USA) buffered with 0.08% (w/v) sodium bicarbonate (Gibco, Paisley, Scotland).

MS data analysis

Proteomics data obtained during previous work (Kessels et al., 2014) were assessed for Wnt-related proteins. MaxQuant software version 1.2.2.5 was used to analyze the raw files from the LTQ-Orbitrap as previously described (Kessels et al., 2014). MS/MS spectra were searched by comparison to the Uniprot zebrafish database downloaded from www.uniprot.org (2012), and a contaminant database including frequently observed contaminants such as human keratins and trypsin. Filtering was performed using the Perseus module (version 1.3.0.4). Reverse hits were removed from the data together with proteins with only 1 identified peptide, no unique peptide, or no unmodified peptide. Proteins with a described connection to Wnt signaling were used for further analysis (Supplemental Table S1-3). Normalized intensity values (LFQ intensity) were used for relative quantification. Database search and quantification results were grouped by combining results for the different replicates of the craniofacial, axial, and caudal fin region for each of the developmental stages.

For quantification purposes, the proteins were additionally filtered and selected for being detected in two or more out of each triplicate LC-MS/MS runs. Selected proteins were further analyzed using the Perseus module. Relative protein abundances were compared by performing a pair-wise t-test (both sides), with a permutation-based on FDR, threshold values of 0.05 or 0.01 and $S_0 = 1$, with 250 number of randomizations and $-\log_{10}$ as selected parameters. The obtained protein ratios were used to assess differences in protein abundance between the different developmental stages.

In situ mRNA hybridization

Spatial and temporal gene expression analysis of *cpz*, *wnt4a* and *wnt4b* was performed by in situ hybridization. Primers were designed using Primer 3 software (Rozen and Skaletsky, 2000) and extended with a T7, or Sp6 transcription initiation sequence on the reverse primer (Supplemental Table S4). cDNA obtained from zebrafish of 15 dpf was used to generate the specific coding sequences of all three genes (0.3-0.9 kb) by PCR, to be used as templates for the DIG labelling reaction. DIG-labelled probes were synthesized according to the manufacturer's instructions (Roche, DIG-labelling) and purified with the Qiagen RNeasy kit (Protocol RNA Cleanup). Zebrafish were euthanized and fixed overnight in 4% paraformaldehyde (PFA) in phosphate-buffered saline (PBS) at 4°C. After washing with PBS (2 x 5 min), fish were dehydrated in 100% methanol at RT (room temperature, 2 x 5 min) and stored at -20°C until further use. Whole-mount in situ hybridization were performed as described by Schulte-Merker (Schulte-Merker, 2002). In situ hybridization on sectioned material was performed as described by Kessels *et al.* (Kessels et al., 2014). For sectioning of zebrafish used for whole-mount in situ hybridization, glycerol was first removed by sequential washing (75%, 50% and 25% glycerol/PBS, 1x5 min), and washed in PBST (PBS + 0.1% v/v Tween 20, 3x5 min). Fish were embedded in 1.5% agar/5% sucrose and incubated overnight in 30% sucrose at 4°C. Embedded fish were frozen in liquid nitrogen and stored at -80°C. Longitudinal or transverse sections of 20 µm were made with a cryostat (Leica CM3050S) and transferred onto polylysine coated slides (Menzel-Gläser, Thermo scientific). Slides were stored in a box with silica gel at -20°C or, if used immediately, dried overnight at RT.

RNA isolation, cDNA synthesis and RT-PCR

For the reverse transcriptase PCR (RT-PCR) experiment, twenty-five zebrafish embryos (0, 1, 2, 4, 6, 8, 10, 12, 24, 48, and 96 hpf) or individual larvae (8 dpf, 15 dpf, 25 dpf and 30 dpf) were collected and euthanized. Total RNA was extracted with the Qiagen Rneasy kit according to the manufacturer's protocol (Qiagen). All samples were DNase treated with DNase I (Invitrogen, California, USA) and stored at -80°C. For RT-PCR, 1 µg of total RNA was reverse transcribed with SuperScript III (Invitrogen) according to the manufacturer's protocol. The RT-PCR reactions were performed using standard PCR using Taq polymerase (Promega) with the oligonucleotides listed in Supplemental Table S4. Samples were pre-denatured at 95°C for 5 min, followed by 40 cycles at 95°C for 5 sec, 60°C for 10 sec and 72°C for 10 sec. For the relative quantification of mRNA levels of the gene of interest (GOI), the housekeeping gene *β-actin* was used as an internal standard.

RESULTS

Cpz expression in the zebrafish skeletal extracellular matrix

Cpz was identified as one of the 262 extracellular proteins that were identified in the zebrafish skeletal ECM during the compositional analysis of the zebrafish skeleton (Kessels et al., 2014). Cpz was one of eight Wnt signaling-related proteins that displayed significant differences in abundance during skeletal development (Table 3.1, Supplemental Table 3.1-3.3). Among these proteins were several antagonists (secreted-frizzled related proteins and Wnt inhibitory protein Dickkopf), as well as proteins that are implicated in activation of Wnt signaling (Cthrc1a, Cthrc1b, Fibin) (Kawano and Kypta, 2003; Moeller et al., 2003; Wakahara et al., 2007; Wang et al., 2009; Yamamoto et al., 2008). The last protein, Cpz, attracted our attention because of its putative role in Wnt signaling through active processing of Wnt proteins (Moeller et al., 2003; Wang et al., 2009). In mammals, CPZ is secreted as an active peptidase and therefore believed to be secreted close to the region it exerts its biological function. Zebrafish *cpz* expression was therefore analyzed in juvenile zebrafish (28 dpf) using whole-mount in situ hybridization. Sections of juvenile zebrafish were used for hematoxylin and eosin staining to create a clear overview of the tissues present (Fig. 3.1A), and consecutive sections were used for in situ hybridization (Fig. 3.1B-D). This spatial expression analysis revealed *cpz* transcripts in the pharyngeal teeth and around several ossified structures, including the vertebral column and the fin rays suggesting a role for Cpz in the formation of mineralized tissues in zebrafish.

Characterization of zebrafish *cpz*

The zebrafish genome contains a single *cpz* gene expressed in the form of two splice variants: *cpz-001* (ENSDART00000147497) and *cpz-201* (ENSDART00000109165). Both splice variants encode a predicted N-terminal signal peptide, a cysteine-rich domain (CRD), and a catalytic carboxypeptidase domain. Like its mammalian orthologues the CRD of the

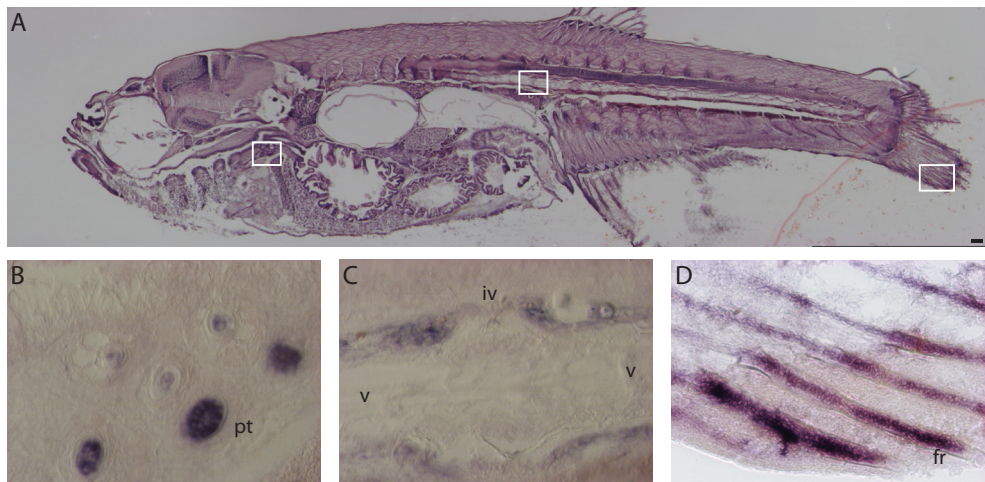


Figure 3.1. Spatial analysis of *cpz* expression in juvenile (28 dpf) zebrafish. Consecutive sections of juvenile zebrafish were used for (A) hematoxylin and eosin staining or (B-D) in situ hybridization using a *cpz* specific probe. Boxed areas in A correspond to the regions depicted for the in situ hybridization. Abbreviations: fr, fin rays; iv, intervertebral disc; pt, pharyngeal tooth; v, vertebra. Scale bars indicate 50 μ m.

Table 3.1. Differences in abundance of identified Wnt signaling-related proteins

Protein name	Gene name	Ratio 28/14	Ratio 358/28	Ratio 358/14	Accession No.	References
carboxypeptidase z	cpz	-1.50*	0.01	-1.48*	F1RCR9	Wang et al., 2009
dickkopf Wnt signaling pathway inhibitor 1a	dkk1a	-	-3.87**	-3.87**	F1RBK0	Kawano and Kypta, 2003
frizzled-related protein	frzb	-2.69**	1.04	-1.65*	Q9W6E0	Enomoto-Iwamoto et al., 2002
secreted frizzled-related protein 1a	sfrp1a	-0.93	-0.24	-1.18*	Q7T2K9	Wang et al., 2005a
secreted frizzled-related protein 1b	sfrp1b	-2.88**	0.44	-2.44**	A3KNP6	Wang et al., 2005a
collagen triple helix repeat containing 1a	cthr1a	-0.11	0.76	-0.86	Q6AXL0	Wakahara et al., 2007
collagen triple helix repeat containing 1b	cthr1b	-0.12	-1.35	-1.47*	F1QYB2	Wakahara et al., 2007
fin bud initiation factor a	finb	-0.68	-1.75**	-2.43**	A1IGX5	Yamamoto et al., 2008

Abundance ratios represent the differences between three developmental stages; 14 dpf, 28 dpf and 358 dpf. FDR = 0.05 (*) or FDR = 0.01 (**)

zebrafish *Cpz* proteins contain 10 conserved cysteine residues, as well as multiple amino acid residues important for substrate binding and catalytic activity (His245, Glu248, Arg320, His377, Gly469) (Fig. S3.1) (Moeller et al., 2003). The only differences between the predicted protein sequences of the splice variants are a 16 amino acid extension of the signal sequence and a 13 amino acid insertion in the carboxypeptidase domain in *cpz-201*. The functional significance of these insertions is not known. RT-PCR of the two *cpz* splice variants showed that predominantly *cpz-001* is maternally transferred and is constitutively

expressed throughout the complete assessed development sequence (Fig S3.2). In contrast, *cpz-201* expression remained almost undetectable up to 10 hours in development. After these 10 hours, *cpz-201* expression increased strongly up to day 4 after which a slight decrease was observed (Fig. S3.2). From here onward, no distinction is made between both splice variants that are collectively described as Cpz.

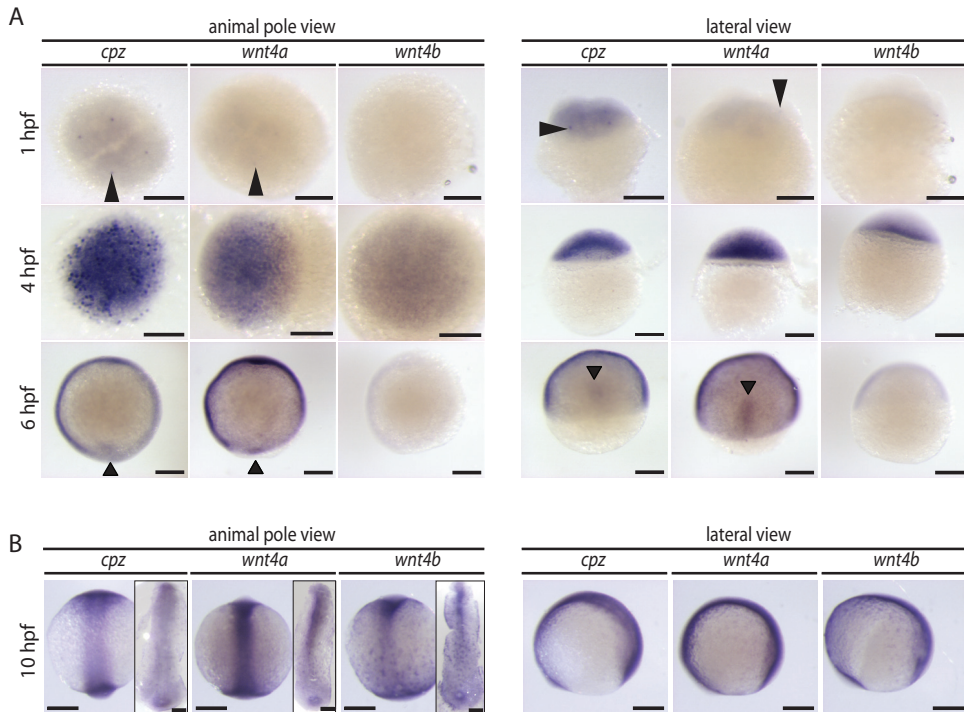


Figure 3.2. Spatial and temporal expression of zebrafish *cpz* during embryogenesis. (A-B) Whole-mount in situ hybridization using specific probes for *cpz*, *wnt4a*, or *wnt4b* to detect spatial expression at 1 hpf, 4 hpf, 6 hpf and 10 hpf. (B) Embryos of 10 hpf, used for in situ hybridization are depicted both as whole-mount and flat mount on the right side of the animal pole views. Views are depicted as indicated, in B anterior on the left. Scale bars indicate 200 μm.

After revealing *cpz* expression in and around ossified structures of juvenile zebrafish, a more thorough examination of the developmental dynamics of zebrafish *cpz* expression was performed. Analysis of *cpz* expression was combined with analysis of two zebrafish *wnt4* isoforms (*wnt4a* and *wnt4b*), based on previous reported interactions of WNT4 and CPZ in mammals (Wang et al., 2009). Transcripts of *cpz* were detected as early as one hour post fertilization (1 hpf), confirming the indicated maternal transfer as detected by RT-PCR analysis. At 1 hpf, *cpz* transcripts were observed as a punctate spot present in each cell (Fig. 3.2A). At sphere stage (4 hpf), *cpz* transcripts were detected in a large number of cells with clear differences in intensity. Transcripts of *wnt4a* but not *wnt4b* were also detected at 1 hpf, overlapping with *cpz* transcripts in the similar punctate spots (Fig. 3.2A). The expression of *wnt4b* was surprisingly not observed before 4 hpf using whole-mount in situ hybridization analysis, while it was detected as maternally transferred using RT PCR analysis (Fig. S3.2) in agreement with previous data (Lu et al., 2011).

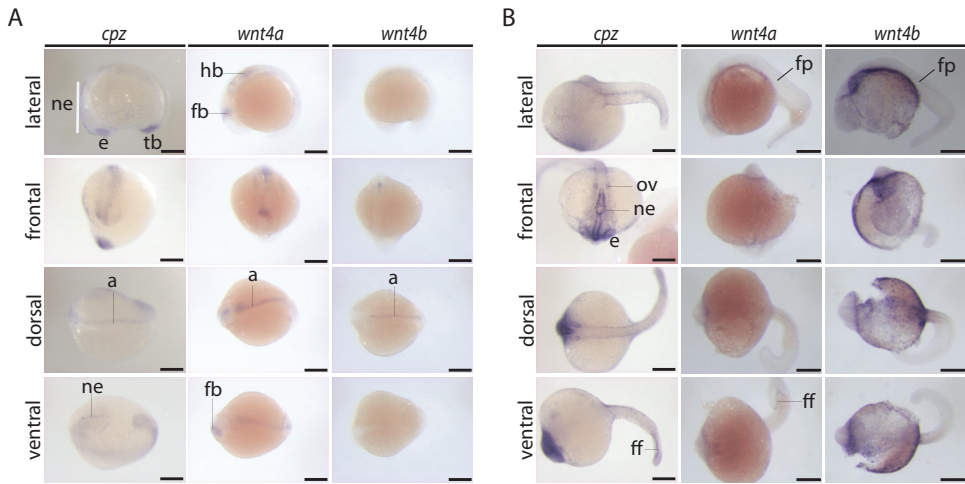


Figure 3.3. Expression of zebrafish *cpz* during embryogenesis. (A-B) Whole-mount in situ hybridization using specific probes for *cpz*, *wnt4a*, or *wnt4b* to detect spatial expression in (A) 14 hpf and (B) 20 hpf embryos. Views are depicted as indicated. Abbreviations: a, axis; e, eye anlagen; fb, forebrain; ff, fin fold; hb, hindbrain; ne, neural epithelium; ov, otic vesicle; tb, tail bud. Scale bars indicate 200 μ m.

During somite stages (14 hpf), *cpz* expression was observed in cells of the eye anlage, the developing tail bud, in neural epithelial cells in the brain region, and in the axis (Fig. 3.3A). At this stage, expression of *wnt4a* was restricted to the forebrain, the hindbrain and the axis of embryos, and notably absent in the eye anlage and tail bud. The expression of *wnt4b* was only observed in the axis. At 20 hpf, *cpz* expression remained evident in the neural epithelial cells, by now surrounding the developing brain ventricles (Fig. 3.3B). Expression of *cpz* was observed in the developing otic vesicles, and the ventral tail fin fold (Fig. 3.3B). Coinciding expression patterns of *wnt4a* and *cpz* were found in the ventral fin fold. Additional *wnt4a* expression was detected in floor plate while *wnt4b* expression was restricted to the floor plate only.

In situ hybridization at 1 dpf revealed expression patterns of *cpz* and *wnt4* genes in adjacent axial structures rather than in the same structures, except for the forebrain region and the midbrain-hindbrain boundary region in which *cpz* expression coincided with that of *wnt4b* (Fig. 3.4A-F). Expression of *cpz* in the axis was observed in the hypochord, while expression of *wnt4a* and *wnt4b* was located in the floor plate, and *wnt4b* additionally in the anterior notochord. Transcripts of *cpz* were also detected in the developing eyes. At 2 dpf, *cpz* expression was found diffusely in the brain region, the posterior part of the notochord, the developing cleithrum and pectoral fins, as well as in the region of the developing heart (Fig. 3.4G-L). Also at this stage, *wnt4a* overlap was observed in several structures such as the brain, the notochord, the developing heart and the pectoral fins. Interestingly, *wnt4a* and *cpz* expression coincided in the pectoral fin ridge while *wnt4b* was more diffusely expressed in the complete pectoral fin. No overlap was observed in the floor plate in which both *wnt4a* and *wnt4b* were expressed. At 6 dpf, *cpz* expression was found in the brain region, the pharyngeal teeth, the swim bladder, the posterior neural tube, in the anterior vertical and

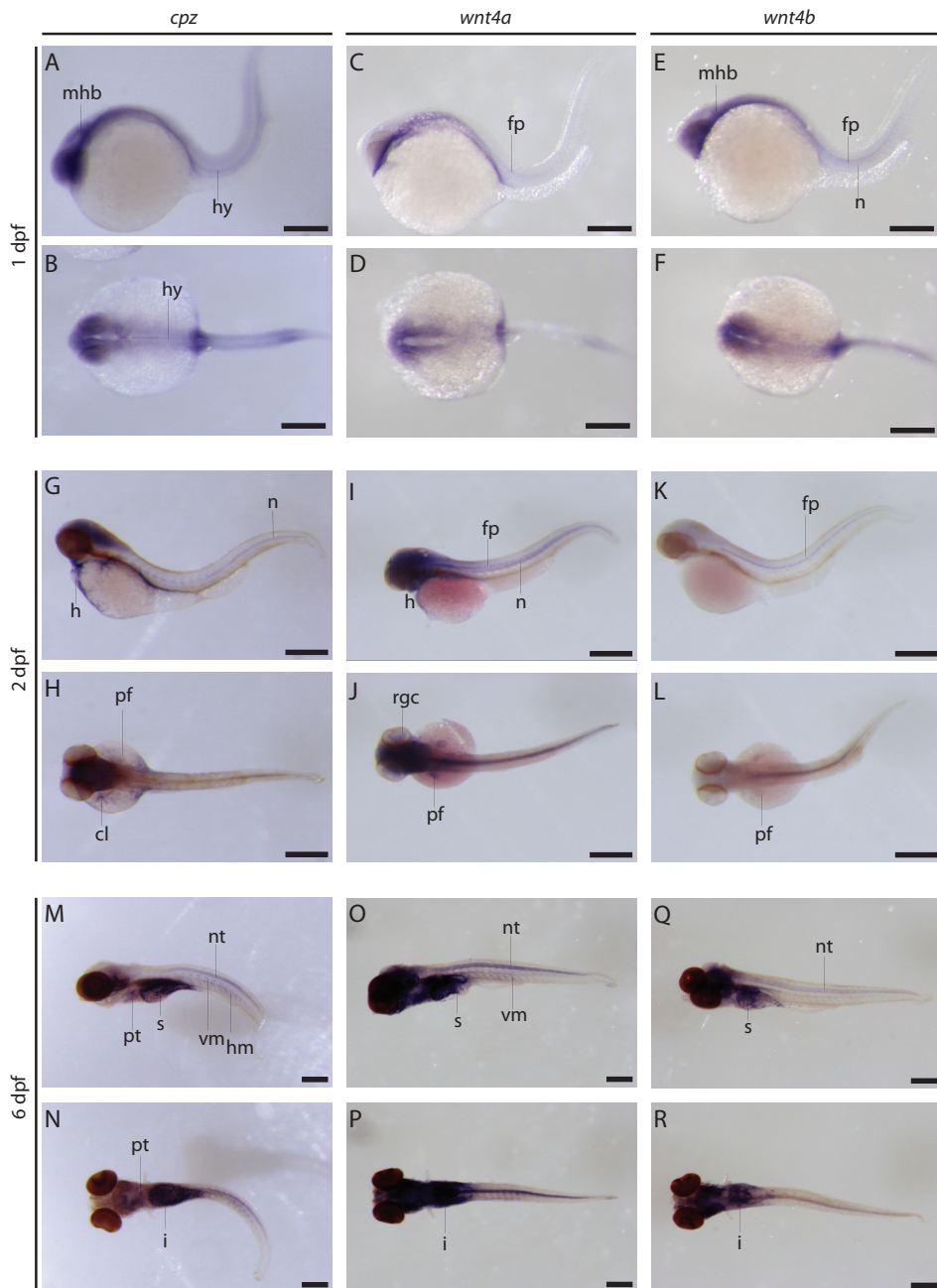


Figure 3.4. Expression of zebrafish *cpz* during larval stages. Whole-mount in situ hybridization using specific probes for *cpz*, *wnt4a*, or *wnt4b* to detect spatial expression in 1 dpf, 2 dpf and 6 dpf embryos. Embryos of all three stages are depicted in a lateral view (top) and dorsal view (bottom). Abbreviations: cl, cleithrum; fp, floor plate; h, heart; hy, hypochord; hm, horizontal myoseptum; mhb, midbrain-hindbrain boundary region; n, notochord; nt, neural tube; pf, pectoral fin; pt, pharyngeal tooth; rgc, retinal ganglion cells; vm, vertical myoseptum. Scale bars indicate 200 μ m.

horizontal myosepta and the intestine (Fig. 3.4M-R). The expression of both *wnt4a* and *wnt4b* overlapped with that of *cpz* in the brain region, the swim bladder and the intestine. In the neural tube, *cpz* expression was distinctive along the length of the axis. In the posterior part, *cpz* was expressed within neural tube tissue, while more anteriorly the expression was located in cells surrounding the neural tube. Both *wnt4a* and *wnt4b* were found within the neural tube only. Additional *wnt4a* expression, but not *wnt4b* was found in vertical myosepta. In summary, transcripts of *cpz* and *wnt4a* were detected in the same cells as early as 1 hpf, indicating a function early in development. During subsequent developmental stages, *cpz* and *wnt4* expression revealed three patterns in which (Fig. 3.5) expression of *cpz* and *wnt4* either overlapped, was observed in spatially adjacent structures, or where expression of *cpz* was restricted to certain cell groups without any immediately adjacent expression of *wnt4*.

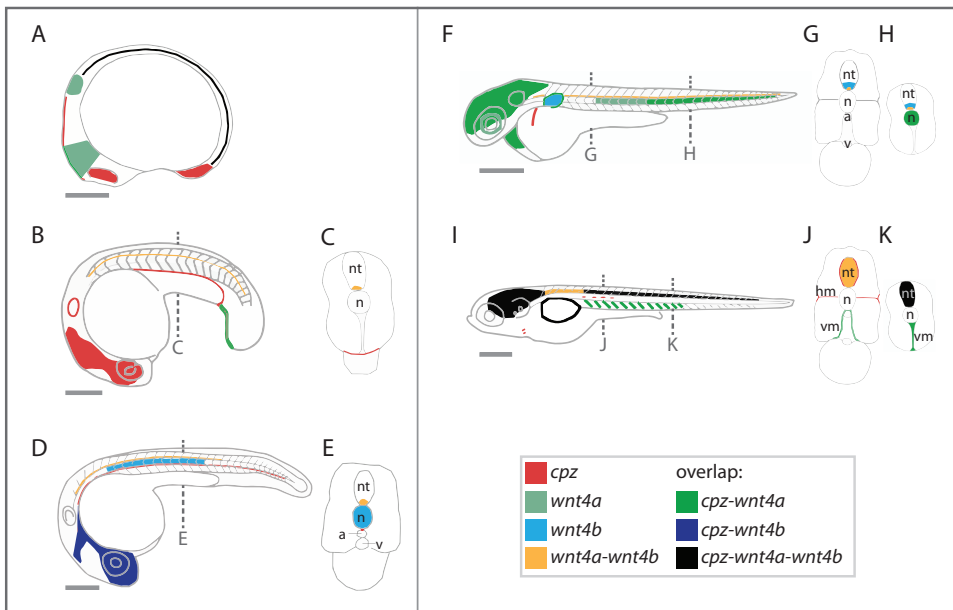


Figure 3.5. Schematic representation of spatial expression of *cpz*, *wnt4a* and *wnt4b* during development. Spatial expression as identified by whole-mount in situ hybridization was marked at (A) 14 hpf, (B-C) 20 hpf, (D-F) 1 dpf, (G-I) 2 dpf and (J-L) 6 dpf. Color combinations are indicated in the legend. Abbreviations: a, aorta; hm, horizontal myoseptum; n, notochord; nt, neural tube; v, vein; vm, vertical myoseptum.

DISCUSSION

Proteomics analysis of the zebrafish skeletal ECM resulted in the identification of 8 components of the Wnt signaling pathway. One of these, Cpz, has not previously been implicated in zebrafish skeletogenesis and was therefore analyzed in more detail. Gene expression analysis using in situ mRNA hybridization revealed expression of *cpz* in cells engaged in forming mineralized structures of the skeleton and the dentary of juvenile zebrafish. Since this is the first description of Cpz in teleosts, *cpz* expression was analyzed throughout development and compared with that of *wnt4a* and *wnt4b*, the two zebrafish isoforms of the proposed Cpz substrate in other vertebrates (Moeller et al., 2003; Wang et al., 2009). This analysis revealed a complex spatiotemporal *cpz* expression pattern, which compared with *wnt4* gene expression in three different temporal and spatially distinct patterns.

The substrate preference of Cpz has been studied in several vertebrate species (Novikova et al., 2001; Song and Fricker, 1997; Wang et al., 2009). In all described cases, Cpz was able to proteolytically cleave C-terminal basic amino acids, with a clear preference for a C-terminal arginine. Based on its amino acid sequence, zebrafish Wnt4a shows high sequence homology with Wnt4 of other vertebrate species. In addition, Wnt4a is the only Wnt protein in zebrafish that contains a C-terminal arginine. Expression analysis places both *wnt4a* and *cpz* in early zebrafish embryonic development. Both are detected throughout the gastrulation process and throughout the here examined developmental stages. Wnt4a as a protein has been described to function in activation of both β -catenin dependent and independent Wnt signaling (Choe et al., 2013; Ramachandran et al., 2011). Recent findings however showed the involvement of Wnt4a in the regulation of CE movements during zebrafish gastrulation, acting via β -catenin independent Wnt signaling (Matsui et al., 2005). The possibility of a function for Cpz in β -catenin independent Wnt signaling is a unconventional concept since existing studies have focused mainly on β -catenin dependent Wnt signaling (Moeller et al., 2003; Wang et al., 2009). In contrast to the arginine in Wnt4a, the zebrafish Wnt4b protein contains a C-terminal glutamic acid, making it a less likely candidate for processing by Cpz. Zebrafish Wnt4b has not yet been implicated in either branch of Wnt signaling pathways but a role in skeletogenesis has been described in the teleost species Medaka (Inohaya et al., 2010).

For both *wnt4a* and *wnt4b*, the early spatial and temporal expression patterns showed a partial overlap with that of *cpz* in several tissues, implicating that the same cells produce the substrate and the modifying protease. This suggests that both the substrate and the protease are produced in the same cells in these tissues with a possible modification due to simultaneous expression or expression separated in time (i.e. first *cpz*, followed by *wnt4*). In contrast, our data also shows instances in which there is no coincidence between the Wnt4 producing cells and the cells that express *cpz*. This introduces the possibility of divergent functions of the Wnt4 protein depending on proteolytic processing, or the ability of Cpz to affect migration of the Wnt protein. In turn, the latter option may create high levels of normally diffusing Wnt proteins in a certain region or prevent Wnt proteins to diffuse out of a specific region or tissue. Finally, *cpz* expression as seen in the cleithrum and tail bud occurs without any nearby *wnt4* expression. Despite the absence of *wnt4*, the expression of Wnt mediators such as transcription factor 7 (*tcf7*) in the cleithrum emphasizes that Wnt signaling is playing a role in the development of these structures (Veien et al., 2005).

Provided that the failure to detect *wnt4* transcripts is not due to detection limitations, this might suggest the possibility of Cpz substrates other than Wnt4.

The extensive expression of *cpz* during zebrafish development was not completely unexpected since it correlates with expression patterns observed in other vertebrate species. In mouse embryos, *Cpz* expression is identified in similar tissues throughout development, including the brain, cell lining the brain ventricles, the intestine and even the connective tissue in the ribs (Reznik and Fricker, 2001). Together with high conservation in amino acid residues observed in the functional domains, this indicates that Cpz function might be comparable among different vertebrate species. The use of zebrafish in this study proved beneficial, since the *ex utero* development of embryos permitted gene expression analysis through in situ hybridization to be performed with relative ease. Also, the use of zebrafish allows for the generation of transgenic lines. The expression of a specific fluorophore under the *cpz* promoter could give full advantage of the optical clarity of the zebrafish embryos in order to study rapid changes in the transient *cpz* expression patterns.

For now, the exact role of zebrafish Cpz in the entirety of the complex interconnected Wnt signaling network remains elusive. We provide however a first glimpse in the extensive and transient expression pattern of *cpz* during development which, like in embryonic development of mammalian species, suggests an important function throughout the vertebrate developmental program. This provides a foundation for future experiments on biochemical properties as well as the biological function of Cpz.

SUPPLEMENTAL DATA

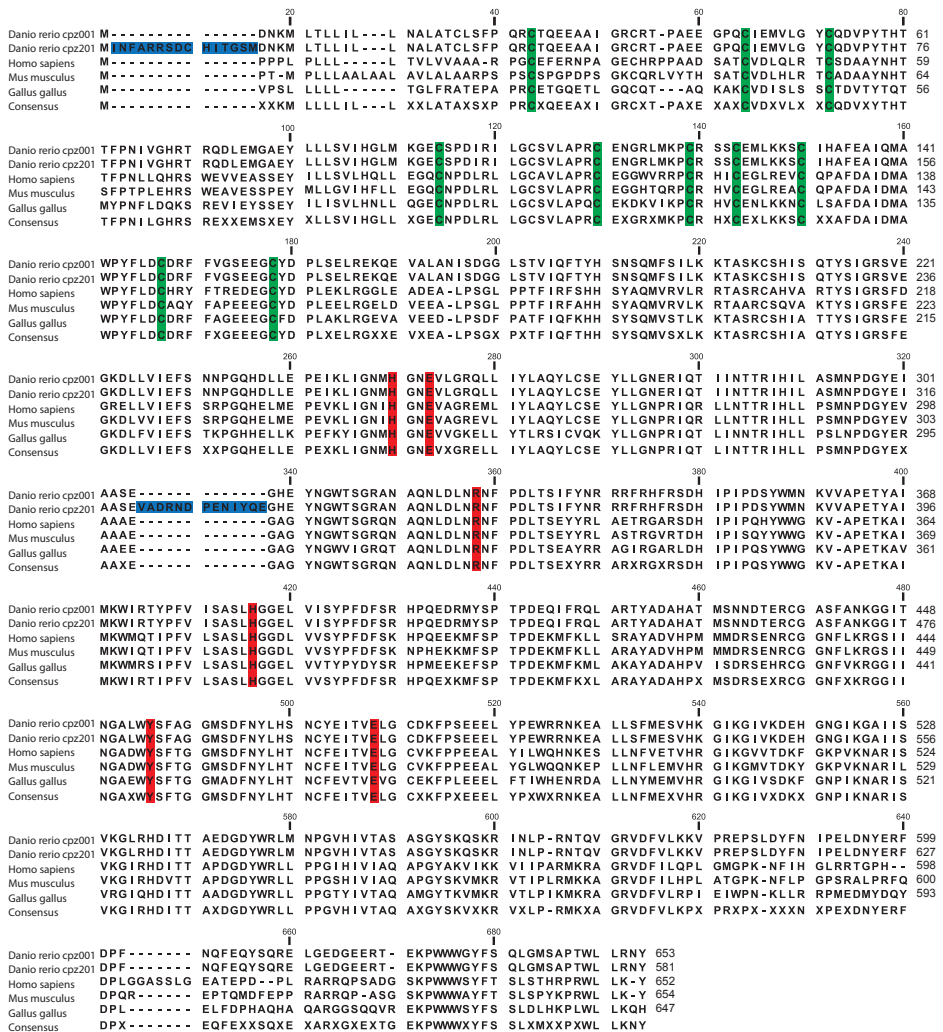


Figure S3.1. Multiple alignment of the predicted zebrafish Cpz proteins and Cpz orthologues of other vertebrate species. Predicted additional amino acids in the zebrafish splice-variants of cpz are indicated in blue. The conserved cysteine residues of the predicted cysteine-rich-domain (CRD) are marked by green boxes. Residues with functions in catalytic activity or substrate binding are marked by red boxes.

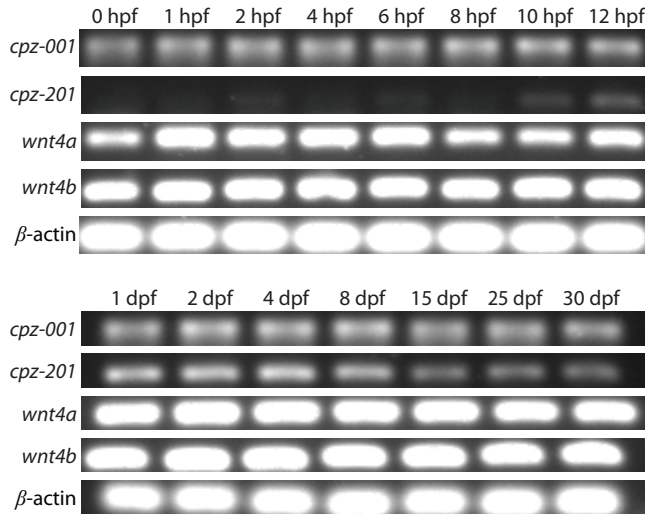


Figure S3.2. RT-PCR analysis of *cpz-001*, *cpz-201*, *wnt4a* and *wnt4b* expression during zebrafish development. RT-PCR analysis performed on cDNA from total embryo RNA extracted from twenty-five zebrafish embryos (0, 1, 2, 4, 6, 8, 10 and 12 hpf, as well as 1, 2, and 4 dpf) or individual larvae (8 dpf, 15 dpf, 25 dpf and 30 dpf). Standard loading was indicated by β -actin expression.

Supplemental Table S3.1. "Protein groups" table as obtained for Wnt-related proteins

id	Protein IDs	total			14 dpf peptides		
		Peptides	Unique Peptides	iBAQ	head region 1	head region 2	head region 3
1168	O42248	9	9	1083100	9	9	4
847	F1QJG6	6	6	1899300	0	0	0
1216	Q1LXD2	6	6	12599000	6	4	6
1667	Q9W6E0	6	6	14561000	1	1	2
1134	F1RBK0	5	5	10760000	0	0	0
1140	F1RCR9	5	5	726540	0	2	1
11	A1IGX5	4	3	1165400	0	0	0
49	A3KNP6	4	4	2245800	0	0	1
1545	Q7T2K9	2	2	492340	0	0	0
987	F1QYB2	4	4	6156800	2	1	1
664	Q6AXL0	3	3	4113000	1	1	1
28 dpf peptides							
id	Protein IDs	head region 1	head region 2	head region 3	axial skeleton 1	axial skeleton 2	axial skeleton 3
1168	O42248	2	5	3	1	1	2
847	F1QJG6	1	0	0	1	1	1
1216	Q1LXD2	0	2	1	0	0	0
1667	Q9W6E0	4	4	4	3	4	4
1134	F1RBK0	0	0	0	0	0	0
1140	F1RCR9	2	3	3	3	4	3
11	A1IGX5	1	0	1	2	2	3
49	A3KNP6	3	2	2	3	3	2
1545	Q7T2K9	2	2	1	2	2	2
987	F1QYB2	3	2	4	3	3	2
664	Q6AXL0	3	3	2	2	1	1
358 dpf peptides							
id	Protein IDs	head region 1	head region 2	head region 3	axial skeleton 1	axial skeleton 2	axial skeleton 3
1168	O42248	0	0	0	0	1	0
847	F1QJG6	0	0	0	1	0	0
1216	Q1LXD2	0	0	0	0	0	1
1667	Q9W6E0	4	2	3	4	1	3
1134	F1RBK0	4	3	3	4	4	4
1140	F1RCR9	2	2	2	2	5	3
11	A1IGX5	2	2	2	3	2	4
49	A3KNP6	1	2	2	3	4	3
1545	Q7T2K9	1	2	2	2	2	2
987	F1QYB2	3	4	3	3	3	3
664	Q6AXL0	3	3	3	1	2	1

Supplemental Table S3.1. Continued

	14 dpf peptides			14 dpf LFQ intensity			
Protein IDs	axial skeleton 1	axial skeleton 2	axial skeleton 3	head region 1	head region 2	head region 3	axial skeleton 1
O42248	0	0	0	1983500	17029000	1665500	0
F1QJG6	6	5	5	0	0	0	1349900
Q1LXD2	4	5	5	7390900	7441000	5429900	4322400
Q9W6E0	3	1	1	0	0	1042200	995350
F1RBK0	0	0	0	0	0	0	0
F1RCR9	2	3	1	0	178760	0	192210
A1IGX5	1	0	0	0	0	0	0
A3KNP6	0	0	1	0	0	0	0
Q7T2K9	2	1	2	0	0	0	88901
F1QYB2	3	3	2	744740	0	0	716990
Q6AXL0	2	2	2	0	0	0	409450
	28 dpf peptides		28 dpf LFQ intensity				
Protein IDs	caudal fin 1	caudal fin 2	head region 1	head region 2	head region 3	axial skeleton 1	axial skeleton 2
O42248	0	0	356250	306180	471400	0	0
F1QJG6	0	0	0	0	0	0	0
Q1LXD2	0	0	0	800810	0	0	0
Q9W6E0	4	4	10262000	2726600	5429900	8533400	4276600
F1RBK0	0	0	0	0	0	0	0
F1RCR9	4	3	210340	337710	197500	1022100	767720
A1IGX5	3	3	0	0	0	125130	0
A3KNP6	3	3	775630	710640	501290	756010	1245100
Q7T2K9	2	2	133610	88583	0	69629	57816
F1QYB2	2	2	2431100	0	1458400	662790	431620
Q6AXL0	1	1	955860	736060	835530	0	0
	358 dpf peptides			358 dpf LFQ intensity			
Protein IDs	caudal fin 1	caudal fin 2	caudal fin 3	head region 1	head region 2	head region 3	axial skeleton 1
O42248	0	0	1	0	0	0	0
F1QJG6	0	0	0	0	0	0	0
Q1LXD2	0	0	0	0	0	0	0
Q9W6E0	0	3	3	13094000	0	7625500	14543000
F1RBK0	2	2	3	4978600	5418100	4672700	20886000
F1RCR9	4	3	3	406600	444550	239120	514820
A1IGX5	4	4	4	533770	186480	117800	650970
A3KNP6	3	2	2	0	946220	1036300	483480
Q7T2K9	0	2	2	0	232170	153660	163050
F1QYB2	4	3	4	1034700	2440100	1256400	4042300
Q6AXL0	2	3	1	1986400	2222600	1669700	0

Supplemental Table S3.1. Continued

	14 dpf LFQ intensity		14 dpf iBAQ				
Protein IDs	axial skeleton 2	axial skeleton 3	head region 1	head region 2	head region 3	axial skeleton 1	axial skeleton 2
O42248	0	0	212570	544690	103760	0	0
F1QJG6	897070	2610800	0	0	0	426980	197780
Q1LXD2	7119200	10957000	961250	748810	445230	789810	1018100
Q9W6E0	0	0	11241	10990	11983	118070	39229
F1RBK0	0	0	0	0	0	0	0
F1RCR9	247450	0	0	3360.5	888.67	17606	21026
A1IGX5	0	0	0	0	0	6761.2	0
A3KNP6	0	0	0	0	9957.9	0	0
Q7T2K9	0	121640	0	0	0	24404	7449.8
F1QYB2	524290	660550	86679	11095	5692.4	153280	74703
Q6AXL0	521570	633040	15696	22329	9772.9	35265	25499
	28 dpf LFQ intensity			28 dpf iBAQ			
Protein IDs	axial skeleton 3	caudal fin 1	caudal fin 2	head region 1	head region 2	head region 3	axial skeleton 1
O42248	202290	0	0	40912	80505	44784	13465
F1QJG6	0	0	0	10614	0	0	32665
Q1LXD2	0	0	0	0	55792	4606.3	0
Q9W6E0	2524500	2401000	2592800	814620	259000	324520	421270
F1RBK0	0	0	0	0	0	0	0
F1RCR9	742740	2148700	1883000	12054	23628	10192	39345
A1IGX5	100570	248270	237940	14206	0	1223.2	15890
A3KNP6	775620	454910	764920	96163	85365	48172	86345
Q7T2K9	91321	107070	140380	18278	10117	1404	5617.8
F1QYB2	0	0	0	408880	286850	244580	158120
Q6AXL0	0	0	0	303520	224820	179730	111460
	358 dpf LFQ intensity					358 dpf iBAQ	
Protein IDs	axial skeleton 2	axial skeleton 3	caudal fin 1	caudal fin 2	caudal fin 3	head region 1	head region 2
O42248	0	0	0	0	0	0	0
F1QJG6	0	0	0	0	0	0	0
Q1LXD2	0	0	0	0	0	0	0
Q9W6E0	0	5349100	0	1917700	3844100	1284200	333450
F1RBK0	3567200	16779000	2289600	3269200	2994200	473780	1468100
F1RCR9	695500	433190	167540	342940	369570	10608	38492
A1IGX5	165870	304190	1503800	375820	405500	46599	49640
A3KNP6	742890	1228200	689810	1902500	1160100	9105.1	131460
Q7T2K9	128580	166520	0	404060	443790	510.73	56904
F1QYB2	1702200	5968100	2384200	1584000	1440700	136040	393870
Q6AXL0	2715200	0	3959900	1352700	0	205950	547020

Supplemental Table S3.1. Continued

	14 dpf iBAQ							
Protein IDs	axial skeleton 3							
O42248	0							
F1QJG6	1159600							
Q1LXD2	8541100							
Q9W6E0	44759							
F1RBK0	0							
F1RCR9	13014							
A1IGX5	0							
A3KNP6	13951							
Q7T2K9	67674							
F1QYB2	153270							
Q6AXL0	100350							
	28 dpf iBAQ							
Protein IDs	axial skeleton 2	axial skeleton 3	caudal fin 1	caudal fin 2				
O42248	2210	23089	0	0				
F1QJG6	29153	25837	0	0				
Q1LXD2	0	0	0	0				
Q9W6E0	593460	724780	324080	310860				
F1RBK0	0	0	0	0				
F1RCR9	46485	44961	82435	64879				
A1IGX5	9924.1	25894	44675	45485				
A3KNP6	244610	119750	40248	71359				
Q7T2K9	5498.3	15465	9570.6	15760				
F1QYB2	130970	129310	108910	107580				
Q6AXL0	92657	85680	75201	62460				
	358 dpf iBAQ							
Protein IDs	head region 3	axial skeleton 1	axial skeleton 2	axial skeleton 3	caudal fin 1	caudal fin 2	caudal fin 3	
O42248	0	0	3987.5	0	0	0	13082	
F1QJG6	0	16754	0	0	0	0	0	
Q1LXD2	0	0	0	34704	0	0	0	
Q9W6E0	2088500	3475400	223000	2249200	0	458440	439530	
F1RBK0	1227700	2371600	1125500	2634500	371060	561810	525630	
F1RCR9	13626	28215	109480	37844	61289	22866	24239	
A1IGX5	19773	76199	33227	82871	507110	86254	99667	
A3KNP6	173920	55130	144510	224250	309270	227650	154610	
Q7T2K9	32480	24619	28011	30222	0	104920	33441	
F1QYB2	380000	490280	298350	831270	856630	329340	381120	
Q6AXL0	531790	38797	307530	50269	757330	306200	23683	

- Provided id in Supplemental Table 3.1 correspond with identified peptides as described in Kessels et al., 2014, Supplemental Table 2.2.

Supplemental Table S3.3. Differential protein abundance

Protein IDs	gene name	Log Protein Abundance Ratios 28dpf/14dpf	-log t-test p value	Significant	Log iBAQ intensity
Q7T2K9	sfrp1a	-0.93	0.95		4.02
A3KNP6	sfrp1b	-2.88	13.10	**	4.77
F1QJG6	sfrp5	1.58	1.30	*	4.92
Q9W6E0	frzb	-2.69	2.73	**	5.05
Q1LXD2	ck2b	3.35	4.36	**	5.59
F1RBK0	dkk1a	-	-	-	-
A1IGX5	fibin	-0.68	0.84		3.95
O42248	gnb2l1	0.12	0.04		4.68
F1RCR9	cpz	-1.50	1.74	*	4.14
F1QYB2	cthrclb	-0.12	0.05		4.99
Q6AXL0	cthrcla	-0.11	0.04		4.79
Protein IDs	gene name	Log Protein Abundance Ratios 358dpf/28dpf	-log t-test p value	Significant	Log iBAQ intensity
Q7T2K9	sfrp1a	-0.24	0.20		4.03
A3KNP6	sfrp1b	0.44	0.41		4.96
F1QJG6	sfrp5	0	0		4.33
Q9W6E0	frzb	1.04	0.61		5.86
Q1LXD2	ck2b	0.48	0.47		4.32
F1RBK0	dkk1a	-3.87	10.32	**	6.13
A1IGX5	fibin	-1.75	2.52	**	4.35
O42248	gnb2l1	1.67	1.99	**	4.23
F1RCR9	cpz	0.01	0.04		4.43
F1QYB2	cthrclb	-1.35	1.18		5.44
Q6AXL0	cthrcla	-0.76	0.35		5.22
Protein IDs	gene name	Log Protein Abundance Ratios 358dpf/14dpf	-log t-test p value	Significant	Log iBAQ intensity
Q7T2K9	sfrp1a	-1.18	1.20	*	4.26
A3KNP6	sfrp1b	-2.44	3.25	**	4.71
F1QJG6	sfrp5	1.58	1.30	*	5.30
Q9W6E0	frzb	-1.65	0.83	*	5.22
Q1LXD2	ck2b	3.83	13.96	**	5.84
F1RBK0	dkk1a	-3.87	10.32	**	6.13
A1IGX5	fibin	-2.43	8.70	**	4.54
O42248	gnb2l1	1.79	1.28	*	4.92
F1RCR9	cpz	-1.48	1.76	*	4.18
F1QYB2	cthrclb	-1.47	1.45		5.18
Q6AXL0	cthrcla	-0.86	0.43	*	4.92

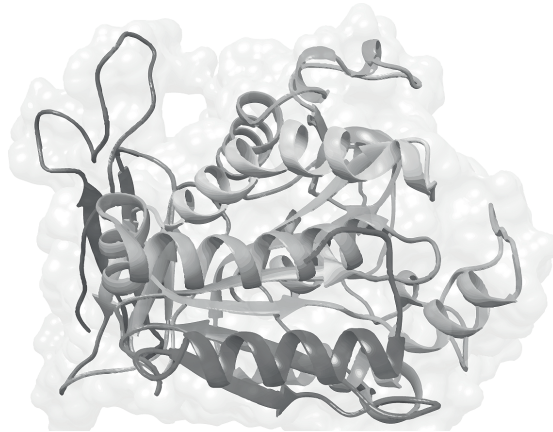
Supplemental Table S3.4. Primer sequences

ISH probes	
Primer name	Sequences
drT7CPZfw1	5'-TAATTACGACTCACTATAGGAAGATGCAGAACACCTG-3'
drSp6CPZrv1	5'-ATTTAGGTGACACTATAGAAGATGGATGTGAGGTCAG-3'
drT7Wnt4Afw1	5'-TAATTACGACTCACTATAGGGGCGAGTGTATAGC-3'
drSp6Wnt4aArv1	5'-ATTTAGGTGACACTATAGAGTCATCGTGACACAGAATC-3'
drT7Wnt4Bfw1	5'-TAATTACGACTCACTATACACACCTGCCGAG-3'
drSp6Wnt4Brv1	5'-ATTTAGGTGACACTATAGAGTTTAATGCTAATGCCTCA-3'
RT-PCR	
Primer name	Sequences
Cpz001 fw	5'-GCCGCTTCTGAGGGTCAT-3'
Cpz001 rev	5'-GAAGTTGCGGTTTCAGATCAAG-3'
Cpz201 fw	5'-ATAGGAACGACCCCGAAAAC-3'
Cpz201 rev	5'-GAAGTTGCGGTTTCAGATCAAG-3'
Wnt4a fw	5'-GAACGCGGAGAAAAGTCAAC-3'
Wnt4a rev	5'-TCAAGCAGCATCACAGGAAC-3'
Wnt4b fw	5'-GAAAGAGCGAAAGGGATGTC-3'
Wnt4b rev	5'-CCGAAACACCATGACACTTG-3'
b-actin fw	5'-CGAGCAGGAGATGGGAACC-3'
b-actin rev	5'-CAACGGAAACGCTCATTGC-3'

Chapter 4

Loss of CPZ affects calcium signaling during zebrafish development

Maurijn Y. Kessels^{1,2}, Karen M. Léon-Kloosterziel², Sander Kranenbarg², Sacco C. de Vries¹, Johan L. van Leeuwen², Stefan Schulte-Merker^{2,3}



¹Laboratory of Biochemistry, Wageningen University, Wageningen, the Netherlands;

²Experimental Zoology Group, Wageningen University, Wageningen, the Netherlands;

³Hubrecht Institute-KNAW and University Medical Centre Utrecht, Utrecht, the Netherlands

ABSTRACT

Carboxypeptidase Z (Cpz) is a metallo-carboxypeptidase which removes carboxyl-terminal basic amino acid residues, particularly arginine residues, from specific proteins. During the analysis of *cpz* expression in zebrafish, a broad and transient expression pattern was identified which, similar to *Cpz* expression during mammalian development, embryonic development of mammalian species, suggests an important function throughout the vertebrate developmental program. With data presently available concerning biochemical properties of CPZ in mammals, a loss-of-function analysis of Cpz remained absent. Here, TALEN-mediated mutagenesis was employed to determine the effect on zebrafish development upon loss-of-function of the Cpz protein function in zebrafish. Zebrafish mutants were generated containing a frame shift mutation in the first exon of the *cpz* gene. Offspring of zebrafish *cpz* mutants displayed a wide range of different phenotypes during early development. These phenotypes include defective cell adhesion resulting in separation of the blastoderm during early cleavage stages, defective dorsal structure development, convergence extension movement defects resulting in microcephaly, shortening of the anterior-posterior axis and undulating notochords, degeneration of the central nervous system, defects in heart development and swim bladder development. In addition, high lethality rates later (5-8 days post fertilization) in development were detected. Except for some uncommon phenotypes (e.g. over-inflation of the swim bladder), most phenotypes were clearly linked to described effects in disruptions of the Wnt/planar cell polarity and the Wnt/Calcium pathway branches, for the first time linking Cpz to β -catenin independent Wnt signaling.

INTRODUCTION

In chapter 3 we described the identification of the Cpz protein in the extracellular matrix of the zebrafish skeleton. The expression pattern of the encoding gene suggested a role in multiple developmental stages most likely linked to the Wnt signaling pathway. Since the discovery of Cpz two decades ago (Song and Fricker, 1997), multiple studies have contributed to unravelling the biochemical properties of Cpz (Moeller et al., 2003; Song and Fricker, 1997; Wang et al., 2009). Cpz is a metallocarboxypeptidase and differs from all other family members in that it is located in the extracellular matrix. Cpz cleaves synthetic peptides at a pH optimum of 7-8, with K_m values of approximately 2 mM and has a clear preference for C-terminal arginines (Reznik and Fricker, 2001). The replacement of the alanine in synthetic substrates (dansyl-phenylalanine-alanine-arginine and dansyl-proline-alanine-arginine) by either a glycine or phenylalanine led to a 10-fold decrease in Cpz activity, while peptides substituted with an isoleucine or proline remained completely unprocessed. Enzymatic activity of Cpz is, as expected for a metallocarboxypeptidase, strongly inhibited by chelating agents such as EDTA. However, serine protease inhibitors and most cysteine protease inhibitors do not affect Cpz activity (Reznik and Fricker, 2001).

The Wnt gene family can be mechanistically grouped based on their signaling functions and the effects they exert during overexpression studies. The hallmark of the β -catenin dependent ('canonical') Wnt signaling pathway, is the accumulation and the translocation of β -catenin into the nucleus. This class of Wnt proteins comprises the majority of Wnt proteins, including Wnt1, Wnt2, Wnt3, Wnt3a, and Wnt-8 (Miller, 2002). β -Catenin dependent Wnt signaling plays an important role in cell fate decisions during early embryogenesis as indicated by overexpression experiments of *wnt1* and *wnt8* that induce hyper-dorsalization and ectopic axis formation in *Xenopus* and zebrafish embryos (Larabell et al., 1997; Nasevicius et al., 1998). The β -catenin independent ('noncanonical') Wnt signaling pathway can be viewed as a complex network with different cellular outputs. Stimulation can trigger functions in coordinated cell migration through regulation of planar cell polarity (PCP) and the release of calcium (Ca^{2+}).

The Wnt/ Ca^{2+} pathway was identified by findings that Wnt signaling components can stimulate intracellular Ca^{2+} release from the endoplasmic reticulum in a G-proteins dependent manner (Kohn and Moon, 2005). Demonstration of Ca^{2+} waves in embryos during gastrulation implicated an important role for Ca^{2+} in early pattern formation (Creton et al., 1998; Wallingford et al., 2001). Wnt4, Wnt5 and Wnt11 are capable to induce intracellular Ca^{2+} release, without affecting β -catenin stabilization (Kuhl et al., 2000). Ca^{2+} release by overexpression of *Xenopus wnt5a* in zebrafish embryos appeared to rescue the effects observed during *wnt1* or *wnt8* overexpression (i.g. hyper-dorsalization, ectopic axis formation). This antagonistic effect on β -catenin dependent signaling was reproduced by overexpression of the ligand-activated serotonin receptor (Slusarski et al., 1997b), concurrently showing that the rescue effects were mediated by Ca^{2+} release downstream of Wnt receptor-ligand interactions. The overlap of the Wnt/ Ca^{2+} and the Wnt/PCP pathways was suggested after identifying PCP-specific components modulating both cell movements and stimulate Ca^{2+} release in zebrafish (Veeman et al., 2003). Misexpression of *wnt5* and *wnt4* alter the morphogenetic movements in zebrafish (Slusarski et al., 1997b; Ungar et al.,

1995) and defects in convergence and extension (CE) movements during gastrulation are observed in genetic mutations of *Wnt5* and *Wnt11* (Heisenberg et al., 2000; Kilian et al., 2003). Wnt proteins that regulate β -catenin independent Wnt signaling therefore appear to have dual roles. On the one hand they modulate Ca^{2+} release and cell movements, on the other hand they act as antagonists towards β -catenin dependent signaling.

Expression of *Cpz* has been identified as widespread during vertebrate embryonic development of several species (Moeller et al., 2003; Reznik and Fricker, 2001), including the zebrafish (chapter 3). The function of CPZ during development however remains elusive. To date, the effect of *cpz* gene knock-out has not been reported. In this study, a *cpz* mutant was generated using transcription activator-like effector nucleases (TALEN)-mediated mutagenesis, creating a null allele that lacks both functional domains (e.g. cysteine rich domain and peptidase domain) due to a frame shift in exon 1. Homozygote and heterozygote mutant embryos revealed multiple morphological defects, including hyper-dorsalization of embryos. Other phenotypic phenomena such as heart defects also copied phenotypic traits observed by inhibition of Ca^{2+} signaling. Together, these observations for a first time implicate *Cpz* as a component of the β -catenin independent Wnt signaling pathway.

MATERIALS AND METHODS

Ethical statement

The performed experiments were approved by the Wageningen University Animal Experiments Committee (protocol nr. 2014125.c).

Animal maintenance

Zebrafish were reared at the fish facility of Wageningen or the fish facility of the Hubrecht Institute (Utrecht) at 27.1°C using standard conditions. Eggs were collected by mating two males with three females. Eggs were kept at 28.5°C at the breeding facility, and transferred to the fish facility at 20 days post fertilization (dpf). For the experimental use of fish, fish were euthanized with 0.1% (w/v) tricaine methane sulphonate (TMS, Crescent Research chemicals, USA) buffered with 0.08% (w/v) sodium bicarbonate (Gibco, Paisley, Scotland).

TALEN mediated mutagenesis

Information on the zebrafish *cpz* gene (ENSDARG00000075521) was obtained from the Ensembl Genome Browser (<http://ensembl.org>). TALEN sequences were identified in candidate genes using TAL Effector Nucleotide Targeter 2.0 (<https://tale-nt.cac.cornell.edu/>). The TALEN target site was designed to target exon 1 of the zebrafish *cpz* gene, which encodes the signal peptide and part of the cysteine-rich domain of *Cpz* (Fig. 4.1D). TALEN-mediated genome editing for the generation of the *cpz* mutant was performed as described (Bedell et al., 2012; van Impel et al., 2014). The TALEN binding sites in *cpz* exon 1 were: TAL1, 5'-T TAATACTTCTGAACG-3'; TAL2, 5'-TGAGCTTCCACAGCGA-3'.

Genotyping

For genotyping purposes, genomic DNA was extracted from complete larvae or from fin clips of juveniles or adults as described (Meeker et al., 2007). PCR primers amplifying an ~300 bp fragment were designed in exon 1 (5'-ACAGTGGGTCCCAGACACAG-3'), and in the adjacent intron (5'-TTGCTGCAACTGAATGAATG-3'). The insertion-deletion mutation was confirmed by gel electrophoresis on a 2% w/v agarose gel (Fig. 4.1C).

Acridine orange vital staining

To detect cell death, embryos were dechorionated and soaked in egg water containing 2 µg/ml acridine orange at 28°C for 30 minutes. After washing with egg water eight times 5 minutes each, embryos were anesthetized with tricaine, and examined by stereomicroscopy.

RESULTS

TALEN mediated targeting of the zebrafish *cpz* gene

The zebrafish *cpz* gene is located on chromosome 1 and consists of 11 exons. The *cpz* gene produces two splice-variants (*cpz-001* and *cpz-201*) which differ in the size of the N-terminal signal peptide and the length of exon 5 (difference of 39 base pairs) (Fig. 4.1A). Two TALEN target sites were designed in exon 1 of zebrafish *cpz* to produce a mutant locus. A *cpz* frame shift mutation was generated by a 33 base pair deletion in combination with a single base pair insertion (Fig. 4.1B). Wild type, heterozygote (*cpz*^{+/-}) and homozygote mutants (*cpz*^{-/-}) were genotyped by PCR (Fig. 4.1C). The insertion-deletion mutation resulted in a frame shift leading to a predicted premature stop codon after 101 and 116 amino acids in Cpz-001 and Cpz-201, respectively. In addition, the frame shift is predicted to result in a defective cysteine-rich domain leading to the premature stop codon. The mutation is therefore expected to constitute a loss-of-function mutation due to the loss of the complete protein, except for a fragment of the signal peptide (Fig. 4.1D).

Zebrafish (founders) that contained the described frame shift mutation in the *cpz* gene after TALEN mRNA injections were outcrossed to wild type zebrafish to generate F1 parents. Heterozygous parents were identified via PCR analysis and used to create an F2 population. Heterozygous and homozygous parent combinations produced viable offspring up to the development of different phenotypic phenomena. Wild type, heterozygote and homozygote fish of the F3 generation were identified after genotyping and used for phenotyping purposes (Supplementary Figure S4.1).

Offspring from heterozygote *cpz* mutant parents display cell-adhesion defects

Embryos produced by *cpz* carrier parents (*cpz*^{+/-} and *cpz*^{-/-}) develop a wide range of developmental anomalies. Unexpectedly, the first detectable developmental defect was observed in embryos produced by heterozygote (*cpz*^{+/-}) parents primarily (Table 4.1). Embryos from heterozygote parents displayed different graduations of cell adhesion defects

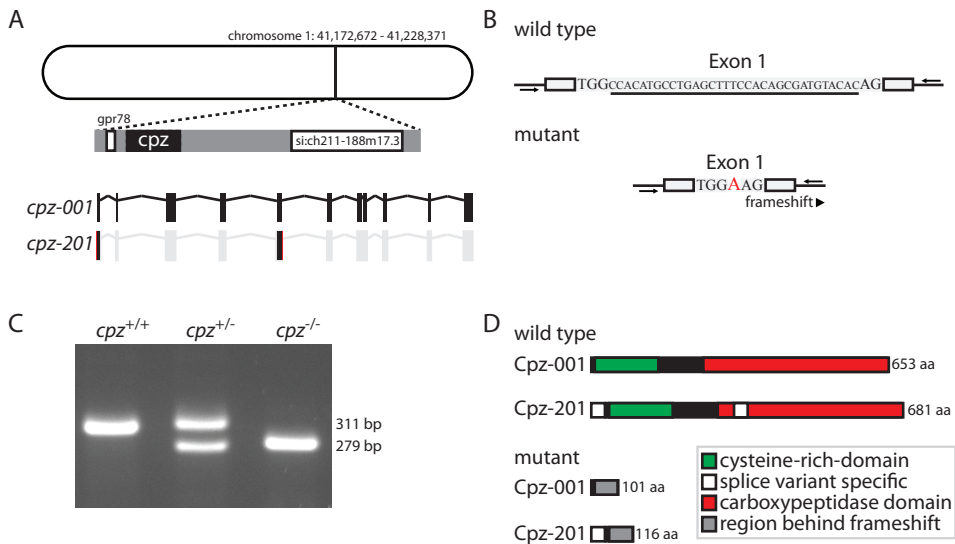


Figure 4.1. TALEN-mediated mutagenesis of the zebrafish *cpz* gene. (A) Genomic location of the zebrafish *cpz* gene on chromosome 1. The gene is comprised of 11 exons and transcribed as two splice-variants with minor differences in exon 1 and exon 5. (B) TALENs were designed to target exon 1 of zebrafish *cpz* resulting in a 33 basepair deletion (underlined) and a single base pair insertion (red). Primers used for genotyping in C are indicated (arrows). (C) Genotyping on genomic DNA isolated from fin clips allowed for clear distinctions between wild type, heterozygous and homozygous genotypes. (D) Schematic representation of the predicted wild type and mutant zebrafish Cpz proteins. Predicted domains are color indicated as described.

(Fig. 4.2). In more severely affected embryos, cells often remained separated from each other during cleavage stages. Cells retained a more rounded shape which can indicate loss of the adhesiveness of the cell membranes. This phenotype showed similarities with the maternal effect mutation *nebel* (Pelegrini et al., 1999). In contrast to the *nebel* mutation in which embryos from homozygote females are affected, offspring of *cpz* heterozygous females (*cpz*^{+/-}) but not homozygous (*cpz*^{-/-}) females showed cell-adhesion defects. In affected embryos, the defective cell adhesion resulted in a separation of the cleavage stage blastoderm into two halves (Fig. 4.2E,I). Both halves underwent development separately, resulting in the formation of the anterior axis by only one of the halves (Fig. 4.2F-H). This phenotype is reminiscent of the phenotype described for the maternal effect mutation *janus* (Abdelilah and Driever, 1997). But in contrast to the described *janus* mutation, the blastoderm of *cpz* mutant eggs in most cases fused before the gastrulation stage (Fig. 4.2J-L). Whether zygotic *cpz* expression is responsible for this phenomena is not yet determined.

The resulting body shape in affected embryos often appeared less elongated. The truncation of the body axis is morphologically consistent with a general reduction of convergence-extension movements during gastrulation (Hammerschmidt et al., 1996). Severely affected embryos that survived up to gastrulation typically died before 24–36 hours post fertilization. These findings indicate that maternally deposited *cpz* mRNA plays a role in cell adhesion during early zebrafish cleavage stages. This defect suggests a dose-dependent function of Cpz during early cleavage stages since the effect was observed in eggs produced by *cpz*^{+/-}

but not *cpz*^{-/-} females. Surprisingly, the here described defects appeared non-linear and were only observed in embryos produced by *cpz*^{+/-} females. Also, a variable phenotypic penetrance was observed within this group in which only 45% of the embryos appeared to be affected (Table 4.1).

Figure 4.2. Offspring of heterozygous *cpz* mutant parents develop cell adhesion defects. Early developmental stages of (A-D) wild type and (E-L) mutant embryos from heterozygous parents. E-H, I-L both depict one embryo throughout development (E,I) Separation between two blastodermal halves at 16-cell stage resulting in (F,G) separate development of the two halves and (H) shortened and severely misshaped embryos or (J, H) fusion of the two halves before gastrulation stages (L) partially restoring embryo phenotypes to wild type.

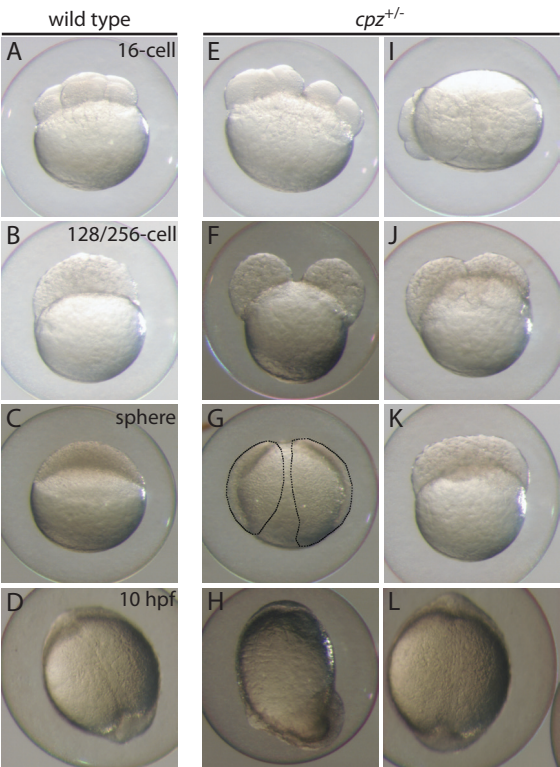
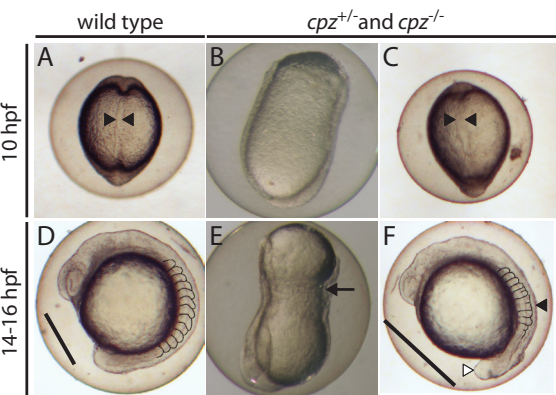


Figure 4.3. Altered levels of *cpz* affect gastrulation. Bright field images of (A,D) wild type embryos and (B-C,E-F) heterozygous and homozygous embryos. (C-D) Mutant embryos appear oblong and display notochord defects compared to the wild type situation (black arrowheads in A and C). (E) Mutant embryos display failure in patterning in which the notochord (arrow) develops in a dorsal-ventral direction. (F) Convergence extension movement defects affect the extension of the anterior-posterior axis as indicated by the black bar in wild type (D) and mutant (F) embryos which additionally display fusion of somites (black arrowhead in F) and early dissociation of the tail bud (white arrowhead).



Offspring of *cpz* mutant parents display gastrulation defects

By the end of epiboly (~10 hours post fertilization), embryos from mutant parents (*cpz*^{+/-} and *cpz*^{-/-}) developed an oblong phenotype and contained an irregular-shaped notochord. During consecutive stages these embryos developed irregular, in some cases fused somites and displayed early separation of the tail bud (Fig. 4.3C-F). Eventually, these morphological defects resulted in different gradations of hyper-dorsalization defects similar to those described by Mullins *et al.* (Mullins *et al.*, 1996). The most severely dorsalized embryos contained a tail structure which curled over their trunk (*snail-house-like*; Fig. 4.4B) or a shortened, twisted trunk axis (*piggy-tail-like*; Fig. 4.4C). Mildly dorsalized *cpz* mutant embryos showed posteriorly shortened body axes and a defective under developed ventral fin fold (Fig. 4.4D). The dorsalization defects appeared in offspring of both *cpz*^{+/-} (8.3%) and *cpz*^{-/-} (11.8%), but was still observed in only a fraction of the embryos.

Other phenotypical traits such as microcephaly, and undulating notochords (Fig. 4.4E-F), copied phenotypical traits observed in defective CE movements (Kilian *et al.*, 2003; Matsui *et al.*, 2005). Overall, these morphological phenotypes suggest a disturbance of normal

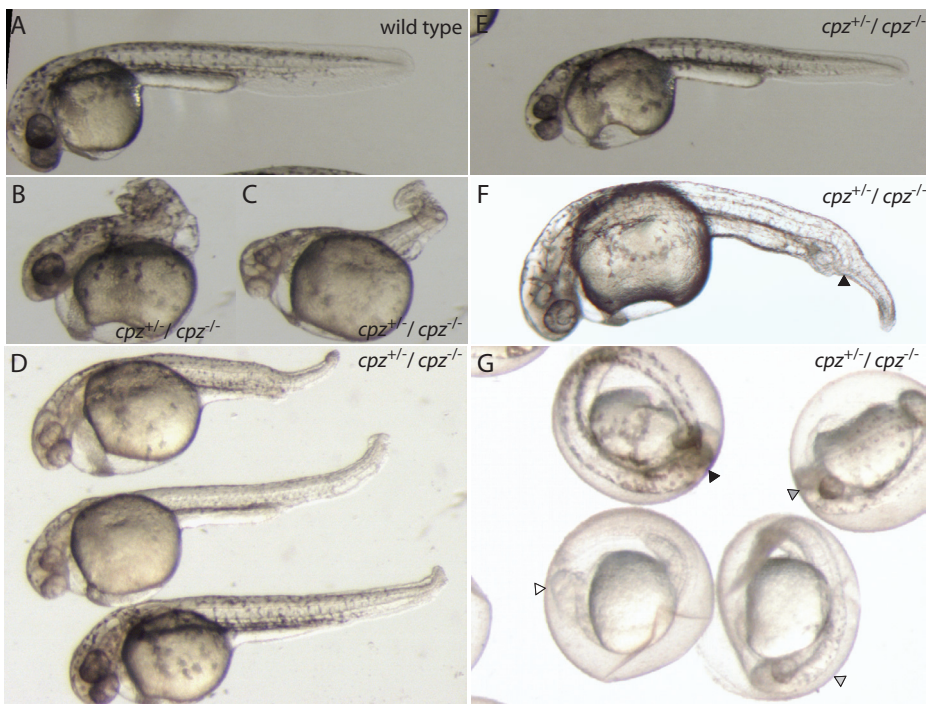


Figure 4.4. Altered levels of *Cpz* affects dorsal-ventral patterning and convergence extension movements. Morphology of wild type (A) and heterozygous and homozygous embryos (B-F) exhibiting different degrees of dorsalization defects. (B-C) Extreme phenotypes displayed severe tail defects, (D) while milder phenotypes mainly showed defects in fin fold development. Compared to wild type, mutant embryos displayed late CE movement-linked phenotypes including (E) microcephaly (F) and undulating notochords (arrowhead in F). (G) Overview of *cpz* mutant embryos at 2 dpf. Normal developing embryos (black arrowhead) and different stages of delayed developmental phenotypes (white-gray arrow heads) appear in embryos from the same clutch.

embryonic cell movements and in dorsoventral patterning. A yet unexplained phenomena observed in offspring from mutant parents ($cpz^{+/-}$ and $cpz^{-/-}$) was the developmental delay observed in embryos after 48 hours of development (Fig. 4.4G). The differences were clearly visible by the reduced level of pigmentation and some of the embryo still displayed similar phenotypic traits observed in 1 day old embryos (Fig. 4.4G). Embryos displaying this developmental arrest typically died within the next 24 hours of development.

Absence of maternal and zygotic *cpz* affects neural development

After 24 hours of development, a fraction (n=11) of $cpz^{-/-}$ mutant embryos developed severe defects resulting in general neural degeneration (Fig. 4.5). The neural phenotype was found similar to previously characterized class IV defects as described by Furutani-Seiki *et al.* (Furutani-Seiki *et al.*, 1996). Acridine orange staining of wild type and apparently unaffected $cpz^{+/-}$ and $cpz^{-/-}$ embryos revealed cell death of distinct single cells mainly in the region of the developing olfactory epithelium in the anterior head region and neural tube (Fig. 4.5A-B). In affected $cpz^{-/-}$ embryos ubiquitous cell degeneration was observed throughout the complete hindbrain and neural tube (Fig. 4.5C-D). Observed cell death was however restricted to these neural tissue while other tissues including the notochord and somites appeared normal. Complete neural degeneration resulted in an upwardly bent body axis and proved lethal within 24-48 hours post fertilization. These observations indicate that complete absence of Cpz can affect the early formation of the central nervous system, but the number of affected embryos remained low.

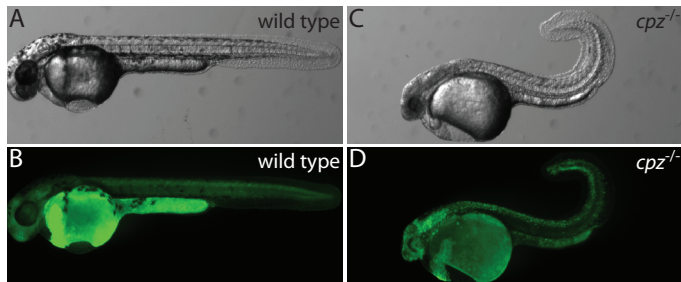


Figure 4.5. Homozygous *cpz* mutant embryos develop neural degeneration. (A-B) Wild type embryo bright field and acridine orange staining. (C-D) Homozygote *cpz* mutant embryo displaying extreme curvature of the body axis resulting from degeneration of the hindbrain and neural tube as visualized by acridine orange staining (green).

cpz mutant embryos display heart deformations

After 48 hours post fertilization embryos of $cpz^{+/-}$ (10.8%) and $cpz^{-/-}$ (20.1%) parents developed heart deformations (Fig. 4.6). Although the atrium and ventricle were formed, the heart remained small and did either not function correctly or not at all. The heart was stretched in a longitudinal direction and was surrounded by profound pericardial edema (Fig. 4.6C-D). In less severe cases, the heart morphology appeared similar to that of wild type embryos. In these milder phenotypes, functioning of the heart was defective with back and forward pumping of blood cells. Embryos that developed heart defects typically died within 72 hours post fertilization.

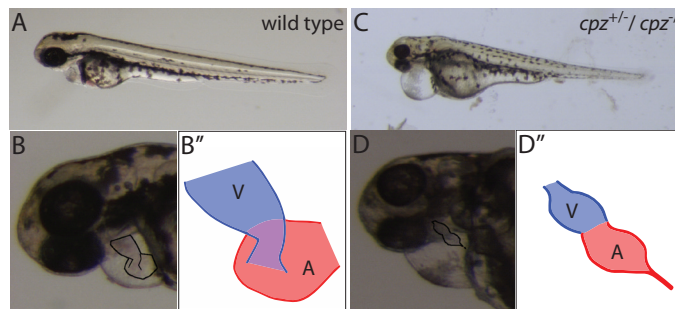


Figure 4.6. Altered levels of *Cpz* results in heart deformations. (A-B) Wild type heart shape at 2 dpf. (C-D) Heart phenotype in heterozygous and homozygous embryos at 2 dpf. The heart remained small and appeared stretched in a longitudinal direction. Representation of the (B'') wild type and (D'') heart phenotype. of A, atrium; V, ventricle.

***cpz* mutant embryos display defective swim bladder development and encounter high late lethality rates**

Both *cpz*^{+/-} (3.9%) and *cpz*^{-/-} (5.9%) mutant embryos displayed failure in swim bladder development in which the swim bladder was missing in some embryos (Fig. 4.7B) but mainly did develop to extreme proportions (Fig. 4.7C). The expansion might be a result of over-inflation of gas, but could also be a result of an increase in swim bladder primordium. Larvae with over-inflated swim bladders became trapped at the surface due to their increased buoyancy and died typically around 5-7 dpf.

Large numbers of embryos that did develop normal sized and functional swim bladders did not survive to later developmental stages (5-8 dpf) due to development of several other phenotypic features. Related or not to the above described neural defects, many zebrafish larvae did not display normal feeding behavior around 5 days post fertilization. Instead of active swimming, larvae floated around in the water column or lay on the bottom. During short resurgences, these larvae proved that swimming itself was not impaired. An abnormal downward bending of the axis starting behind the head region (Fig 4.7D) probably contributed to swimming difficulties, and also strongly impaired intake of food. These severe morphological defects proved lethal in subsequent stages most likely due to starvation. For now it is unclear whether the morphological defects originate from the reduced or absent prior feeding behavior, defective development of the intestinal tract (in which *cpz* is expressed as well, chapter 3) or yet another reason. The range of observed phenotypes observed in *cpz* mutant embryos shows that *Cpz* is involved in a number of key processes during zebrafish development.

Incidence of *cpz* mutant phenotypes

The quantitative analysis of the here described phenotypes revealed a number of defects common to both homozygous *cpz*^{-/-} and heterozygous *cpz*^{+/-} embryos, albeit at different penetrance: e.g. the observed penetrance reached a two-fold increase in the number of *cpz*^{-/-} embryos compared to *cpz*^{+/-} embryos (Table 4.1). Whether the phenotypes that become evident later in development could be traced back to earlier defects, remains unclear. The

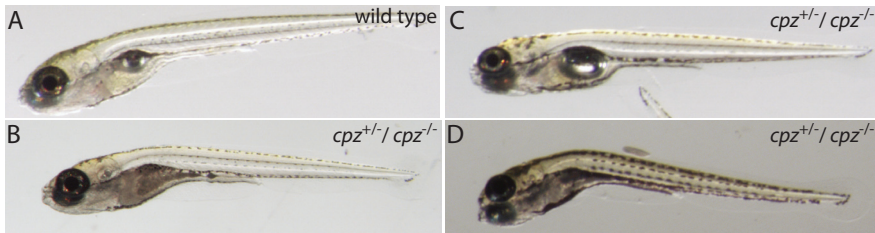


Figure 4.7. Altered levels of Cpz results in developmental defects. Bright field images depicting (A) wild type embryos, (C) embryos missing a swim bladder or (D) the observed over-inflation phenotype. (E) Large numbers of embryos developed an extreme curvature of their axis and remained thin.

identification of common defects in offspring of both *cpz*^{+/-} and *cpz*^{-/-} females reveals that these defects were not a result of the absence of maternally deposited *cpz* mRNA or Cpz protein. A possible exception to this is notion are the observed defects in neural development which were only observed in offspring from *cpz*^{-/-} females. This finding is best explained by a requirement for maternally provided *cpz* mRNA or Cpz protein, even though formally a lower requirement for Cpz during neural development is also a possibility.

Strangely, defective cell adhesion during early cleavage stages was mainly observed in offspring of *cpz*^{+/-} mothers. The early nature of these defects suggest a function of *cpz* as a maternal effect gene. This is supported by preliminary experiments in which crossings of *cpz*^{+/-} females with wild type males and vice versa (*cpz*^{+/-} male with wildtype females) led to the described cell adhesion defects only in offspring of *cpz*^{+/-} females (data not shown). Early lethality due to failure in egg activation was considered but this notion was excluded since *cpz*^{-/-} parents produce partially viable offspring and the offspring of *cpz*^{+/-} parents developed with the expected Mendelian ratios. There is the possibility that phenotypic phenomena are modulated by genetic background of an inbred strain in which the mutation is maintained (Sanders and Whitlock, 2003). This is not unusual and could be addressed in future experiments by an out-cross to a different wild type background.

Taken together, *cpz* mutants display a wide range of both early and late morphological defects, apparent from 1 hour to stages exceeding 5 days post fertilization. Interestingly, a subpopulation of heterozygous and homozygous *cpz* mutants appeared completely unaffected and develop into fertile adults, arguing for different dose requirements for *cpz* during development.

Table 4.1. Quantitative analysis of *cpz* mutant phenotypes

genotype	+/+ F2		-/- F2		+/- F2	
date parent generation	09-05-2014	03-12-2013	09-05-2014	03-12-2013	09-05-2014	03-12-2013
total	427	315	353	309	195	278
unfertilized	139	82	184	104	62	51
blastoderm separation	0	0	1	0	56	106
	0%		0%		45%	
dorsalization	0	0	40	4	1	29
	0%		12%		8%	
neural degeneration	0	0	11	0	0	0
	0%		3%		0%	
heart defects	0	0	23	56	11	28
	0%		21%		11%	
swim bladder defects	0	0	15	7	9	5
	0%		6%		4%	
normal 5 dpf	270	214	79	138	56	59
	92%		58%		32%	
normal 20 dpf	245	195	18	15	14	8

percentages are based on the initial total of fertilized eggs per parental genotype

DISCUSSION

The metalloprotease Cpz processes specific proteins through proteolytic cleaving of carboxyl-terminal basic amino acid residues. After identification of the Cpz protein in the developing skeletal extracellular matrix (chapter 2), the analysis of *cpz* expression during zebrafish development revealed an extensive and transient pattern partially overlapping with that of zebrafish *wnt4* genes (chapter 3). The presence of a cysteine-rich domain, the localization in the extracellular matrix and the overlap of *cpz* expression during development with *wnt4* genes suggests that Cpz may function as a Wnt-binding and processing protein. Indeed, modulation of the WNT4 protein by CPZ was previously detected in mammalian species, resulting in a more potent activation of the β -catenin dependent Wnt signaling pathway (Moeller et al., 2003). Here, a loss-of-function analysis of *cpz* was performed by TALEN-mediated mutagenesis of the zebrafish *cpz* gene. The loss-of-function mutation resulted in a series of morphological defects throughout zebrafish development. Based on literature descriptions (as discussed below) of similar morphological defects, we suggest a role for zebrafish Cpz in the regulation of Ca^{2+} signaling during development, likely through β -catenin independent Wnt signaling.

Localized elevation of Ca^{2+} is associated with many of the sequential processes that are common to vertebrate development, including fertilization and the subsequent cleavage events, but also axis specification and coordinated cell movements. In zebrafish, misexpression of specific Wnt proteins (i.g. Wnt4, Wnt5, and Wnt11) stimulates Ca^{2+} release, defining the

Wnt/Ca²⁺ class (Westfall et al., 2003). Zebrafish *wnt5b* mutant (*pipetail*) embryos that are depleted of both maternal and zygotic Wnt5 display cell movement defects as well as hyper-dorsalization (Westfall et al., 2003). The cell movement defects described in the *pipetail* mutant have also been observed in *wnt11* (*silberblick*) mutants (Heisenberg et al., 2000) and correlate with convergence and extension (CE) defects in other PCP component mutants such as *van gogh-like protein 2* (*vangl2/trilobite*) (Sepich et al., 2000), and *glypican 4* (*knypek*) which is believed to act as a co-receptor for β -catenin independent Wnt signaling (Topczewski et al., 2001). Expression of *wnt5b*, *wnt11* but also of *wnt4a* is observed during zebrafish gastrulation and has therefore been implicated in activation and/or regulation of PCP (Heisenberg et al., 2000; Kilian et al., 2003; Ungar et al., 1995). Blocking translation of *wnt4a* indeed revealed CE movement defects in zebrafish (Matsui et al., 2005). *cpz* mutant embryos display considerable similarities to the phenotypes such as various degrees of hyper-dorsalization and CE movement defects. The underlying mechanism of the hyper-dorsalization phenotype observed in *wnt5b* mutant embryos is a result of a decrease in Wnt/Ca²⁺ signaling activity. The reduced antagonism of Wnt/Ca²⁺ signaling on β -catenin dependent Wnt signaling leads to the dorsalized phenotypes (Westfall et al., 2003). The hyper-dorsalization observed in *cpz* mutant embryos requires further investigation, but for now we propose that a decrease of functional Cpz results in a reduction of the described antagonistic role of Wnt/Ca²⁺ signaling on β -catenin dependent Wnt signal activation. Concurrently, decreased Ca²⁺ modulation affects coordinated cell movement as observed in *wnt4a*, *wnt5* and *wnt11* mutants during gastrulation (Heisenberg et al., 2000; Kilian et al., 2003; Matsui et al., 2005; Ungar et al., 1995).

The defects observed during the cleavage period, e.g. the cell adhesion defects resulting in blastoderm separation, have not previously been linked to Wnt/Ca²⁺ signaling and are therefore more difficult to interpret. During early cell divisions, elevated Ca²⁺ levels associate with all the major processes vital for correct separation of daughter cells. These include furrow positioning (Lee et al., 2006), propagation (Webb et al., 1997), deepening (Lee et al., 2003), and apposition (Webb et al., 1997). The initial increase of cytoplasmic Ca²⁺ when fertilized eggs are placed in Ca²⁺-free medium, indicates that the Ca²⁺ involved in these first transients is derived from internal stores. However, after the first divisions embryos develop a lack of cohesiveness between the blastoderm cells (Webb et al., 1997), an effect also observed in our *cpz* mutants. The lack of cohesiveness has not been identified in the zebrafish *wnt5b* mutant, even when *wnt5b* was maternally depleted. Also the more recently described *wnt4a*^{fh295} mutant (Choe et al., 2013), did not display such defects. Suggesting genetic redundancy within the Wnt/Ca²⁺ class of proteins or possibly a more severe effect upon mutation of *cpz* due to its likely function in processing of such Wnt proteins. The importance of Ca²⁺ signals is also observed using pharmacological inhibitors of Ca²⁺ signals during development. For instance, when Ca²⁺ signals are completely blocked by injection of the calcium buffer BAPTA (1,2-bis(o-aminophenoxy)ethane-N,N,N',N'-tetraacetic acid), cleavage divisions remain absent (Creton et al., 1998). Lowering these BAPTA concentrations results in developing embryos that show microcephaly and heart deformation. Strikingly, these phenotypical defects were also observed in our *cpz* mutants. This suggests that a reduction in the level of *cpz* affects early Ca²⁺ signals leading to different defects.

The above described morphological defects suggest a yet to be determined role for Cpz

in Ca^{2+} regulation in which the loss-of-function correlates with a decrease in Ca^{2+} signals. The importance of Ca^{2+} signaling exceeds however early developmental stages as indicated by defective heart development. Ca^{2+} signals have also been implicated in formation and functioning of ciliated structures such as the neural tube, the pronephric kidney and Kupffer's vesicle. The latter is for instance of vital importance for the left-right asymmetry of the heart, liver and gut (Essner et al., 2005). Malformation of such structures could contribute to phenotypic defects. The formation and functioning of cilia and the possible loss of laterality should therefore be included in future experiments. Examining the morphological developmental defects in offspring of both $\text{cpz}^{+/-}$ and $\text{cpz}^{-/-}$ parents, mainly revealed common phenotypical defects (e.g. hyper-dorsalization, heart defects, swim bladder defects, high lethality rates). Only two specific defects were detected in $\text{cpz}^{+/-}$ (e.g. cell adhesion defects) and $\text{cpz}^{-/-}$ embryos (e.g. neural degeneration). The low-penetrance of phenotypes remains a puzzling observation but considering the complexity of the Wnt signaling pathways, may be an effect of genetic redundancy. Considering the proposed function of Cpz in Wnt/ Ca^{2+} signaling, the output (Ca^{2+}) is dependent on the phosphatidylinositol (PI) cycle. The PI cycle can however be activated in response to many different hormones and growth factors (Lapetina and Michell, 1973; Michell, 1975), which might explain the ability of embryos to cope with the proposed reduction of Wnt/ Ca^{2+} activation.

The recent description of a high-resolution crystal structure of a Wnt protein (*Xenopus* Wnt8) in complex with a Frizzled receptor binding domain, provided a first insight in how Wnt proteins engage their receptors (Janda et al., 2012). Wnt proteins reveal a highly unusual two-domain structure forming a thus far unique protein fold (Fig. 4.8A) (Janda et al., 2012). This structure is best described through a hand analogy in which Wnt extends a thumb from the N-terminal and an index finger from the C-terminal domain. Together these domains are involved in 'grasping' the cysteine-rich domain of the Frizzled receptor. The thumb domain extends a lipid residue which nestles in a hydrophobic groove of the cysteine-rich domain of Frizzled upon receptor binding. The thumb and index finger are connected by the palm which provides the region with a large amount of flexibility. This linker region is solvent exposed and most likely not involved in direct binding of Frizzled. It took three decades, to go from the identification of Wnt to obtaining a high-resolution structure of Wnt in complex with the Frizzled receptor. Still, little is known on the complex formation with the various other receptors and co-receptors of Wnt (Niehrs, 2012). To speculate on the regulatory role of Cpz in Wnt signaling, one has to consider the effects of the removal of only one C-terminal arginine residue. Arginine is a positively-charged, polar amino acid which is often observed on the protein surface where it can interact with the polar environment. Therefore arginines are quite frequently involved in protein activity or observed in protein binding sites (Barnes, 2007). Regarding the structure of Wnt proteins, the C-terminus is located at the base of the index finger oriented towards the protein surface (also in zebrafish Wnt4a, based on predicted 3-dimensional structure; Fig. 4.8B). Since the base of this index finger contains a disulfide bridge, its conformation is not likely affected. We therefore propose that removal of the C-terminal arginine, which is exposed on the surface of Wnt4a, leads to alterations in protein interactions; e.g. co-receptors. In the absence of available information on co-receptor binding sites, we hypothesize that changes in co-receptor affinity could be responsible for the here implicated differences in Ca^{2+} output resulting in the various phenotypical defects (Fig. 4.8C).

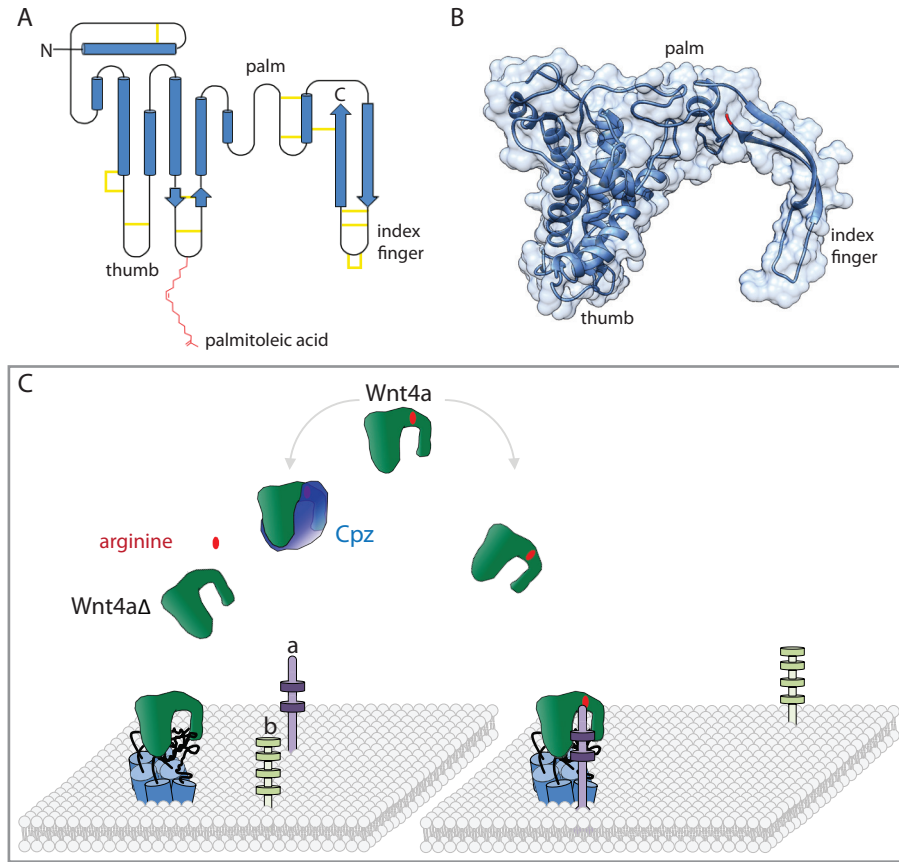


Figure 4.8. Proposed model for the function of Cpz in regulating Wnt4a signal activation. (A) Secondary structure Wnt proteins. Disulfide bridges are indicated in yellow. α -helices are depicted as cylinders whereas β -sheets are represented as arrows. (B) Predicted 3D structure of the zebrafish Wnt4a protein. C-terminus is depicted in red. Prediction was produced in ModBase (Pieper et al., 2014). (C) Hypothetical model that depicts the possible regulatory role of Cpz in Wnt4a activated signaling. The processing of the C-terminal arginine (red) of Wnt4a (green) by the metalloprotease Cpz (blue) changes the affinity between Wnt4a and (a) a specific yet to determine traditional co-receptor or (b) increases Wnt4a affinity towards a different co-receptor.

SUPPLEMENTAL DATA

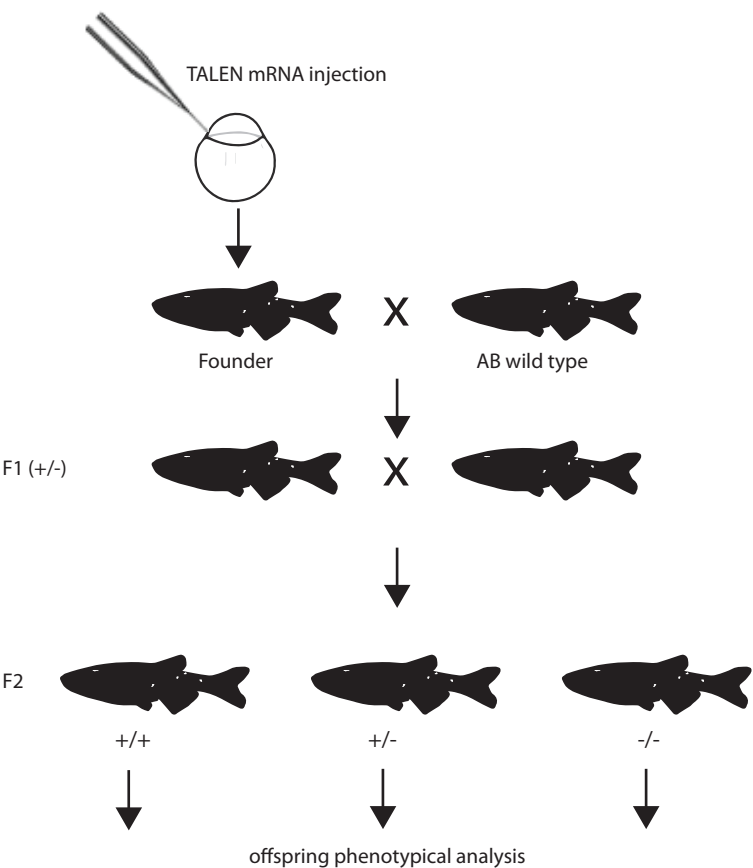
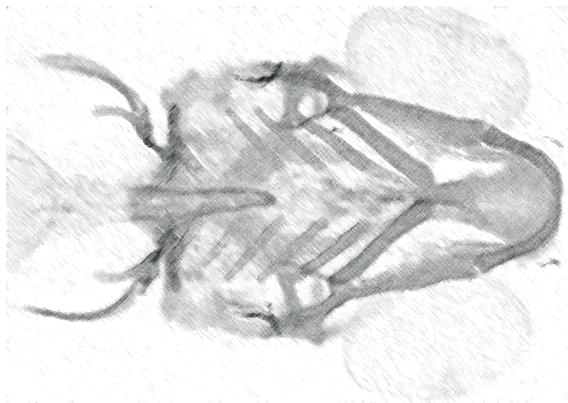


Figure S4.1. Schematic outline of *cpz* mutant zebrafish generation. TALEN-injected founders were out-crossed with wild type AB zebrafish to produce F1 parents. After genotype screening for mutations, the here used frame shift mutation was selected and used to generated F2 generations of homozygote and heterozygote *cpz* mutants, as well as wild type zebrafish generations used for phenotypical comparison. F3 embryos were used for phenotyping purposes.

Chapter 5

Effect of thyroid hormone on bone development of early stage zebrafish larvae

Barae Jomaa¹, Maurijn Y. Kessels^{2,3}, Hans H.J. van den Berg¹, Jac M.M.J.G. Aarts¹, Sacco C. de Vries², Ivonne M.C.M. Rietjens¹



¹Division of Toxicology, Wageningen University, Wageningen, The Netherlands; ²Department of Biochemistry, Wageningen University, Wageningen, The Netherlands; ³Experimental Zoology Group, Wageningen University, Wageningen, the Netherlands.

ABSTRACT

Thyroid hormones are required for skeletal development and the establishment of peak bone mass in vertebrates. The role of thyroid hormone is well documented in humans and studied extensively in rodent models, however to what extent thyroid hormone affects early bone development in zebrafish remains unclear. In order to assess the effect of thyroid hormone on zebrafish skeletal development, zebrafish embryos were exposed to the thyroid hormone triiodothyronine (T3) as well as the antithyroid drug propylthiouracil (PTU) from 2–120 hours post fertilization (hpf). Modulation of the zebrafish thyroid system by exposure to PTU only slightly affected the growth of cartilage elements without influencing cartilage column organization. In contrast, exposure to T3 significantly decreased the size of the posterior craniofacial region of 120 hpf zebrafish in a concentration-dependent manner and led to the morphological defects of ceratobranchial, palatoquadrate and ceratohyal skeletal elements as well as the opercle. In addition, the total length of T3-exposed larvae at 120 hpf decreased in a concentration-dependent manner. Significant changes in bone formation were observed upon exposure to T3. Ossified structures of both dermal and chondral origin displayed accelerated ossification upon exposure to increased levels of the thyroid hormone. The results confirm the importance of the thyroid hormone system with regard to osteogenesis in not only mammals, but also teleosts.

INTRODUCTION

The importance of the thyroid in bone development became apparent during the latter part of the 19th century with the linking of cretinism, in which affected individuals exhibit short stature, after the surgical removal of the thyroid (Reverdin and Reverdin, 1883). It is now established that the thyroid hormones (THs) triiodothyronine (T3) and tetraiodothyronine (T4) are regulators of bone development in vertebrates (Bucher et al., 1985; Kini and Nandeesh, 2012; Thorngren and Hansson, 1973). They exert their effects both directly by activating thyroid hormone receptors (THRs) in bone-forming cells or indirectly by stimulating the secretion of growth hormone (GH) and insulin-like growth factor-1 (IGF-1) (Abu et al., 1997; Gothe et al., 1999). While both THs bind THRs, T4 has 20–40x lower binding affinity and is deiodinated intracellularly at the outer ring by deiodinase type II (DIO2) to form the more active T3 (Sandler et al., 2004). *Dio2* knockout mice have revealed that this local conversion of T4 to T3 is especially important in bone formation (Bassett et al., 2010; Schroeder and Privalsky, 2014). Deiodinase type III (DIO3) inactivates T3 and T4 by catalyzing inner ring deiodination while deiodinase type I (DIO1) catalyzes both activation and inactivation reactions (Maia et al., 2011).

Endochondral and intramembranous ossification are the two main mechanisms involved in the formation of the vertebrate skeleton. Endochondral ossification relies on the formation of a cartilage scaffold by chondrocytes that serves as a template for the formation of long bones. At each end of the long bone are epiphyseal growth plate zones which are the centers of longitudinal bone growth until epiphyseal fusion at the onset of adulthood. Hypothyroidism results in endochondral ossification while hyperthyroidism results in accelerated linear growth accompanied by a premature fusion of the epiphyseal growth plate. In this manner, both hypothyroid and hyperthyroidism result in short stature (Wojcicka et al., 2013). In intramembranous ossification, bone is formed directly from mesenchymal cells instead of going through a cartilage intermediate. For example, the formation of the flat bones of the skull, mandibles and clavicles relies on intramembranous ossification (Otto et al., 1997). Intramembranous ossification is also involved in foramen lacerum (triangular opening at the base of the skull) closure as well as fracture healing (Santaolalla-Montoya et al., 2012; Thompson et al., 2002). In zebrafish, intramembranous ossification mediates the formation of the flat bones such as the opercle or circumorbital bones as well as the fracture healing of bony fin rays (Chang and Franz-Odenaal, 2014; Geurtzen et al., 2014).

As has been demonstrated in vertebrate models, the essential role of thyroid hormones in bone development can be disrupted by anti-thyroid drugs (Goddard, 1948). The serendipitous discovery by Ana Soto and her colleagues in 1991 that a ubiquitous man-made chemical, p-nonyl-phenol, can have inadvertent estrogenic activity *in vitro*, has launched the field of endocrine disruption as well as legislation to protect the general public from being exposed to harmful levels of such compounds (EEC, 2006; Soto et al., 1991). In a previous study, the zebrafish was reported as an animal model for detecting developmental toxicity due to thyroid-active compounds (Jomaa et al., 2014). Considering the effect thyroid hormones elicit during human bone development, the current study aims to explore the extent to which zebrafish skeletal development is influenced by thyroid hormone.

MATERIALS AND METHODS

Compounds

All compounds were obtained from Sigma-Aldrich Chemie (Zwijndrecht, The Netherlands) and were of high purity ($\geq 95\%$). All test chemicals were added from 500-fold concentrated stock solutions in dimethylsulfoxide (DMSO, Acros Organics, Geel, Belgium) to Dutch Standard Water (DSW; demineralized water supplemented with NaHCO_3 (100 mg/l), $\text{CaCl}_2 \cdot \text{H}_2\text{O}$ (200 mg/l), KHCO_3 (20 mg/l), and $\text{MgSO}_4 \cdot 7\text{H}_2\text{O}$ (180 mg/l)). The exposure medium was then aerated for 24 h at 27°C, the pH was adjusted to 7.4–8.4 and O_2 concentration was above 6.5 mg/l.

Fish maintenance and experimental design

Zebrafish strains were reared at the fish facility of Wageningen University at 27.1°C with a 14:10 light dark cycle and raised at a density of 5 fish/L. All fish were fed *ad libitum* three times a day with both *Artemia* and Tetramin flakes. For the experiments, matings were set up with two males and four females. Spawned eggs were rinsed in DSW and unfertilized eggs were removed. Embryos were examined between the 4 to 32-cell stage and at 2 hpf, embryos of similar developmental stages were placed in separate glass beakers containing the exposure medium. Subsequently, the embryos were individually placed in a well of a 24-well plate containing 2 ml of test medium (0.4, 0.2, 0.1, 0.05 and 0.025 mM for PTU; 0.05, 0.5, 5.0, 50 and 500 nM for T3). The 24-well plates were kept in an incubator at 27 °C \pm 1 °C with a 14:10 light dark cycle. The exposure solutions were renewed halfway the experimental period (day 2). For the exposure with T3, the concentration range was considered with the intermediate concentration close to the estimated physiological levels (Chang et al., 2012). At the end of each experiment, the 5 day old larvae were euthanized with 0.1% (w/v) tricaine methane sulphonate (TMS, Crescent Research chemicals, USA) buffered with 0.08% (w/v) sodium bicarbonate (Gibco, Paisley, Scotland).

Alcian blue and Alizarin red staining

Whole-mount staining of cartilage and bone structures was performed as described previously (Spoorendonk et al., 2008; Walker and Kimmel, 2007).

Surface calculations

Images of whole-mount cartilage and bone stained larvae were taken with an Olympus DP50 digital camera (Olympus Corporation Inc., Japan) mounted on a Zeiss Stemi SV11 microscope (Carl Zeiss AG, Germany). Measurements were performed in AnalysisD software (version 2.2, Soft Imaging System GmbH, Germany). Length and width of the ossified area (for example around the near-cylindrical structure of the ceratohyal) were used to calculate the surface area with the exception of the early phases where only half of the cylindrical value was used. For the opercle, the structure was considered to be 2 dimensional and measured by calculating the surface area. Results are based on 8 replicates per concentration (n=8).

Statistical analysis was performed comparing the replicates from each concentration to the pooled 0.1% DMSO control larvae in a two tailed Student t-test assuming unequal variance.

RESULTS

Morphological defects in the zebrafish craniofacial skeleton upon exposure to thyroid-active compounds

Modulation of the thyroid system was performed by exposing zebrafish to the bioactive thyroid hormone T3 or to the antithyroid drug propylthiouracil (PTU), which inhibits the synthesis of the thyroid hormones T3 and T4 (Fig. 5.1) (Moriyama et al., 2007). Exposure to a concentration range of T3 or PTU occurred from 2–120 hpf. Modulation of the thyroid system did not affect the initial development of craniofacial cartilage elements as was observed by the presence of all elements in both exposed and control larvae (Fig. 5.2A-F). Moreover, the inhibition of the thyroid system with PTU did not result in obvious morphological defects. In contrast, exposure to T3 concentrations $\geq 5 \times 10^{-2} \mu\text{M}$ altered the morphology of the posteriorly-located craniofacial elements. A shortening of the posterior head region resulted in the bending of the ceratobranchials and the outward extension of the hyosymplectic (Fig. 5.2F,H,I). The jaw region of the larvae did not display morphological abnormalities due to T3 exposure. Furthermore, exposure to T3 reduced total lengths of larvae in a dose-dependent manner resulting in significant differences in larvae exposed to T3 concentration $\geq 5 \times 10^{-3} \mu\text{M}$ (Fig. 5.2J).

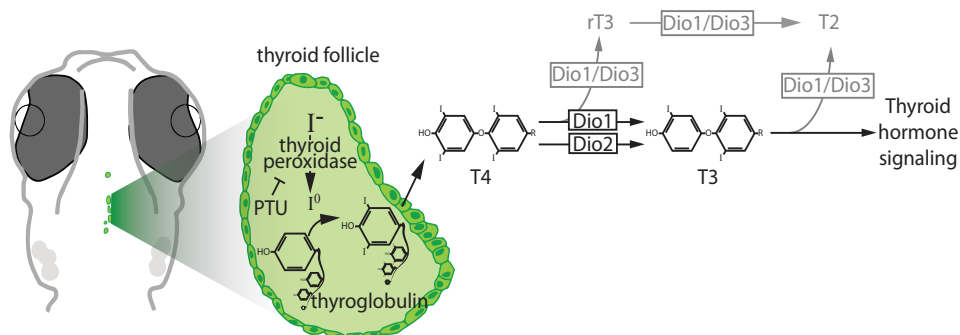


Figure 5.1. The zebrafish thyroid system. Schematic representation of key components in the zebrafish thyroid system. The thyroid follicles in the zebrafish are located in the midline, close to the dorsal side of the pharynx. Iodide (I^-) is transported into the follicles and oxidized to iodine (I^0) by thyroid peroxidase. In the follicular lumen, the reactive iodine incorporates into tyrosyl residues in thyroglobulin. Tyrosyl residues are coupled together and thyroglobulin is taken up by the follicular cells through pinocytosis. In the cell, thyroglobulin is proteolytically processed, thereby liberating thyroxine (T_4) and triiodothyronine (T_3) molecules that cross the membrane and enter the bloodstream. The metabolism of T_3 and T_4 into active and inactive intermediates involves the action of 3 types of deiodinases (Dio). T_4 is activated when it is converted to T_3 through the removal of an iodine atom from its outer ring by Dio1 and Dio2. Deactivation of T_4 to reverse (r) T_3 and T_3 to T_2 happens by Dio1 and Dio3-mediated inner ring deiodination. By inhibiting the enzyme thyroid peroxidase, PTU is able to prevent the iodination and coupling of thyroglobulin and the formation of both T_3 and T_4 .

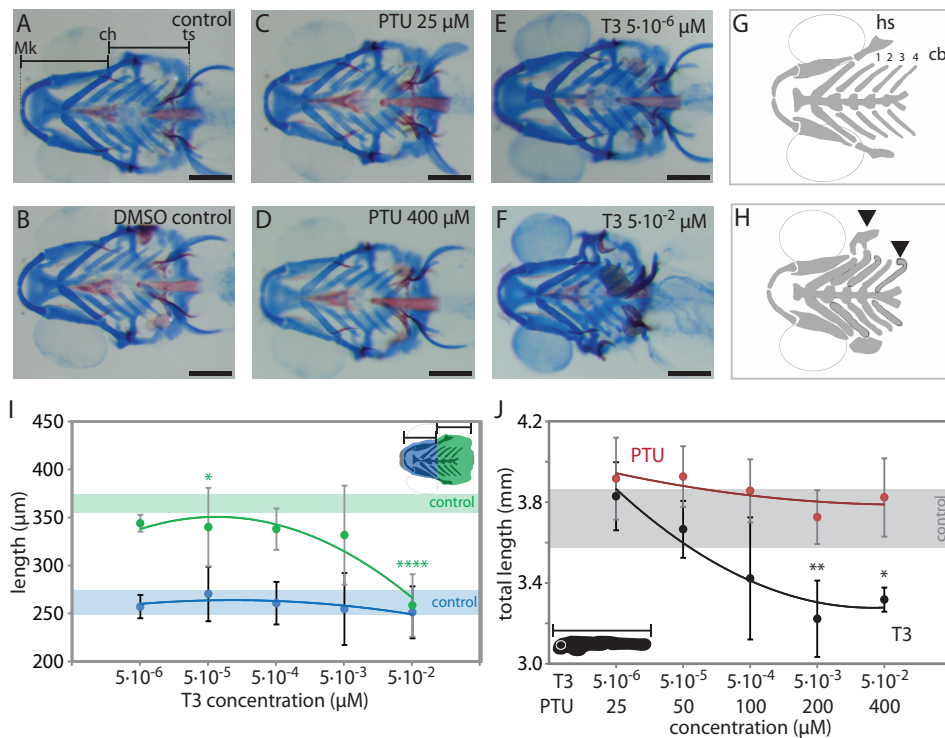


Figure 5.2. Exposure to T3 affects embryonic growth rate and induces abnormal morphology of the head region and skeletal elements. (A-F) Alcian blue/alizarin red double stain of cartilage/bone structures in 5 dpf (A) control, (B) DMSO control larvae and larvae exposed to different levels of (C-D) PTU or (E-F) T3. Scale bars indicate 200 μm . (G-H) Schematic representation of the craniofacial cartilage elements in larvae of the DMSO control group and T3 treated group (extrapolated from A and F, respectively). (G) The hyosymplectic (hs) and ceratobranchials (cb) 1–4 in control larvae display malformations due to exposure of T3 (arrow heads in H). (I) Average lengths of the jaw (blue dots; tip of the Meckel's cartilage to the attachment site of the ceratohyal) and the region behind the jaw (green dots; attachment site of the ceratohyal to the posterior of the tectum synoticum) \pm standard deviation, of larvae from the DMSO control (green and blue areas) and T3 exposed group. (J) Average total lengths (dots) \pm standard deviation of larvae from the DMSO control (grey area) and T3 or PTU exposed group at 5 dpf. * $P \leq 0.05$; ** $P \leq 0.01$; *** $P \leq 0.001$; **** $P \leq 0.0001$ compared to the DMSO control group. Abbreviations: ch, ceratohyal; Mk, Meckel's cartilage; ts, tectum synoticum.

Modulation of the thyroid system affects growth of the palatoquadrate cartilage

No irregular chondrocyte stacking of cartilage elements was observed by exposure to T3 or PTU. Length measurements were performed on cartilage structures to determine whether thyroid modulation affected cartilage growth rate. Most structures (e.g. ceratohyal, ethmoid plate) did not exhibit any significant differences (data not shown). However, the length of the palatoquadrate showed several significant differences upon thyroid modulation (Fig. 5.3). The palatoquadrate of larvae exposed to concentrations of T3 5×10^{-6} μM , 5×10^{-5} μM and 5×10^{-2} μM were significantly shorter compared to these structures in the DMSO control group (Fig. 5.3C). Exposure to PTU resulted in an opposite effect on palatoquadrate length showing a concentration-dependent decrease with significant length differences at PTU concentrations of ≥ 100 μM and higher.

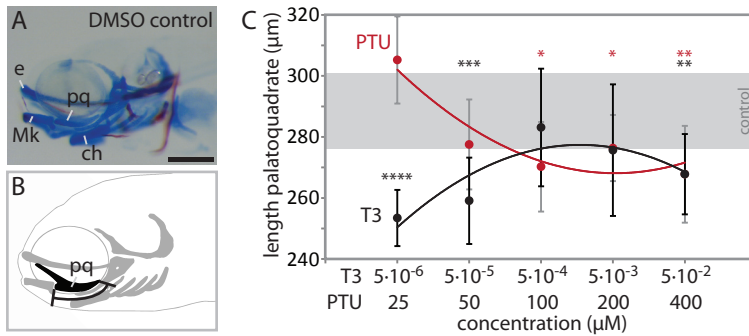


Figure 5.3. Modulation of the thyroid system affects palatoquadrate cartilage growth. (A) Alcian blue/alizarin red double stain of cartilage/bone structures of a DMSO control larva (5 dpf) indicating the (e) ethmoid plate, (Mk) Meckel's cartilage, (ch) ceratohyal and (pq) palatoquadrate. (B) Schematic representation of the same larva highlighting the measured region of the palatoquadrate. (C) Average lengths of the palatoquadrate (dots) \pm standard deviation of larvae from the DMSO control (grey area) or the PTU (red) and T3 (blue) exposed groups. * $P \leq 0.05$; ** $P \leq 0.01$; *** $P \leq 0.001$; **** $P \leq 0.0001$ compared to the DMSO control group. Scale bar indicates 200 μm .

T3 exposure accelerates ossification in the zebrafish craniofacial skeleton

Exposure of embryos to T3 concentrations $\geq 5 \times 10^{-4} \mu\text{M}$ clearly affected ossification in zebrafish larvae, as determined by Alizarin red staining (Fig. 5.4). The acceleration of ossification was supported by two parameters, namely initial ossification of the ceratobranchial elements and the ossified area of elements present in all 5 day old zebrafish larvae. First, 5 day old larvae exposed to T3 concentrations $\geq 5 \times 10^{-4} \mu\text{M}$ revealed an advanced ossification sequence compared to that of lower T3 concentrations or control larvae of the same age (Fig. 5.4A-B, E-H). During wild type zebrafish bone development, the ossification of the ceratohyal precedes that of ceratobranchial 1–4. In contrast to control larvae or larvae exposed to lower levels of T3 ($\leq 5 \times 10^{-4} \mu\text{M}$), high T3 levels revealed advanced maturation in perichondral ossification by ossification of the ceratobranchial elements (Fig. 5.4H), while at the same time total length of these larvae was reduced significantly (Fig. 5.2J). Subsequent analysis of ossified areas of either chondral (ceratohyal) or dermal (opercle) origin present in exposed and control larvae supported the notion of increased ossification in T3 treated larvae (Fig. 5.4C-D). The opercle, a dermally-derived bone element displayed a more mature shape and an increased ossified area compared to control animals (Fig. 5.4A,G,I). The ceratohyal is a cylindrical structure in which the ossified areas arise on the surface. Ossification begins in the form of two parallel stripes on opposite sides of the cylinder, slowly extending over the entire surface. T3 exposure resulted in an significant increase in the ossified surface area of these chondral-derived elements (Fig. 5.4B,H,J). The concentrations of T3 used during this analysis were compared to the whole-body content as determined in zebrafish larvae where the average thyroid concentration from 1–5 dpf was determined to increase from 0.1 to 0.2 ng g^{-1} (Chang et al., 2012). Assuming that 1 g of larval wet weight equals 0.8 ml, this amounts to a whole-body concentration of 0.19–0.38 nM. Significant changes in ossification of the ceratohyal were observed at T3 concentrations of $\geq 0.5 \text{ nM}$, which therefore represents an approximately 2-fold increase of the endogenous levels as predicted by the whole-body content of 5 day old zebrafish larvae. Significant changes in ossification

based on the ossified surface area of the opercle were observed in T3 concentrations of ≥ 5 nM.

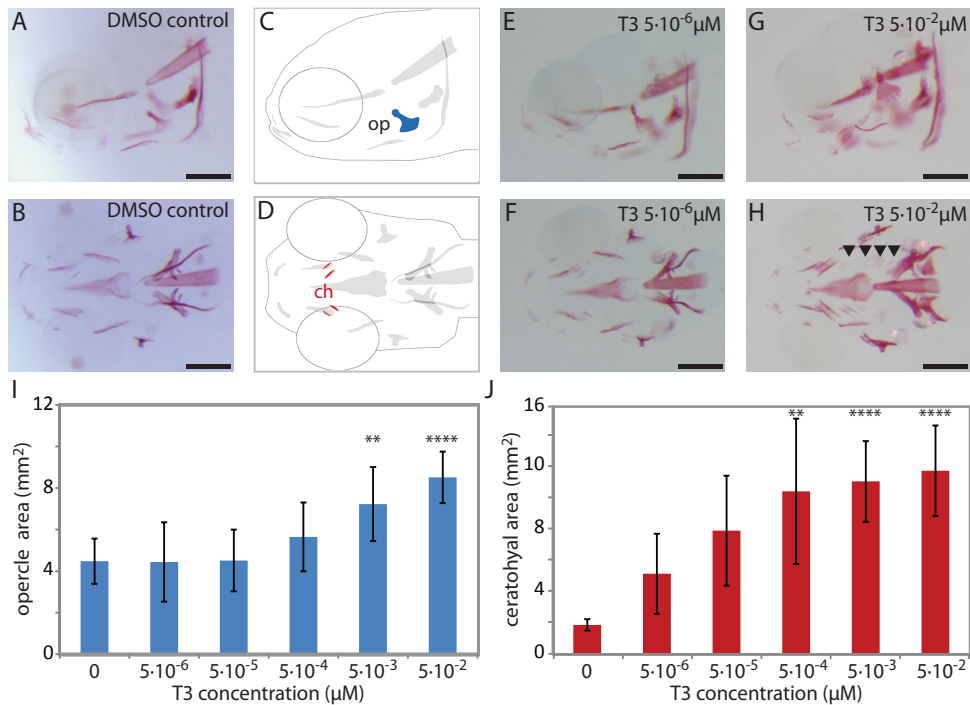


Figure 5.4. T3 exposure accelerates chondral and dermal ossification in the zebrafish craniofacial skeleton. (A-B,E-H) Alizarin red stain on ossified structures in the craniofacial skeleton of 5 dpf (A-B) DMSO control larvae and larvae exposed to different levels of T3 (E-H). (H) Arrow heads indicate ossification of the ceratobranchials. (C-D) Schematic representation of ossified structures used for quantification purposes in control larvae with the (C) opercle and (D) ceratohyal indicated in blue and red, respectively. (I,J) Quantitative analysis of the ossified surface areas of the opercle (I) and ceratohyals (J) in control and T3 exposed larvae. * $P \leq 0.05$; ** $P \leq 0.01$; *** $P \leq 0.001$; **** $P \leq 0.0001$ compared to DMSO controls. Abbreviations: ch, ceratohyal; op, opercle. Scale bars indicate 200 μm .

DISCUSSION

Thyroid hormones regulate directly or indirectly many morphological, physiological and biochemical changes in fish during early development (Liu and Chan, 2002). Previously, zebrafish bone development was shown to be affected by thyroid-active compounds, but this was not documented in detail (Jomaa et al., 2014). In the present work the effect of thyroid hormone modulation on bone development was studied at the level of individual skeletal elements. The results show that treatment with the thyroid hormone T3 does not affect the initial formation of cartilage elements in the craniofacial skeleton but exerts an effect on the growth of the palatoquadrate. Furthermore, T3 accelerates ossification of chondral (ceratohyal) and dermal (opercle) elements of the developing skeleton. The thyroid inhibitor PTU has a much less pronounced effect on these processes.

The original hypothesis underlying the use of thyroid hormone was that changes in this system could be employed that affect early zebrafish skeletal development. The use of the anti-thyroid drug PTU did not reveal major changes in bone formation. PTU functions mainly by inhibiting the synthesis of T3 and T4 by interfering with thyroid peroxidase-mediated iodination of tyrosyl residues in thyroglobulin (Nakamura et al., 2007). Moreover, PTU has also been found to also affect the conversion of T4 to T3 by inhibiting D2 (Abuid and Larsen, 1974). Until T3 and T4 production begins at 60 hpf (Bohnsack et al., 2011), embryonic thyroid hormone is derived from maternal supplies stored in the yolk sac (Power et al., 2001) and therefore the effect of PTU on the thyroid system prior to that time point is predominantly at the level of D2 inhibition. However, in contrast to mammals, PTU has a less potent effect on deiodinases in fish and therefore is less effective at inhibiting the conversion of T4 to the active hormone T3 in peripheral tissues (Orozco and Valverde, 2005). The absence of major morphological phenotypes in PTU exposed embryos might therefore be a result of PTU's inefficient inhibition of D2 in zebrafish in combination with the compound's inability to affect maternally transferred thyroid hormones which are present in the yolk. The absence in cartilage deformities correlates with previous findings though these studies used shorter windows of exposure (Bohnsack et al., 2011; Bohnsack and Kahana, 2013). Also craniofacial development of zebrafish has been attributed to interplay between thyroid hormones, retinoic acid and insulin-like growth factor in which inhibition of thyroid hormone alone did not reveal morphological defects (Bohnsack et al., 2011; Bohnsack and Kahana, 2013). The treatment with PTU in combination with inhibition of insulin-like growth factor however disrupted development of the jaw and extraocular muscles whereas PTU-treated controls appear morphologically normal (Bohnsack and Kahana, 2013).

To date the effects of thyroid hormones in fish have mainly been restricted to morphological descriptions and changes in gene expression. For example, development of different skeletal elements, including the craniofacial skeleton (Bohnsack and Kahana, 2013), paired and unpaired fins (Brown, 1997; Shkil et al., 2012) and the development of the supraneurals (Kapitanova and Shkil, 2014) have been described. In most cases, the effects of alterations in thyroid hormone levels affect the developmental rate and timing of skeletal structures which leads to changes in their definitive morphology. In the present study, exposure to T3 resulted in significant dose-dependent reduction of zebrafish total lengths as well as a reduced growth rate of the posterior skull region. As a consequence, the reduction in length of the posterior skull resulted in deformities of the posterior located ceratobranchials. However, the ceratobranchials as well as other craniofacial cartilage structures appeared structurally unaffected.

High levels of exogenous T3 clearly affected the process of ossification in developing zebrafish larvae. A dose-dependent acceleration of ossification in bone structures of dermal and chondral origin was observed upon exposure of zebrafish to excess T3. Interestingly, this corresponds with human childhood thyrotoxicosis in which the skeleton displays accelerated skeletal development and growth with advanced bone age (Segni et al., 1999). It remains unclear what the underlying mechanism entails; whether the increased ossification rate is a result of enhanced secretory activity of osteoblasts, increased osteoblasts differentiation or a normal developmental sequence with accelerated speed. Like in mammals, zebrafish exposure to thyroid hormones has been linked to changes in gene expression in the skeletal

system (Pelayo et al., 2012). The effect of thyroid hormones on osteoblast differentiation in vertebrates remains however contradictory and has been found to stimulate, inhibit, or exert no effect on osteoblastic cell proliferation (Kanatani et al., 2004; Kim and Mohan, 2013). The consensus suggests that T3 stimulates osteoblast differentiation (Harvey et al., 2002), and does so in an FGF-dependent manner (Stevens et al., 2003; Su et al., 2008). Accelerated growth resulting in advanced endochondral and intramembranous ossification was previously described in human patients and a corresponding mouse mutant, with both humans and mice displaying thyroid hormone resistance resulting in elevated circulating T3 and T4 concentrations (O'Shea et al., 2003; Weiss and Refetoff, 1996). Because this study focused on early development of the skeleton rather than the overall developmental speed of exposed zebrafish larvae, we cannot suggest a similar mode of action in which increased T3 levels accelerated development.

As introduced in the result section, the concentrations of T3 that resulted in significant increases of the ossified areas in the opercle and ceratohyal were observed in a 2 to 30-fold increase compared to the whole-body content of T3 in zebrafish larvae (Chang et al., 2012). However, whole body content of thyroid hormone does not accurately reflect the intracellular and thus transcriptionally active thyroid hormone levels since this is tissue dependent (Irvine, 1974). Endogenous thyroid hormone is mainly produced as the prohormone T4, which is converted to T3 in peripheral target tissue cells by deiodinases. Local elevations of thyroid hormone play an important regulatory role as is observed in the developing mouse brain. Different parts of the brain are sensitive to thyroid hormone at different time points during development whereas there appears to be local control of hormone levels (Zoeller, 2004). Local production of T3 is mainly regulated through the actions of deiodinases, especially Dio2 which is implicated in local elevations of cytoplasmic T3 rather than the maintenance of T3 serum concentration. This finding is supported by the expression of *Dio2* which is more limited during development (Bianco and Kim, 2006). Bursts of D2 activity occur in some tissues, allowing for increased thyroid hormone signaling in both spatially and temporally specific patterns (Bianco and Kim, 2006).

In summary, the modulation of the zebrafish thyroid system clearly reflects observations made in other vertebrate species. Exposure of zebrafish to excess T3 resulted in growth retardation and accelerated bone maturation, similar to what is observed in clinical hyperthyroidism. Future research is needed to elucidate whether the skeletal effects result from disruption of primary thyroid actions in bone cells or whether they are secondary and/or systemic effects on other endocrine pathways that regulate skeletal development and bone mass. This study is the first to provide histological evidence of increased ossification in zebrafish due to thyroid hormone exposure.

ACKNOWLEDGEMENTS

This project was financially supported by the Netherlands Genomics Initiative (Netherlands Toxicogenomics Centre, grant number 6162500134). The authors would like to thank Azath Hamza for her participation in the project during her MSc studies.

Chapter 6

General Discussion

COMBINING PROTEOMICS AND GENETIC APPROACHES: AN EVALUATION

In this thesis, I have employed a combined approach – proteomics followed by reverse genetics – to enhance our understanding of the zebrafish skeleton and its development.

While some proteomics techniques have been employed in zebrafish (Greiling et al., 2009; Tay et al., 2006), the zebrafish has been selected primarily as a tool for genetic approaches. Therefore, the main focus in skeletal research has been on genetic regulation of skeletogenesis. As a result only a handful of structural components of the zebrafish skeleton are presently known and characterized which have predominately been used as markers of skeletal cells (expression-based) or the matrices themselves (antibody-based). Over the years, the zebrafish was developed as a disease model for skeletal defects including osteogenesis imperfecta (Mackay, 2013) and osteoarthritis (Mitchell et al., 2013), without extensive knowledge on its skeletal composition.

First, I compared the protein content of the zebrafish skeleton during three major stages of development; late larval, juvenile and adult (chapter 2). By analyzing the differential abundance of proteins, I detected major changes in the developing skeleton and identified potential regulatory proteins.

For the proteomics approach to be successful, two requirements had to be fulfilled:

1. To minimize contamination with cellular proteins in order to produce an extensive overview of the protein content of the zebrafish skeletal matrix
2. To identify major and minor matrix components and determine their change in abundance during development.

If the proteomics approach did not meet our initial expectations, was there any additional value to this strategy? In the case that both requirements could not be achieved, follow-up studies could still have provided some insights in regulatory proteins. This, however, would have made it more difficult to identify candidates that are linked to skeletal development. Since a similar approach has not previously been attempted in zebrafish, the identification of highly abundant skeletal matrix proteins only could still have had an added value to current understanding of extracellular matrix formation during development. Because I have achieved both of the requirements, minimizing cellular contamination and identifying less abundant components, the proteomics approach is clearly feasible and worthwhile.

The skeletal proteome of the zebrafish

Various studies aimed to identify the composition of bone (Onnerfjord et al., 2012; Wilson et al., 2012) and cartilage (Alves et al., 2011; Schreiweis et al., 2007) and their changes during development. These studies targeted either bone or cartilage to prevent detection limits of low-abundance proteins in a matrix primarily composed of a limited number of highly abundant structural proteins. Only one study presented developmental differences in cartilage, while others focused more on differences between particular skeletal structures and between individuals. So, the analysis of the whole skeleton as performed in this thesis on zebrafish presents novel information on changes that occur throughout the formation of

bone. This study provides a foundation for future analysis in which available pathological mineralized zebrafish mutants (Spoorendonk et al., 2010) or the use of mechanical loading (Fiaz et al., 2012), could generate valuable insights in the functioning of the vertebrate skeleton.

Combination of proteomics and genetics

The identification of the carboxypeptidase Z (Cpz) protein during the proteomic analysis paved the way for a more elaborate analysis of this molecule (chapters 3 and 4). The initial goal here was to provide new insight into the role of Cpz in skeletal development of the zebrafish by studying a loss-of-function mutation. This appeared difficult due to a surprisingly wide variety of phenotypes that this mutation induced. Even though I was unable to pinpoint the exact mechanism of Cpz and identify a clear skeletal phenotype, the observed correspondence between Cpz phenotypes and those found for mutants in the β -catenin independent Wnt signaling pathway suggested a role of zebrafish Cpz in that important general signaling pathway.

This study compellingly demonstrates the complications that can occur when a component of an elaborate signaling pathway is examined during a relatively late stage of development. Historically, genes were studied through the identification of naturally occurring mutant phenotypes to characterize and determine the role of particular pathways and processes. These forward genetic approaches relied on observable phenotypic variations and aimed to find genes that are essential to certain biological phenomena. While studies used to depend on spontaneous mutations for introducing genetic variation, the mutation frequency is presently often accelerated using chemical agents such as ethylmethanesulphonate (EMS) or N-ethyl-N-nitrosourea (ENU) which induce primarily point mutations in single genes (de Bruijn et al., 2009; O'Brien and Frankel, 2004). Reverse genetic approaches provide several advantages over the more classical techniques. They allow for targeted mutations in specified regions and do not rely on chance to introduce mutations by circumventing the possibility of intergenic hits during random mutagenesis.

The use of a proteomics approach as a starting position proved to be effective in the study of the extracellular matrix of the skeleton. Identification of proteins in the skeletal ECM does not exclude functions elsewhere. Regulatory proteins present often the most interesting candidates for functional analysis but are hardly ever constrained to a specific tissue or stage in development. This was also observed in this thesis with regard to the extensive spatio-temporal expression pattern of *cpz*. Studying development of a specific tissue with a loss-of function mutation is therefore challenging. When Cpz would not have been identified by proteomics, the link with the skeleton would presumably not have been made.

Genetic approaches, often identify the role of genes up to the earliest lethal phenotype. This is the case in the majority of studies in zebrafish that focus on gene mutations affecting key developmental genes. A good example is the research performed on the *knypek* gene, the zebrafish homolog of mammalian glypican 4 (SolnicaKrezel et al., 1996; Topczewski et al., 2001). *Knypek* was identified during a large-scale genetic screen in which mutant embryos displayed defects in axis extension (SolnicaKrezel et al., 1996). *Knypek* appeared to be a co-receptor for β -catenin independent Wnt signaling with a role in convergence and extension

movements. Mutant embryos were shorter and broader than wild type embryos and did not survive past 5–7 days post fertilization (Topczewski et al., 2001). By overcoming this lethality rate via injections of Knypek mRNA into embryos, mutant embryos could be reared to adult size which uncovered an important role of this protein in zebrafish cartilage and bone morphogenesis (LeClair et al., 2009).

In conclusion, the combination of proteomics and reverse genetics approaches provided valuable insights and a solid foundation for future studies on the composition and the regulation of the morphogenesis of the vertebrate skeleton.

ZEBRAFISH CARBOXYPEPTIDASE Z

An extracellular protein?

In this thesis, I studied Cpz in zebrafish under the presumption that Cpz is secreted into the extracellular matrix. Secreted Wnt glycoproteins function by binding to receptors and receptor combinations on the plasma membrane. Extra-cellular localization of the functional Cpz protein is required to process Wnt proteins.

Cpz was studied in species including the mouse, rat, chicken and human (Moeller et al., 2003; Novikova et al., 2001; Novikova et al., 2000; Xin et al., 1998). The protein sequence displays high homology in the functional domains (i.e. cysteine-rich domain and peptidase domain). In addition, all Cpz orthologues contain a N-terminal signal peptide that suggests that Cpz enters the endoplasmic reticulum (Song and Fricker, 1997; Xin et al., 1998). Human CPZ has indeed been detected in the secretory pathway by *in vitro* experiments and as a component of the extracellular matrix in human tissues (Novikova et al., 2000). Also, the biochemical properties such as the functional pH range (7–8) predict an extracellular function for Cpz, rather than an intracellular one (Novikova and Fricker, 1999). Despite our efforts, I was unable to detect the cellular localization of zebrafish Cpz. In the absence of an functional antibody, I studied the localization *in vitro*. I successfully cloned both zebrafish splice variants of *cpz* and expressed them as fusion proteins C-terminally linked to Gfp. However, transfection experiments in PAC2 zebrafish fibroblast proved difficult and without further experimentation, we cannot reach a definite conclusion on the localization of zebrafish Cpz.

Substrate specificity; lessons from frizzled receptors?

In chapters 3 and 4 of this thesis, I propose a role for Cpz in Wnt4 induced signaling, with Wnt4a as most likely substrate based on its high sequence homology with Wnt4 proteins from mammalian species and the partial overlap in expression patterns during zebrafish development (chapter 3).

Despite the preference of CPZ to process substrates with a C-terminal arginine, *in vitro* studies revealed its ability to process synthetic peptides with other basic amino acid residues as well (Song and Fricker, 1997). This raises concerns on its substrate specificity, especially because a majority of the Wnt proteins contain a basic C-terminal amino acid. One of the two important domains in Cpz is the cysteine-rich domain (CRD) which is also present

in the frizzled (Fzd) family of Wnt receptors. Fzd receptors present a family of seven-pass transmembrane receptors in which the CRD is presented at the cell-surface on the N-terminus of the protein. Wnt ligands bind this CRD with high affinity (K_d of 1-10 nM) (Hsieh et al., 1999; Rulifson et al., 2000). Studies that aimed to identify the specificity of the CRD produced contradictory results. While one provides evidence that the CRD is replaceable and functions only by bringing Wnt proteins in close proximity of the membrane portion of the receptor (Povelones and Nusse, 2005), another shows that Wnt affinity is different for specific receptors and a determinant in the pathway specificity of Wnt signaling (Rulifson et al., 2000). A breakthrough came with the recent discovery of the co-crystal structure of *Xenopus* Wnt8 in complex with the mouse FZD8-CRD (Janda et al., 2012). These data suggest a certain selectivity by the protein-protein interactions but most strikingly is the palmitoleic acid residue on the Wnt protein that inserts in a hydrophobic groove of the CRD. The high degree of conservation of apolar amino acids in the region of the CRD contacting the acyl group implies that the lipid-binding site is conserved in other Fzd-CRD proteins. However, amino acid substitutions in the composition of the groove of different Fzd proteins indicates that ligand specificity could be modulated to some extent through this interaction.

In conclusion, it appears that the CRD in Fzd proteins is at least in part responsible for the binding specificity of Wnt proteins. It remains unclear whether subsequent interactions with the membrane portion of the receptor are involved in this Wnt-receptor specificity or interactions of Wnt proteins with other binding proteins such as inhibitors or in this case Cpz. This is of vital importance in creating a better understanding of Wnt function and complexity which should be addressed in future research.

PHENOTYPE PENETRANCE; GENETIC MODIFIERS AND CILIARY DYSFUNCTION

In chapter 4, I show that *cpz* mutant embryos and larvae display a variety of relatively low-penetrant phenotypes. It is not uncommon for components of complex signaling pathways, such as the Wnt signaling pathway, to display pleiotropic mutant phenotypes upon loss-of-function. Interestingly, the observed phenotypes in *cpz* mutant embryos do not resemble the phenotypical traits presently assigned to zebrafish *wnt4a* (Choe et al., 2013; Matsui et al., 2005; Ungar et al., 1995). Whether this argues for the importance of proteolytic processing of Wnt4a or the ability of Cpz to act on different substrates should be resolved by future experimentation. The latter concern is emphasized by the partial overlap of phenotypical traits between *cpz* and *wnt5b* mutants (Westfall et al., 2003). Redundant (or parallel) pathway components can be responsible for the partial survival of embryos. In chapter 4, I introduced two additional important factors that can undermine normal phenotype distribution; genetic modifiers and ciliary dysfunction. Here, I discuss these topics in more depth providing some insight in their role.

The use of genetic analysis to interpret and predict phenotypes in genetic diseases is promising though not always accurate. Many human diseases, including malformation syndromes, have no clear phenotype to genotype relationship. Some variations in phenotype or penetrance cannot be explained by loss or alteration of a single gene and are likely the result of contiguous genes, transporter proteins or activator proteins. These so-called

modifier genes have become increasingly recognized as an important source for phenotypic variation (Dipple and McCabe, 2000; Nadeau, 2001). A good example of a modified gene in zebrafish is the *squint* (*sqt*) gene (Pei et al., 2007). Loss of the Nodal-related protein Squint causes a spectrum of phenotypes including cyclopia and midline bifurcations. However, the *sqt* deficiency is incompletely penetrant, which allows homozygous mutant embryos to frequently escape cyclopia and even develop as viable and fertile adults. By examining the parameters controlling *sqt* penetrance the authors found that the variable penetrance of this phenotype is substantially influenced by the use of fish from the same genetic background, as well as environmental temperature. A follow-up study revealed a link between Nodal and non-canonical Wnt pathways in the production of midline bifurcations (Pei and Feldman, 2009), providing evidence that Wnt5b and Wnt11 were genetic modifiers of separate phenotypic traits.

A second process that results in variable phenotype penetrance is caused by cilia. Cilia are almost ubiquitously present in vertebrate cells. In mammals, motile cilia normally concentrate in large numbers on the cell surface, beat in an orchestrated wave-like fashion, and are involved in fluid and cell movement. In contrast to motile cilia, primary cilia (monocilia) project as single immotile organelles from the cell surface. Primary cilia are found on nearly all cell types in mammals (Wheatley et al., 1996). Recent discoveries have revealed that cilia have crucial roles in the signal transduction pathways that regulate intracellular Ca^{2+} levels, as well as in the Hedgehog (Hh) and planar cell polarity (PCP) pathways (Goetz and Anderson, 2010). Dysfunction of cilia gives rise to a broad range of human diseases and the diversity in phenotypes caused by ciliary dysfunction reflect the wide variety of functions and the extensive number of ciliary components and regulators (Badano et al., 2006). Studies that link cilia-related proteins to human genetic disorders have shown that compromised ciliary function can have profound consequences for cellular homeostasis. Dysfunction of ciliary proteins gives rise to phenotypes that range from being organ specific (e.g. some polycystic kidney diseases) to broadly pleiotropic (e.g. Bardet-Biedl syndrome). Emerging from this complex spectrum of disease and developmental mutant phenotypes are a set of phenotypic indicators of ciliary dysfunction, including such seemingly unrelated phenotypes as cystic disease of the kidney, liver and pancreas, neural tube defects, postaxial polydactyly, situs inversus, and retinal degeneration. The variance in phenotypic severity can be attributed to the role of the affected protein; for example, structural proteins produce a higher severity than proteins that affect motility.

So, how does this relate to the phenotypes observed in *cpz* mutant embryos? First, mutants were produced and outcrossed in the same genetic background (chapter 4). The evidence for modifier effects comes from a range of phenotypes in different inbred strain backgrounds and multiple human families that are not explained by the disease gene. To exclude the effect of genetic modifiers in the experiments described here, it is necessary to examine the effect on the various phenotypes when the loss-of-function mutation is outcrossed to a different genetic background. Next to this, *cpz* mutants displayed several phenotypic phenomena in tissues that can be affected by ciliopathies in zebrafish (e.g. neural tube, heart formation). To address this in future experiments, ciliated structures such as the Kupffer's vesicle and the neural tube could be examined more closely as well as their secondary effects, including left-right asymmetry (Essner et al., 2005).

WNT/ Ca^{2+} SIGNALING IN THE SKELETON

After identification of Cpz in chapter 2, I determined its expression in and around several ossified structures in the zebrafish skeleton (chapter 3). Loss-of-function analysis in chapter 4 revealed a variety of relatively low penetrant phenotypic phenomena which allowed for a percentage of mutant embryos to develop into full grown fertile adults. The embryos that were affected displayed phenotypes suggesting a role for Cpz in the β -catenin independent signaling Wnt/ Ca^{2+} pathway. Histological analysis of these embryos did however not reveal any phenotypic abnormalities in their skeletal structures. Despite an obvious role for the β -catenin-dependent pathway in bone development and disease (Urano, 2006), the function for the β -catenin-independent Wnt pathways is slowly taking shape. For instance, the planar cell polarity pathway has been implicated in limb morphogenesis (Wang et al., 2011), osteoblast formation (Liu et al., 2007) and chondrocyte formation (DeChiara et al., 2000; Randall et al., 2012). The Wnt/ Ca^{2+} pathway was initially identified as a crucial mediator in development (chapter 1). However, there is substantial evidence that the signaling cascade is also involved in many other molecular phenomena. Although many aspects of Wnt/ Ca^{2+} pathway are yet to be resolved, there is some evidence of a role in the formation of osteoclasts, in which osteoclast precursors express the co-receptor for β -catenin-independent Wnt signaling, Ror2 (Maeda et al., 2007).

Despite our efforts, a skeletal phenotype remained absent and the potential role of Cpz in the formation and functioning of the skeleton is still unclear. The possible effect of the Wnt/ Ca^{2+} pathway on osteoclastogenesis suggests that the efforts in future experimentation should be more directed toward bone homeostasis (e.g. osteoclasts) than bone formation.

HORMONAL REGULATION OF THE SKELETON: A PERSPECTIVE

While the identification of the Cpz protein provided evidence that the Wnt pathway is involved in zebrafish skeletal matrix formation, other signaling pathways are also known to play an important role in bone morphogenesis. In chapter 5 of this thesis, I show the effect of thyroid hormone on bone development in zebrafish. Exposure of zebrafish embryos to different concentrations of thyroid hormone revealed a dose-dependent acceleration of ossification in bone structures. The importance of thyroid hormone in the regulation of skeletal growth and maintenance has been well established, mainly through clinical studies involving human patients and data from genetic mouse models. Here I will provide a perspective on a number of key growth factor signaling pathways that are regulated by thyroid hormone and compare these with the present knowledge from studies in zebrafish.

Thyroid hormone effects on the target cells are mediated via ligand-inducible nuclear receptors/transcription factors, thyroid hormone receptor α and β . Thyroid hormone receptor α seems to be critically important in regulating bone cell functions (Cheng, 2005). Both receptors are expressed in virtually all tissues, but their abundance and roles differ depending on the developmental stage of the organism and the particular tissue type (Forrest et al., 1990). In terms of mechanisms for thyroid hormone action, studies suggest that thyroid hormone regulates a number of key growth factor signaling pathways including fibroblast growth factor, insulin-like growth factor 1 and Wnt to influence skeletal growth.

Fibroblast growth factor (Fgf) signaling is involved in proliferation and specification of many cell types (Ornitz and Itoh, 2001). In humans, mutations in fibroblast growth factor receptors (FGFRs), causing either increased or decreased FGF signaling, generate craniofacial malformations resulting from deficient chondrogenesis (Nie et al., 2006). In mice, FGFR1 controls endoderm patterning in the pharyngeal region and plays a crucial role in cranial neural crest cell migration into the branchial arches (Trokovic et al., 2003). FGFR2 mutant mice develop abnormalities of the skeleton, including defects in normal osteoblastic proliferation and differentiation (Wang et al., 2005). A crucial role for FGFR3 in mediating the effects of T3 in chondrogenesis was suggested after analysis of thyroid receptor mutant mice, in which FGFR3 was reduced in growth plates of thyroid hormone receptor alpha mutants (Barnard et al., 2005). In zebrafish, Fgf receptors control the function of pharyngeal endoderm in late cranial cartilage development (Larbuissou et al., 2013). Depletion of Fgfr1a or Fgfr2 by microinjection of antisense morpholinos results in severe defects in cartilage formation. Despite expression patterns during fin regeneration that suggest a function for Fgfr3 in skeletal formation (Santos-Ruiz et al., 2001), a role for zebrafish Fgfr3 in chondrogenesis and the link to thyroid hormone remains unexplored. In addition, the in chapter 5 discussed consensus that T3 stimulates osteoblast differentiation in an FGF-dependent manner (Harvey et al., 2002; Stevens et al., 2003; Su et al., 2008) is a topic of particular interest since thyroid hormone exposure revealed an accelerated ossification rate (this thesis).

The second important factor is the insulin-like growth factor (IGF) 1, which plays a role in a number of different growth and differentiation processes across a wide variety of tissues including the skeleton (Guntur and Rosen, 2013). This important role in the skeleton is reflected by the peak bone mass which is considerably reduced as a consequence of deficiency of IGF1 action in both humans and experimental animals (Mohan et al., 2003; Zhang et al., 2002). The link between thyroid hormone and IGF1 was determined in studies using genetic mouse models deficient in thyroid hormone (Xing et al., 2012). Serum levels of IGF1 reduced by more than 50% after 21 days as a consequence of a decrease in *Igf1* expression in liver and bone, while daily administration of thyroid hormone increased *Igf1* expression in both liver and bone and normalized the serum IGF1 levels. In zebrafish, thyroid hormone is also able to enhance hepatic *igf1* expression *in vitro* (Reinecke et al., 2005). Moreover, exposure of zebrafish to thyroid hormone *in vivo* induces a significant increase in the expression of the *igf1* gene in the liver, suggesting that zebrafish share a similar regulatory mechanism of the *igf1* gene expression in response to thyroid hormone. This provides evidence for the presence of a vertebrate-like thyroid hormone-Igf signaling pathway (Wang and Zhang, 2011). As discussed in chapter 5, inhibition of both thyroid hormone formation and Igf1 signaling disrupts the jaw development through alterations in neural crest patterning (Bohnsack et al., 2011). In terms of the target cell types for the thyroid hormone effects on *Igf1* expression, several studies found that thyroid hormone treatment increased *Igf1* expression in bone cells and chondrocytes (O'Shea et al., 2005; Xing et al., 2012). However, whether this can be extrapolated to the zebrafish needs yet to be determined.

The Wnt/ β -Catenin signaling pathway has also been recognized as an important signal-transduction pathway in the regulation of growth plate chondrocytes. Inhibition of β -catenin

signaling in mice results in reduced chondrocyte proliferation and differentiation, delayed formation of the secondary ossification center, and reduced skeletal growth (Chen et al., 2008). Thyroid hormone promotes the terminal differentiation of chondrocytes by increasing the expression of *Wnt4*, and thereby the activation of Wnt/ β -Catenin signaling and the expression of the target gene *Runx2/Cbfa1* (Wang et al., 2009). (Interestingly, CPZ is implicated in this process by enhancing β -Catenin signaling activity of *Wnt4*). In addition, thyroid hormone treatment stimulates PI3K/Akt/GSK-3 β signaling (Wang et al., 2010). Both PI3K and Akt are important signal transducers of IGF-1 signaling in which Akt can inactivate GSK-3 β , a negative regulator of the canonical Wnt/ β -catenin pathway (Brazil et al., 2004). The inhibition of PI3K/Akt activity prevents T3-induced *Wnt4* expression and β -catenin activation. This indicates that thyroid hormone promotes growth plate cell differentiation and longitudinal bone growth by activating β -catenin signaling via modulation of IGF1/IGFR1 signaling through the Wnt and PI3K/Akt pathways. In zebrafish, regulation of *igfr1* expression is mediated by the Wnt/ β -catenin pathway during caudal fin regeneration (Wehner et al., 2014), and increased expression of *runx2/cbfa1* results in a significant upregulation of several genes involved in osteogenesis (Li et al., 2009). This process is however not been linked to thyroid hormone actions.

In conclusion, a number of growth factor signaling pathways have been implicated to play an important role in the thyroid hormone regulation of skeletal development growth. In addition with the in chapter 5 introduced and discussed deiodinases, the thyroid system provides a complex and highly regulated system. To what extent these growth factor signaling pathways contribute to thyroid hormone metabolism and action *in vivo* remains to be resolved. There is however substantial overlap in thyroid hormone regulatory pathways between mammals and zebrafish. The use of the zebrafish model in future experimentation will likely contribute to a better understanding of the thyroid axis in development of the vertebrate skeleton.

CONCLUDING REMARKS

For future experiments, it would be advisable to first provide evidence of the nature of Cpz activity by making use of synthetic peptides. These assays have been applied in several studies and are relatively straightforward once the Cpz protein can be expressed *in vitro* (Song and Fricker, 1997; Wang et al., 2009). The same approach could in turn be used to prove the loss-of-function of the mutated zebrafish *cpz* gene. Once able to express *cpz in vitro*, the localization experiments of Cpz (intracellular or extracellular) could be repeated. Also, approaches to detect pathway activation by transiently expressing a *cpz* construct in zebrafish cells that are fitted with a Wnt-dependent reporter assays (Wang et al., 2009) could help to elucidate the function of Cpz. In parallel to these *in vitro* experiments, the *cpz* mutant line should be outcrossed with a different wildtype strain to exclude the possible influence of modifier genes on the representation of phenotypes.

The exploration of the function of Cpz in the zebrafish skeleton remains an attractive option for further investigations. Combining the *cpz* mutant with a transgenic zebrafish line that mark osteoclast (Chatani et al., 2011), could provide insights in the possible function in osteoclastogenesis. To allow analysis of Cpz function in late-stage embryos, techniques that

allow a temporally controlled disruption of gene function should be employed. The use of conditional approaches are essential for determining stage- and tissue-specific functions of genes. One of such techniques is Cre-mediated site-specific recombination (Akagi et al., 1997). Cre mediates the recombination between two *loxP* sites in an efficient site-specific way. Placing the *loxP* sequences appropriately results in the removal of the intervening DNA sequence upon translation of the Cre enzyme. In zebrafish, this system has been successfully converted to an inducible system by placing the *cre* gene under control of a zebrafish heat shock-inducible promoter (Thummel et al., 2005). This allows for manipulation of the host gene at different time points and in specific tissue/cell types, an approach that should be pursued in the future to unravel the precise function of proteins such as the zebrafish carboxypeptidase Z. In addition, such experiments could give insights in the regulation of *cpz* expression by thyroid hormone and the effect on chondral ossification as observed in mammals.

So far, our knowledge of Cpz has been confined to *in vitro* studies and a few independent vertebrate experiments. In this thesis, I show the importance of Cpz in a number of key processes during zebrafish development. The loss-of-function of *cpz* presented a range of phenotypical defects that for the first time implicates Cpz as a component of the β -catenin independent Wnt signaling pathway.

Reference list

- Abdelilah, S., and W. Driever. 1997. Pattern formation in janus-mutant zebrafish embryos. *Developmental biology*. 184:70-84.
- Abu, E.O., S. Bord, A. Horner, V.K. Chatterjee, and J.E. Compston. 1997. The expression of thyroid hormone receptors in human bone. *Bone*. 21:137-142.
- Abuid, J., and P.R. Larsen. 1974. Triiodothyronine and Thyroxine in Hyperthyroidism - Comparison of Acute Changes during Therapy with Antithyroid Agents. *J Clin Invest*. 54:201-208.
- Ahrens, C.H., E. Brunner, E. Qeli, K. Basler, and R. Aebersold. 2010. Generating and navigating proteome maps using mass spectrometry. *Nat Rev Mol Cell Bio*. 11:789-801.
- Akagi, K., V. Sandig, M. Vooijs, M. VanderValk, M. Giovannini, M. Strauss, and A. Berns. 1997. Cre-mediated somatic site-specific recombination in mice. *Nucleic Acids Res*. 25:1766-1773.
- Alves, R.D.A.M., J.A.A. Demmers, K. Bezstarosti, B.C.J. van der Eerden, J.A.N. Verhaar, M. Eijken, and J.P.T.M. van Leeuwen. 2011. Unraveling the Human Bone Microenvironment beyond the Classical Extracellular Matrix Proteins: A Human Bone Protein Library. *J Proteome Res*. 10:4725-4733.
- Anderson, L., and J. Seilhamer. 1997. A comparison of selected mRNA and protein abundances in human liver. *Electrophoresis*. 18:533-537.
- Andress, D.L. 2001. IGF-binding protein-5 stimulates osteoblast activity and bone accretion in ovariectomized mice. *Am J Physiol-Endoc M*. 281:E283-E288.
- Apschner, A., S. Schulte-Merker, and P.E. Witten. 2011. Not All Bones are Created Equal - Using Zebrafish and Other Teleost Species in Osteogenesis Research. *Zebrafish: Disease Models and Chemical Screens, 3rd Edition*. 105:239-255.
- Ashton, B.A., H.J. Hohling, and J.T. Triffitt. 1976. Plasma-Proteins Present in Human Cortical Bone - Enrichment of Alpha-2hs-Glycoprotein. *Calcified tissue research*. 22:27-33.
- Avaron, F., L. Hoffman, D. Guay, and M.A. Akimenko. 2006. Characterization of two new zebrafish members of the hedgehog family: atypical expression of a zebrafish indian hedgehog gene in skeletal elements of both endochondral and dermal origins. *Developmental dynamics : an official publication of the American Association of Anatomists*. 235:478-489.
- Badano, J.L., N. Mitsuma, P.L. Beales, and N. Katsanis. 2006. The ciliopathies: An emerging class of human genetic disorders. *Annu Rev Genom Hum G*. 7:125-148.
- Baggiolini, A., S. Varum, J.M. Mateos, D. Bettosini, N. John, M. Bonalli, U. Ziegler, L. Dimou, H. Clevers, R. Furrer, and L. Sommer. 2015. Premigratory and migratory neural crest cells are multipotent in vivo. *Cell stem cell*. 16:314-322.
- Balooch, G., M. Balooch, R.K. Nalla, S. Schilling, E.H. Filvaroff, G.W. Marshall, S.J. Marshall, R.O. Ritchie, R. Derynck, and T. Alliston. 2005. TGF-beta regulates the mechanical properties and composition of bone matrix. *P Natl Acad Sci USA*. 102:18813-18818.
- Barker, N. 2008. The canonical Wnt/beta-catenin signalling pathway. *Methods in molecular biology*. 468:5-15.
- Barnard, J.C., A.J. Williams, B. Rabier, O. Chassande, J. Samarut, S.Y. Cheng, J.H.D. Bassett, and G.R. Williams. 2005. Thyroid hormones regulate fibroblast growth factor receptor signaling during

- chondrogenesis. *Endocrinology*. 146:5568-5580.
- Barnes, M.R. 2007. Bioinformatics for geneticists : a bioinformatics primer for the analysis of genetic data. Wiley, Chichester, England ; Hoboken, NJ. xxii, 554 p. pp.
- Baron, R., and M. Kneissel. 2013. WNT signaling in bone homeostasis and disease: from human mutations to treatments. *Nat Med*. 19:179-192.
- Bassett, J.H., A. Boyde, P.G. Howell, R.H. Bassett, T.M. Galliford, M. Archanco, H. Evans, M.A. Lawson, P. Croucher, D.L. St Germain, V.A. Galton, and G.R. Williams. 2010. Optimal bone strength and mineralization requires the type 2 iodothyronine deiodinase in osteoblasts. *Proc Natl Acad Sci U S A*. 107:7604-7609.
- Bedell, V.M., Y. Wang, J.M. Campbell, T.L. Poshusta, C.G. Starker, R.G. Krug, W.F. Tan, S.G. Penheiter, A.C. Ma, A.Y.H. Leung, S.C. Fahrenkrug, D.F. Carlson, D.F. Voytas, K.J. Clark, J.J. Essner, and S.C. Ekker. 2012. In vivo genome editing using a high-efficiency TALEN system. *Nature*. 491:114-U133.
- Bell, D.M., K.K.H. Leung, S.C. Wheatley, L.J. Ng, S. Zhou, K.W. Ling, M.H. Sham, P. Koopman, P.P.L. Tam, and K.S.E. Cheah. 1997. SOX9 directly regulates the type-II collagen gene. *Nat Genet*. 16:174-178.
- Bernard, P., A. Fleming, A. Lacombe, V.R. Harley, and E. Vilain. 2008. Wnt4 inhibits beta-catenin/TCF signalling by redirecting beta-catenin to the cell membrane. *Biology of the cell / under the auspices of the European Cell Biology Organization*. 100:167-177.
- Bernardo, B.C., D. Belluoccio, L. Rowley, C.B. Little, U. Hansen, and J.F. Bateman. 2011. Cartilage Intermediate Layer Protein 2 (CILP-2) Is Expressed in Articular and Meniscal Cartilage and Down-regulated in Experimental Osteoarthritis. *Journal of Biological Chemistry*. 286:37758-37767.
- Berridge, M.J., M.D. Bootman, and H.L. Roderick. 2003. Calcium signalling: dynamics, homeostasis and remodelling. *Nature reviews. Molecular cell biology*. 4:517-529.
- Bhatia, V.N., D.H. Perlman, C.E. Costello, and M.E. McComb. 2009. Software Tool for Researching Annotations of Proteins: Open-Source Protein Annotation Software with Data Visualization. *Anal Chem*. 81:9819-9823.
- Bi, W.M., J.M. Deng, Z.P. Zhang, R.R. Behringer, and B. de Crombrughe. 1999. Sox9 is required for cartilage formation. *Nat Genet*. 22:85-89.
- Bialek, P., B. Kern, X.L. Yang, M. Schrock, D. Sosic, N. Hong, H. Wu, K. Yu, D.M. Ornitz, E.N. Olson, M.J. Justice, and G. Karsenty. 2004. A twist code determines the onset of osteoblast differentiation. *Dev Cell*. 6:423-435.
- Bianco, A.C., and B.W. Kim. 2006. Deiodinases: implications of the local control of thyroid hormone action. *J Clin Invest*. 116:2571-2579.
- Bikle, D.D., and Y. Wang. 2012. Insulin like growth factor-I: a critical mediator of the skeletal response to parathyroid hormone. *Current molecular pharmacology*. 5:135-142.
- Bird, N.C., and P.M. Mabee. 2003. Developmental morphology of the axial skeleton of the zebrafish, *Danio rerio* (Ostariophysi : Cyprinidae). *Dev Dynam*. 228:337-357.
- Blader, P., and U. Strahle. 2000. Zebrafish developmental genetics and central nervous system development. *Hum Mol Genet*. 9:945-951.
- Bohnsack, B.L., D. Gallina, and A. Kahana. 2011. Phenothiourea sensitizes zebrafish cranial neural crest and extraocular muscle development to changes in retinoic acid and IGF signaling. *PLoS one*. 6:e22991.
- Bohnsack, B.L., and A. Kahana. 2013. Thyroid hormone and retinoic acid interact to regulate zebrafish craniofacial neural crest development. *Developmental biology*. 373:300-309.

- Brazil, D.P., Z.Z. Yang, and B.A. Hemmings. 2004. Advances in protein kinase B signalling: AKTion on multiple fronts. *Trends Biochem Sci.* 29:233-242.
- Brellier, F., E. Martina, M. Chiquet, J. Ferralli, M. van der Heyden, G. Orend, J.C. Schittny, R. Chiquet-Ehrismann, and R.P. Tucker. 2012. The adhesion modulating properties of tenascin-W. *International journal of biological sciences.* 8:187-194.
- Brown, D.D. 1997. The role of thyroid hormone in zebrafish and axolotl development. *Proc Natl Acad Sci U S A.* 94:13011-13016.
- Bucher, H., A. Prader, and R. Illig. 1985. Head Circumference, Height, Bone-Age and Weight in 103 Children with Congenital Hypothyroidism before and during Thyroid-Hormone Replacement. *Helv Paediatr Acta.* 40:305-316.
- Cadigan, K.M., and R. Nusse. 1997. Wnt signaling: a common theme in animal development. *Genes Dev.* 11:3286-3305.
- Cerda, J., C. Grund, W.W. Franke, and M. Brand. 2002. Molecular characterization of Calymmin, a novel notochord sheath-associated extracellular matrix protein in the zebrafish embryo. *Developmental dynamics : an official publication of the American Association of Anatomists.* 224:200-209.
- Chang, C.T., and T.A. Franz-Odenaal. 2014. Perturbing the developing skull: using laser ablation to investigate the robustness of the infraorbital bones in zebrafish (*Danio rerio*). *Bmc Dev Biol.* 14.
- Chang, J., W. Sonoyama, Z. Wang, Q. Jin, C. Zhang, P.H. Krebsbach, W. Giannobile, S. Shi, and C.Y. Wang. 2007. Noncanonical Wnt-4 signaling enhances bone regeneration of mesenchymal stem cells in craniofacial defects through activation of p38 MAPK. *The Journal of biological chemistry.* 282:30938-30948.
- Chang, J.H., M.H. Wang, W.J. Gui, Y. Zhao, L. Yu, and G.N. Zhu. 2012. Changes in Thyroid Hormone Levels during Zebrafish Development. *Zool Sci.* 29:181-184.
- Chassot, A.A., I. Gillot, and M.C. Chaboissier. 2014. R-spondin1, WNT4, and the CTNNB1 signaling pathway: strict control over ovarian differentiation. *Reproduction.* 148:R97-R110.
- Chatani, M., Y. Takano, and A. Kudo. 2011. Osteoclasts in bone modeling, as revealed by in vivo imaging, are essential for organogenesis in fish. *Developmental biology.* 360:96-109.
- Chen, M., M. Zhu, H. Awad, T.F. Li, T.J. Sheu, B.F. Boyce, D. Chen, and R.J. O'Keefe. 2008. Inhibition of beta-catenin signaling causes defects in postnatal cartilage development. *Journal of cell science.* 121:1455-1465.
- Cheng, S.Y. 2005. Isoform-dependent actions of thyroid hormone nuclear receptors: Lessons from knockin mutant mice. *Steroids.* 70:450-454.
- Chiang, E.F.L., C.I. Pai, M. Wyatt, Y.L. Yan, J. Postlethwait, and B.C. Chung. 2001. Two sox9 genes on duplicated zebrafish chromosomes: Expression of similar transcription activators in distinct sites. *Developmental biology.* 231:149-163.
- Choe, C.P., A. Collazo, A. Trinh le, L. Pan, C.B. Moens, and J.G. Crump. 2013. Wnt-dependent epithelial transitions drive pharyngeal pouch formation. *Dev Cell.* 24:296-309.
- Church, V.L., and P. Francis-West. 2002. Wnt signalling during limb development. *Int J Dev Biol.* 46:927-936.
- Creton, R., J.E. Speksnijder, and L.F. Jaffe. 1998. Patterns of free calcium in zebrafish embryos. *J Gen Physiol.* 112:36a-36a.
- Cruciat, C.M., and C. Niehrs. 2013. Secreted and transmembrane wnt inhibitors and activators. *Cold Spring Harbor perspectives in biology.* 5:a015081.

- Cubbage, C.C., and P.M. Mabee. 1996. Development of the cranium and paired fins in the zebrafish *Danio rerio* (Ostariophysi, cyprinidae). *J Morphol.* 229:121-160.
- D'Costa, A., and I.T. Shepherd. 2009. Zebrafish development and genetics: introducing undergraduates to developmental biology and genetics in a large introductory laboratory class. *Zebrafish.* 6:169-177.
- Day, T.F., X. Guo, L. Garrett-Beal, and Y. Yang. 2005a. Wnt/beta-catenin signaling in mesenchymal progenitors controls osteoblast and chondrocyte differentiation during vertebrate skeletogenesis. *Dev Cell.* 8:739-750.
- de Bruijn, E., E. Cuppen, and H. Feitsma. 2009. Highly Efficient ENU Mutagenesis in Zebrafish. *Methods in molecular biology.* 546:3-12.
- DeChiara, T.M., R.B. Kimble, W.T. Poueymirou, J. Rojas, P. Masiakowski, D.M. Valenzuela, and G.D. Yancopoulos. 2000. Ror2, encoding a receptor-like tyrosine kinase, is required for cartilage and growth plate development. *Nat Genet.* 24:271-274.
- Dentice, M., A. Bandyopadhyay, B. Gereben, I. Callebaut, M.A. Christoffolete, B.W. Kim, S. Nissim, J.P. Mornon, A.M. Zavacki, A. Zeold, L.P. Capelo, C. Curcio-Morelli, R. Ribeiro, J.W. Harney, C.J. Tabin, and A.C. Bianco. 2005. The Hedgehog-inducible ubiquitin ligase subunit WSB-1 modulates thyroid hormone activation and PTHrP secretion in the developing growth plate. *Nat Cell Biol.* 7:698-U687.
- Deshpande, A.S., and E. Beniash. 2008. Bio-inspired Synthesis of Mineralized Collagen Fibrils. *Crystal growth & design.* 8:3084-3090.
- Dijksterhuis, J.P., J. Petersen, and G. Schulte. 2014. WNT/Frizzled signalling: receptor-ligand selectivity with focus on FZD-G protein signalling and its physiological relevance: IUPHAR Review 3. *Br J Pharmacol.* 171:1195-1209.
- Dipple, K.M., and E.R.B. McCabe. 2000. Phenotypes of patients with "simple" mendelian disorders are complex traits: Thresholds, modifiers, and systems dynamics. *American journal of human genetics.* 66:1729-1735.
- EEC. 2006. Regulation (EC) No 1907/2006 of the European parliament and of the council of 18 December 2006 concerning the Registration, Evaluation, Authorisation and Restriction of Chemicals (REACH), establishing a European Chemicals Agency, amending Directive 1999/45/EC and repealing Council Regulation (EEC) No 793/93 and Commission Regulation (EC) No 1488/94 as well as Council Directive 76/769/EEC and Commission Directives 91/155/EEC, 93/67/EEC, 93/105/EC and 2000/21/EC. . E. Commission, editor.
- Engeszer, R.E., L.B. Patterson, A.A. Rao, and D.M. Parichy. 2007. Zebrafish in the wild: a review of natural history and new notes from the field. *Zebrafish.* 4:21-40.
- Enomoto-Iwamoto, M., J. Kitagaki, E. Koyama, Y. Tamamura, C.S. Wu, N. Kanatani, T. Koike, H. Okada, T. Komori, T. Yoneda, V. Church, P.H. Francis-West, K. Kurisu, T. Nohno, M. Pacifici, and M. Iwamoto. 2002. The Wnt antagonist Frzb-1 regulates chondrocyte maturation and long bone development during limb skeletogenesis. *Developmental biology.* 251:142-156.
- Erlebacher, A., and R. Derynck. 1996. Increased expression of TGF-beta 2 in osteoblasts results in an osteoporosis-like phenotype. *J Cell Biol.* 132:195-210.
- Essner, J.J., J.D. Amack, M.K. Nyholm, E.B. Harris, and J. Yost. 2005. Kupffer's vesicle is a ciliated organ of asymmetry in the zebrafish embryo that initiates left-right development of the brain, heart and gut. *Development.* 132:1247-1260.
- Felber, K., P. Croucher, and H.H. Roehl. 2011. Hedgehog signalling is required for perichondral osteoblast differentiation in zebrafish. *Mechanisms of development.* 128:141-152.
- Fiaz, A.W., K.M. Leon-Kloosterziel, G. Gort, S. Schulte-Merker, J.L. van Leeuwen, and S. Kranenbarg. 2012. Swim-training changes the spatio-temporal dynamics of skeletogenesis in zebrafish

- larvae (*Danio rerio*). *PLoS one*. 7:e34072.
- Fitzgerald, J., C. Rich, F.H. Zhou, and U. Hansen. 2008. Three novel collagen VI chains, alpha 4(VI), alpha 5(VI), and alpha 6(VI). *Journal of Biological Chemistry*. 283:20170-20180.
- Flores, M.V., V.W.K. Tsang, W.J. Hu, M. Kalev-Zylinska, J. Postlethwait, P. Crosier, K. Crosier, and S. Fisher. 2004. Duplicate zebrafish runx2 orthologues are expressed in developing skeletal elements. *Gene Expression Patterns*. 4:573-581.
- Forrest, D., M. Sjöberg, and B. Vennström. 1990. Contrasting Developmental and Tissue-Specific Expression of Alpha-Thyroid and Beta-Thyroid Hormone Receptor Genes. *Embo Journal*. 9:1519-1528.
- Freyria, A.M., and M. Becchi. 2004. Changes of chondrocyte metabolism in vitro: an approach by proteomic analysis. *Methods in molecular medicine*. 100:165-182.
- FurutaniSeiki, M., Y.J. Jiang, M. Brand, C.P. Heisenberg, C. Houart, D. Beuchle, F.J.M. van Eeden, M. Granato, P. Haffter, M. Hammerschmidt, D.A. Kane, R.N. Kelsh, M.C. Mullins, J. Odenthal, and C. Nüsslein-Volhard. 1996. Neural degeneration mutants in the zebrafish, *Danio rerio*. *Development*. 123:229-239.
- Georgiou, H.M., G.E. Rice, and M.S. Baker. 2001. Proteomic analysis of human plasma: failure of centrifugal ultrafiltration to remove albumin and other high molecular weight proteins. *Proteomics*. 1:1503-1506.
- Geurtzen, K., F. Knopf, D. Wehner, L.F.A. Huitema, S. Schulte-Merker, and G. Weidinger. 2014. Mature osteoblasts dedifferentiate in response to traumatic bone injury in the zebrafish fin and skull. *Development*. 141:2225-2234.
- Giacomotto, J., and L. Segalat. 2010. High-throughput screening and small animal models, where are we? *Brit J Pharmacol*. 160:204-216.
- Gilbert, S.F. 2000. *Developmental biology*. Sinauer Associates, Sunderland, Mass. xviii, 749 p. pp.
- Gilbert, S.F. 2014. *Developmental biology*. Sinauer Associates, Inc., Publishers, Sunderland, MA, USA. 1 volume (various pagings) pp.
- Glowacki, J., K.A. Cox, J. Osullivan, D. Wilkie, and L.J. Deftos. 1986. Osteoclasts Can Be Induced in Fish Having an Acellular Bony Skeleton. *P Natl Acad Sci USA*. 83:4104-4107.
- Goddard, R.F. 1948. Anatomical and Physiological Studies in Young Rats with Propylthiouracil-Induced Dwarfism. *Anatomical Record*. 101:539-575.
- Goessling, W., and T.E. North. 2011. Hematopoietic stem cell development: using the zebrafish to identify the signaling networks and physical forces regulating hematopoiesis. *Methods in cell biology*. 105:117-136.
- Goetz, S.C., and K.V. Anderson. 2010. The primary cilium: a signalling centre during vertebrate development. *Nat Rev Genet*. 11:331-344.
- Golubkov, V.S., A.V. Chekanov, P. Cieplak, A.E. Aleshin, A.V. Chernov, W.H. Zhu, I.A. Radichev, D.H. Zhang, P.D. Dong, and A.Y. Strongin. 2010. The Wnt/Planar Cell Polarity Protein-tyrosine Kinase-7 (PTK7) Is a Highly Efficient Proteolytic Target of Membrane Type-1 Matrix Metalloproteinase IMPLICATIONS IN CANCER AND EMBRYOGENESIS. *Journal of Biological Chemistry*. 285:35740-35749.
- Goodrich, L.V., and D. Strutt. 2011. Principles of planar polarity in animal development. *Development*. 138:1877-1892.
- Gothe, S., Z.D. Wang, L. Ng, J.M. Kindblom, A.C. Barros, C. Ohlsson, B. Vennström, and D. Forrest. 1999. Mice devoid of all known thyroid hormone receptors are viable but exhibit disorders of the pituitary-thyroid axis, growth, and bone maturation. *Gene Dev*. 13:1329-1341.

- Graham, J.R., A. Chamberland, Q. Lin, X.J. Li, D. Dai, W. Zeng, M.S. Ryan, M.A. Rivera-Bermudez, C.R. Flannery, and Z. Yang. 2013. Serine Protease HTRA1 Antagonizes Transforming Growth Factor-beta Signaling by Cleaving Its Receptors and Loss of HTRA1 In Vivo Enhances Bone Formation. *PLoS one*. 8:e74094.
- Greene, N.D.E., and A.J. Copp. 2009. Development of the vertebrate central nervous system: formation of the neural tube. *Prenatal Diag.* 29:303-311.
- Greiling, T.M., S.A. Houck, and J.I. Clark. 2009. The zebrafish lens proteome during development and aging. *Molecular vision*. 15:2313-2325.
- Grumolato, L., G.Z. Liu, P. Mong, R. Mudbhary, R. Biswas, R. Arroyave, S. Vijayakumar, A.N. Economides, and S.A. Aaronson. 2010. Canonical and noncanonical Wnts use a common mechanism to activate completely unrelated coreceptors. *Gene Dev.* 24:2517-2530.
- Grunz, H. 2004. The vertebrate organizer. Springer, Berlin ; New York. xix, 428 p. pp.
- Guntur, A.R., and C.J. Rosen. 2013. IGF-1 regulation of key signaling pathways in bone. *BoneKEy reports*. 2:437.
- Hammerschmidt, M., F. Pelegri, M.C. Mullins, D.A. Kane, M. Brand, F.J.M. vanEeden, M. FurutaniSeiki, M. Granato, P. Haffter, C.P. Heisenberg, Y.J. Jiang, R.N. Kelsh, J. Odenthal, R.M. Warga, and C. NussleinVolhard. 1996. Mutations affecting morphogenesis during gastrulation and tail formation in the zebrafish, *Danio rerio*. *Development*. 123:143-151.
- Hammond, C.L., and S. Schulte-Merker. 2009. Two populations of endochondral osteoblasts with differential sensitivity to Hedgehog signalling. *Development*. 136:3991-4000.
- Hao, H.X., Y. Xie, Y. Zhang, O. Charlat, E. Oster, M. Avello, H. Lei, C. Mikanin, D. Liu, H. Ruffner, X. Mao, Q. Ma, R. Zamponi, T. Bouwmeester, P.M. Finan, M.W. Kirschner, J.A. Porter, F.C. Serluca, and F. Cong. 2012. ZNRF3 promotes Wnt receptor turnover in an R-spondin-sensitive manner. *Nature*. 485:195-200.
- Harvey, C.B., P.J. O'Shea, A.J. Scott, H. Robson, T. Siebler, S.M. Shalet, J. Samarut, O. Chassande, and G.R. Williams. 2002. Molecular mechanisms of thyroid hormone effects on bone growth and function. *Mol Genet Metab.* 75:17-30.
- Hegde, P.S., I.R. White, and C. Debouck. 2003. Interplay of transcriptomics and proteomics. *Curr Opin Biotech.* 14:647-651.
- Heisenberg, C.P., M. Tada, G.J. Rauch, L. Saude, M.L. Concha, R. Geisler, D.L. Stemple, J.C. Smith, and S.W. Wilson. 2000. Silberblick/Wnt11 mediates convergent extension movements during zebrafish gastrulation. *Nature*. 405:76-81.
- Hou, J., D.R. Clemmons, and S. Smeekens. 2005. Expression and characterization of a serine protease that preferentially cleaves insulin-like growth factor binding protein-5. *J Cell Biochem.* 94:470-484.
- Houston, C.S., J.M. Opitz, J.W. Spranger, R.I. Macpherson, M.H. Reed, E.F. Gilbert, J. Herrmann, and A. Schinzel. 1983. The Campomelic Syndrome - Review, Report of 17 Cases, and Follow-up on the Currently 17-Year-Old Boy 1st Reported by Maroteaux Et Al in 1971. *Am J Med Genet.* 15:3-28.
- Howe, K., M.D. Clark, C.F. Torroja, J. Torrance, C. Berthelot, M. Muffato, J.E. Collins, S. Humphray, K. McLaren, L. Matthews, S. McLaren, I. Sealy, M. Caccamo, C. Churcher, C. Scott, J.C. Barrett, R. Koch, G.J. Rauch, S. White, W. Chow, B. Kilian, L.T. Quintais, J.A. Guerra-Assuncao, Y. Zhou, Y. Gu, J. Yen, J.H. Vogel, T. Eyre, S. Redmond, R. Banerjee, J.X. Chi, B.Y. Fu, E. Langley, S.F. Maguire, G.K. Laird, D. Lloyd, E. Kenyon, S. Donaldson, H. Sehra, J. Almeida-King, J. Loveland, S. Trevanion, M. Jones, M. Quail, D. Willey, A. Hunt, J. Burton, S. Sims, K. McLay, B. Plumb, J. Davis, C. Clee, K. Oliver, R. Clark, C. Riddle, D. Elliott, G. Threadgold, G. Harden, D. Ware, B. Mortimer, G. Kerry, P. Heath, B. Phillimore, A. Tracey, N. Corby, M.

- Dunn, C. Johnson, J. Wood, S. Clark, S. Pelan, G. Griffiths, M. Smith, R. Glithero, P. Howden, N. Barker, C. Stevens, J. Harley, K. Holt, G. Panagiotidis, J. Lovell, H. Beasley, C. Henderson, D. Gordon, K. Auger, D. Wright, J. Collins, C. Raisen, L. Dyer, K. Leung, L. Robertson, K. Ambridge, D. Leongamornlert, S. McGuire, R. Gilderthorp, C. Griffiths, D. Manthravadi, S. Nichol, G. Barker, S. Whitehead, M. Kay, et al. 2013. The zebrafish reference genome sequence and its relationship to the human genome. *Nature*. 496:498-503.
- Hsieh, J.C., A. Rattner, P.M. Smallwood, and J. Nathans. 1999. Biochemical characterization of Wnt-Frizzled interactions using a soluble, biologically active vertebrate Wnt protein. *P Natl Acad Sci USA*. 96:3546-3551.
- Hsu, L.S., and C.Y. Tseng. 2010. Zebrafish Calcium/Calmodulin-Dependent Protein Kinase II (cam-kii) Inhibitors: Expression Patterns and Their Roles in Zebrafish Brain Development. *Dev Dynam*. 239:3098-3105.
- Huitema, L.F.A., A. Apschner, I. Logister, K.M. Spoorendonk, J. Bussmann, C.L. Hammond, and S. Schulte-Merker. 2012. Entpd5 is essential for skeletal mineralization and regulates phosphate homeostasis in zebrafish. *P Natl Acad Sci USA*. 109:21372-21377.
- Inada, M., Y.M. Wang, M.H. Byrne, M.U. Rahman, C. Miyaura, C. Lopez-Otin, and S.M. Krane. 2004. Critical roles for collagenase-3 (Mmp13) in development of growth and in endochondral plate cartilage ossification. *P Natl Acad Sci USA*. 101:17192-17197.
- Inohaya, K., Y. Takano, and A. Kudo. 2010. Production of Wnt4b by floor plate cells is essential for the segmental patterning of the vertebral column in medaka. *Development*. 137:1807-1813.
- Irvine, C.H.G. 1974. Concentration of Thyroxine in Cellular and Extracellular Tissues of Sheep and Rate of Equilibration of Labeled Thyroxine. *Endocrinology*. 94:1060-1071.
- Ishitani, T., S. Kishida, J. Hyodo-Miura, N. Ueno, J. Yasuda, M. Waterman, H. Shibuya, R.T. Moon, J. Ninomiya-Tsuji, and K. Matsumoto. 2003. The TAK1-NLK mitogen-activated protein kinase cascade functions in the Wnt-5a/Ca²⁺ pathway to antagonize Wnt/beta-catenin signaling. *Molecular and cellular biology*. 23:131-139.
- James, C.G., C.T.G. Appleton, V. Ulici, T.M. Underhill, and F. Beier. 2005. Microarray analyses of gene expression during chondrocyte differentiation identifies novel regulators of hypertrophy. *Molecular biology of the cell*. 16:5316-5333.
- Janda, C.Y., D. Waghray, A.M. Levin, C. Thomas, and K.C. Garcia. 2012. Structural Basis of Wnt Recognition by Frizzled. *Science*. 337:59-64.
- Jiang, X.G., M.L. Ye, X.N. Jiang, G.P. Liu, S. Feng, L. Cui, and H.F. Zou. 2007. Method development of efficient protein extraction in bone tissue for proteome analysis. *J Proteome Res*. 6:2287-2294.
- Jomaa, B., S.A. Hermsen, M.Y. Kessels, J.H. van den Berg, A.A. Peijnenburg, J.M. Aarts, A.H. Piersma, and I.M. Rietjens. 2014. Developmental toxicity of thyroid-active compounds in a zebrafish embryotoxicity test. *Altex*. 31:303-317.
- Jorgensen, E.M., and S.E. Mango. 2002. The art and design of genetic screens: *Caenorhabditis elegans*. *Nat Rev Genet*. 3:356-369.
- Kanatani, M., T. Sugimoto, H. Sowa, T. Kobayashi, M. Kanzawa, and K. Chihara. 2004. Thyroid hormone stimulates osteoclast differentiation by a mechanism independent of RANKL-RANK interaction. *Journal of cellular physiology*. 201:17-25.
- Kapitanova, D.V., and F.N. Shkil. 2014. Effects of thyroid hormone level alterations on the development of supraneural series in zebrafish, *Danio rerio*. *J Appl Ichthyol*. 30:821-824.
- Karaplis, A.C., A. Luz, J. Glowacki, R.T. Bronson, V.L. Tybulewicz, H.M. Kronenberg, and R.C. Mulligan. 1994. Lethal skeletal dysplasia from targeted disruption of the parathyroid hormone-related peptide gene. *Genes Dev*. 8:277-289.

- Karp, S.J., E. Schipani, B. St-Jacques, J. Hunzelman, H. Kronenberg, and A.P. McMahon. 2000. Indian hedgehog coordinates endochondral bone growth and morphogenesis via parathyroid hormone related-protein-dependent and -independent pathways. *Development*. 127:543-548.
- Karve, T.M., and A.K. Cheema. 2011. Small changes huge impact: the role of protein posttranslational modifications in cellular homeostasis and disease. *Journal of amino acids*. 2011:207691.
- Kawano, Y., and R. Kypta. 2003. Secreted antagonists of the Wnt signalling pathway. *Journal of cell science*. 116:2627-2634.
- Kessels, M.Y., L.F. Huitema, S. Boeren, S. Kranenbarg, S. Schulte-Merker, J.L. van Leeuwen, and S.C. de Vries. 2014. Proteomics analysis of the zebrafish skeletal extracellular matrix. *PLoS one*. 9:e90568.
- Kilian, B., H. Mansukoski, F.C. Barbosa, F. Ulrich, M. Tada, and C.P. Heisenberg. 2003. The role of Ppt/Wnt5 in regulating cell shape and movement during zebrafish gastrulation. *Mechanisms of development*. 120:467-476.
- Kim, H.Y., and S. Mohan. 2013. Role and Mechanisms of Actions of Thyroid Hormone on the Skeletal Development. *Bone Res*. 2.
- Kim, T., K. Kim, S.H. Lee, H.S. So, J. Lee, N. Kim, and Y. Choi. 2009. Identification of LRRc17 as a Negative Regulator of Receptor Activator of NF-kappa B Ligand (RANKL)-induced Osteoclast Differentiation. *Journal of Biological Chemistry*. 284:15308-15316.
- Kimmel, C.B., A. DeLaurier, B. Ullmann, J. Dowd, and M. McFadden. 2010. Modes of developmental outgrowth and shaping of a craniofacial bone in zebrafish. *PLoS one*. 5:e9475.
- Kini, U., and B.N. Nandeesh. 2012. Physiology of Bone Formation, Remodeling, and Metabolism. In *I. Fogelman, G. Gnanasegaran, and H. van der Wall (eds.), Radionuclide and Hybrid Bone Imaging*
- Kohn, A.D., and R.T. Moon. 2005. Wnt and calcium signaling: beta-Catenin-independent pathways. *Cell Calcium*. 38:439-446.
- Komori, T., H. Yagi, S. Nomura, A. Yamaguchi, K. Sasaki, K. Deguchi, Y. Shimizu, R.T. Bronson, Y.H. Gao, M. Inada, M. Sato, R. Okamoto, Y. Kitamura, S. Yoshiki, and T. Kishimoto. 1997. Targeted disruption of Cbfa1 results in a complete lack of bone formation owing to maturational arrest of osteoblasts. *Cell*. 89:755-764.
- Kronenberg, H.M. 2003. Developmental regulation of the growth plate. *Nature*. 423:332-336.
- Kronenberg, H.M. 2004. Twist genes regulate Runx2 and bone formation. *Dev Cell*. 6:317-318.
- Kuhl, M., L.C. Sheldahl, M. Park, J.R. Miller, and R.T. Moon. 2000. The Wnt/Ca2+ pathway: a new vertebrate Wnt signaling pathway takes shape. *Trends in genetics : TIG*. 16:279-283.
- Kvist, A.J., A. Nystrom, K. Hultenby, T. Sasaki, J.F. Talts, and A. Aspberg. 2008. The major basement membrane components localize to the chondrocyte pericellular matrix - A cartilage basement membrane equivalent? *Matrix Biology*. 27:22-33.
- Lammi, M.J., J. Hayrinen, and A. Mahonen. 2006. Proteomic analysis of cartilage- and bone-associated samples. *Electrophoresis*. 27:2687-2701.
- Lapetina, E.G., and R.H. Michell. 1973. Phosphatidylinositol Metabolism in Cells Receiving Extracellular Stimulation. *FEBS letters*. 31:1-10.
- Larabell, C.A., M. Torres, B.A. Rowning, C. Yost, J.R. Miller, M. Wu, D. Kimelman, and R.T. Moon. 1997. Establishment of the dorso-ventral axis in *Xenopus* embryos is presaged by early asymmetries in beta-catenin that are modulated by the Wnt signaling pathway. *J Cell Biol*. 136:1123-1136.
- Larbuissou, A., J. Dalcq, J.A. Martial, and M. Muller. 2013. Fgf receptors Fgfr1a and Fgfr2 control the

- function of pharyngeal endoderm in late cranial cartilage development. *Differentiation*. 86:192-206.
- Lawson, N.D., and S.A. Wolfe. 2011. Forward and Reverse Genetic Approaches for the Analysis of Vertebrate Development in the Zebrafish. *Dev Cell*. 21:48-64.
- LeClair, E.E., S.R. Mui, A. Huang, J.M. Topczewska, and J. Topczewski. 2009. Craniofacial Skeletal Defects of Adult Zebrafish glypican 4 (knypek) Mutants. *Dev Dynam*. 238:2550-2563.
- Lee, C., E. Bongcam-Rudloff, C. Sollner, W. Jahnen-Dechent, and L. Claesson-Welsh. 2009. Type 3 cystatins; fetuins, kininogen and histidine-rich glycoprotein. *Front Biosci*. 14:2911-2922.
- Lee, K.W., S.E. Webb, and A.L. Miller. 2003. Ca²⁺ released via IP3 receptors is required for furrow deepening during cytokinesis in zebrafish embryos. *Int J Dev Biol*. 47:411-421.
- Lee, K.W., S.E. Webb, and A.L. Miller. 2006. Requirement for a localized, IP3R-generated Ca²⁺ transient during the furrow positioning process in zebrafish zygotes. *Zygote*. 14:143-155.
- Li, N., K. Felber, P. Elks, P. Croucher, and H.H. Roehl. 2009. Tracking Gene Expression During Zebrafish Osteoblast Differentiation. *Dev Dynam*. 238:459-466.
- Li, Q., A. Kannan, A. Das, F.J. Demayo, P.J. Hornsby, S.L. Young, R.N. Taylor, M.K. Bagchi, and I.C. Bagchi. 2013. WNT4 acts downstream of BMP2 and functions via beta-catenin signaling pathway to regulate human endometrial stromal cell differentiation. *Endocrinology*. 154:446-457.
- Li, S.D., R. Esterberg, V. Lachance, D.D. Ren, K. Radde-Gallwitz, F.L. Chi, J.L. Parent, A. Fritz, and P. Chen. 2011. Rack1 is required for Vangl2 membrane localization and planar cell polarity signaling while attenuating canonical Wnt activity. *P Natl Acad Sci USA*. 108:2264-2269.
- Lieschke, G.J., and P.D. Currie. 2007. Animal models of human disease: zebrafish swim into view. *Nat Rev Genet*. 8:353-367.
- Liu, A.P., A. Majumdar, H.E. Schauerte, P. Haffter, and I.A. Drummond. 2000. Zebrafish wnt4b expression in the floor plate is altered in sonic hedgehog and gli-2 mutants. *Mechanisms of development*. 91:409-413.
- Liu, Y., R.A. Bhat, L.M. Seestaller-Wehr, S. Fukayama, A. Mangine, R.A. Moran, B.S. Komm, P.V. Bodine, and J. Billiard. 2007. The orphan receptor tyrosine kinase Ror2 promotes osteoblast differentiation and enhances ex vivo bone formation. *Mol Endocrinol*. 21:376-387.
- Liu, Y.W., and W.K. Chan. 2002. Thyroid hormones are important for embryonic to larval transitory phase in zebrafish. *Differentiation*. 70:36-45.
- Lu, C., Y. Wan, J.J. Cao, X.M. Zhu, J. Yu, R.J. Zhou, Y.Y. Yao, L.L. Zhang, H.X. Zhao, H.J. Li, J.Z. Zhao, L. He, G. Ma, X. Yang, Z.J. Yao, and X.Z. Guo. 2013. Wnt-mediated reciprocal regulation between cartilage and bone development during endochondral ossification. *Bone*. 53:566-574.
- Lu, F.I., C. Thisse, and B. Thisse. 2011. Identification and mechanism of regulation of the zebrafish dorsal determinant. *Proc Natl Acad Sci U S A*. 108:15876-15880.
- Mackay, E., Apschner, A., and Schulte-Merker, S. 2013. A Bone To Pick with Zebrafish. *BoneKey*. in press.
- Mackie, E.J., Y.A. Ahmed, L. Tatarczuch, K.S. Chen, and M. Mirams. 2008. Endochondral ossification: How cartilage is converted into bone in the developing skeleton. *Int J Biochem Cell B*. 40:46-62.
- Maeda, K., Y. Kobayashi, T. Mizoguchi, Y. Nakamichi, T. Yamashita, S. Kinugawa, N. Udagawa, K. Marumo, and N. Takahashi. 2007. Wnt5a enhances RANKL-induced osteoclastogenesis. *J Bone Miner Res*. 22:S43-S43.

- Maia, A.L., I.M. Goemann, E.L. Meyer, and S.M. Wajner. 2011. Deiodinases: the balance of thyroid hormone: type 1 iodothyronine deiodinase in human physiology and disease. *The Journal of endocrinology*. 209:283-297.
- Manza, L.L., S.L. Stamer, A.J.L. Ham, S.G. Codreanu, and D.C. Liebler. 2005. Sample preparation and digestion for proteomic analyses using spin filters. *Proteomics*. 5:1742-1745.
- Matsui, T., A. Raya, Y. Kawakami, C. Callol-Massot, J. Capdevila, C. Rodriguez-Esteban, and J.C.I. Belmonte. 2005. Noncanonical Wnt signaling regulates midline convergence of organ primordia during zebrafish development. *Gene Dev*. 19:164-175.
- Meeker, N.D., S.A. Hutchinson, L. Ho, and N.S. Treacle. 2007. Method for isolation of PCR-ready genomic DNA from zebrafish tissues. *Biotechniques*. 43:610-+.
- Michell, R.H. 1975. Inositol Phospholipids and Cell-Surface Receptor Function. *Biochimica et biophysica acta*. 415:81-147.
- Mikels, A.J., and R. Nusse. 2006. Purified Wnt5a protein activates or inhibits beta-catenin-TCF signaling depending on receptor context. *Plos Biol*. 4:e115.
- Miller, J.R. 2002. The Wnts. *Genome biology*. 3:REVIEWS3001.
- Mitchell, R.E., L.F.A. Huitema, R.E.H. Skinner, L.H. Brunt, C. Severn, S. Schulte-Merker, and C.L. Hammond. 2013. New tools for studying osteoarthritis genetics in zebrafish. *Osteoarthritis Cartilage*. 21:269-278.
- Moeller, C., E.C. Swindell, A. Kispert, and G. Eichele. 2003. Carboxypeptidase Z (CPZ) modulates Wnt signaling and regulates the development of skeletal elements in the chicken. *Development*. 130:5103-5111.
- Mohan, S., J.R. Farley, and D.J. Baylink. 1995. Age-related changes in IGFBP-4 and IGFBP-5 levels in human serum and bone: implications for bone loss with aging. *Progress in growth factor research*. 6:465-473.
- Mohan, S., C. Richman, R.Q. Guo, Y. Amaar, L.R. Donahue, J. Wergedal, and D.J. Baylink. 2003. Insulin-like growth factor regulates peak bone mineral density in mice by both growth hormone-dependent and -independent mechanisms. *Endocrinology*. 144:929-936.
- Moriyama, K., T. Tagami, T. Usui, M. Naruse, T. Nambu, Y. Hataya, N. Kanamoto, Y.S. Li, A. Yasoda, H. Arai, and K. Nakao. 2007. Antithyroid drugs inhibit thyroid hormone receptor-mediated transcription. *J Clin Endocr Metab*. 92:1066-1072.
- Mullins, M.C., M. Hammerschmidt, D.A. Kane, J. Odenthal, M. Brand, F.J. van Eeden, M. Furutani-Seiki, M. Granato, P. Haffter, C.P. Heisenberg, Y.J. Jiang, R.N. Kelsh, and C. Nusslein-Volhard. 1996. Genes establishing dorsoventral pattern formation in the zebrafish embryo: the ventral specifying genes. *Development*. 123:81-93.
- Nadeau, J.H. 2001. Modifier genes in mice and humans. *Nat Rev Genet*. 2:165-174.
- Nagayama, M., M. Iwamoto, A. Hargett, N. Kamiya, Y. Tamamura, B. Young, T. Morrison, H. Takeuchi, M. Pacifici, M. Enomoto-Iwamoto, and E. Koyama. 2008. Wnt/beta-catenin signaling regulates cranial base development and growth. *J Dent Res*. 87:244-249.
- Nakamura, H., J.Y. Noh, K. Itoh, S. Fukata, A. Miyauchi, and N. Hamada. 2007. Comparison of methimazole and propylthiouracil in patients with hyperthyroidism caused by Graves' disease. *The Journal of clinical endocrinology and metabolism*. 92:2157-2162.
- Nakamura, H., G. Sato, A. Hirata, and T. Yamamoto. 2004. Immunolocalization of matrix metalloproteinase-13 on bone surface under osteoclasts in rat tibia. *Bone*. 34:48-56.
- Nasevicius, A., T. Hyatt, H. Kim, J. Guttman, E. Walsh, S. Sumanas, Y.S. Wang, and S.C. Ekker. 1998. Evidence for a frizzled-mediated wnt pathway required for zebrafish dorsal mesoderm formation. *Development*. 125:4283-4292.

- Nicol, B., A. Guerin, A. Fostier, and Y. Guiguen. 2012. Ovary-predominant wnt4 expression during gonadal differentiation is not conserved in the rainbow trout (*Oncorhynchus mykiss*). *Molecular reproduction and development*. 79:51-63.
- Nie, X.G., K. Luukko, and P. Kettunen. 2006. FGF signalling in craniofacial development and developmental disorders. *Oral Dis*. 12:102-111.
- Niehrs, C. 2012. The complex world of WNT receptor signalling. *Nature reviews. Molecular cell biology*. 13:767-779.
- Nishino, J., K. Yamashita, H. Hashiguchi, H. Fujii, T. Shimazaki, and H. Hamada. 2004. Meteorin: a secreted protein that regulates glial cell differentiation and promotes axonal extension. *The EMBO journal*. 23:1998-2008.
- Novikova, E., L.D. Fricker, and S.E. Reznik. 2001. Metalloproteinase Z is dynamically expressed in mouse development. *Mechanisms of development*. 102:259-262.
- Novikova, E.G., and L.D. Fricker. 1999. Purification and characterization of human metalloproteinase Z. *Biochemical and biophysical research communications*. 256:564-568.
- Novikova, E.G., S.E. Reznik, O. Varlamov, and L.D. Fricker. 2000. Carboxypeptidase Z is present in the regulated secretory pathway and extracellular matrix in cultured cells and in human tissues. *Journal of Biological Chemistry*. 275:4865-4870.
- Nunez, C., A. Esteve-Nunez, C. Giometti, S. Tollaksen, T. Khare, W. Lin, D.R. Lovley, and B.A. Methe. 2006. DNA microarray and proteomic analyses of the RpoS regulon in *Geobacter sulfurreducens*. *J Bacteriol*. 188:2792-2800.
- Nusse, R., and H. Varmus. 2012. Three decades of Wnts: a personal perspective on how a scientific field developed. *Embo Journal*. 31:2670-2684.
- O'Brien, T.P., and W.N. Frankel. 2004. Moving forward with chemical mutagenesis in the mouse. *J Physiol-London*. 554:13-21.
- O'Shea, P.J., J.H. Bassett, S. Srisankharajah, H. Ying, S.Y. Cheng, and G.R. Williams. 2005. Contrasting skeletal phenotypes in mice with an identical mutation targeted to thyroid hormone receptor alpha1 or beta. *Mol Endocrinol*. 19:3045-3059.
- O'Shea, P.J., C.B. Harvey, H. Suzuki, M. Kaneshige, K. Kaneshige, S.Y. Cheng, and G.R. Williams. 2003. A thyrotoxic skeletal phenotype of advanced bone formation in mice with resistance to thyroid hormone. *Mol Endocrinol*. 17:1410-1424.
- Onnerfjord, P., A. Khabut, F.P. Reinholt, O. Svensson, and D. Heinegard. 2012. Quantitative Proteomic Analysis of Eight Cartilaginous Tissues Reveals Characteristic Differences as well as Similarities between Subgroups. *Journal of Biological Chemistry*. 287:18913-18924.
- Ornitz, D.M., and N. Itoh. 2001. Fibroblast growth factors. *Genome biology*. 2.
- Orozco, A., and R.C. Valverde. 2005. Thyroid hormone deiodination in fish. *Thyroid : official journal of the American Thyroid Association*. 15:799-813.
- Otto, F., A.P. Thornell, T. Crompton, A. Denzel, K.C. Gilmour, I.R. Rosewell, G.W.H. Stamp, R.S.P. Beddington, S. Mundlos, B.R. Olsen, P.B. Selby, and M.J. Owen. 1997. *Cbfa1*, a candidate gene for cleidocranial dysplasia syndrome, is essential for osteoblast differentiation and bone development. *Cell*. 89:765-771.
- Pei, W., and B. Feldman. 2009. Identification of common and unique modifiers of zebrafish midline bifurcation and cyclopia. *Developmental biology*. 326:201-211.
- Pei, W., P.H. Williams, M.D. Clark, D.L. Stemple, and B. Feldman. 2007. Environmental and genetic modifiers of squint penetrance during zebrafish embryogenesis. *Developmental biology*. 308:368-378.

- Peifer, M., and P. Polakis. 2000. Wnt signaling in oncogenesis and embryogenesis--a look outside the nucleus. *Science*. 287:1606-1609.
- Pelayo, S., E. Oliveira, B. Thienpont, P.J. Babin, D. Raldua, M. Andre, and B. Pina. 2012. Triiodothyronine-induced changes in the zebrafish transcriptome during the eleutheroembryonic stage: implications for bisphenol A developmental toxicity. *Aquat Toxicol*. 110-111:114-122.
- Pelegri, F., H. Knaut, H.M. Maischein, S. Schulte-Merker, and C. Nusslein-Volhard. 1999. A mutation in the zebrafish maternal-effect gene *nebel* affects furrow formation and *vasa* RNA localization. *Curr Biol*. 9:1431-1440.
- Pelegri, F.J. 2011. Vertebrate embryogenesis : embryological, cellular, and genetic methods. Humana Press : Springer, New York. xi, 605 p. pp.
- Peruzzi, B., A. Cappariello, A. Del Fattore, N. Rucci, F. De Benedetti, and A. Teti. 2012. c-Src and IL-6 inhibit osteoblast differentiation and integrate IGFBP5 signalling. *Nat Commun*. 3.
- Pieper, U., B.M. Webb, G.Q. Dong, D. Schneidman-Duhovny, H. Fan, S.J. Kim, N. Khuri, Y.G. Spill, P. Weinkam, M. Hammel, J.A. Tainer, M. Nilges, and A. Sali. 2014. ModBase, a database of annotated comparative protein structure models and associated resources. *Nucleic Acids Res*. 42:D336-D346.
- Povelones, M., and R. Nusse. 2005. The role of the cysteine-rich domain of Frizzled in Wntless-Armadillo signaling. *Embo Journal*. 24:3493-3503.
- Power, D.M., L. Llewellyn, M. Faustino, M.A. Nowell, B.T. Bjornsson, I.E. Einarsdottir, A.V. Canario, and G.E. Sweeney. 2001. Thyroid hormones in growth and development of fish. *Comparative biochemistry and physiology. Toxicology & pharmacology : CBP*. 130:447-459.
- Quondamatteo, F. 2002. Assembly, stability and integrity of basement membranes in vivo. *Histochem J*. 34:369-381.
- Ramachandran, R., X.F. Zhao, and D. Goldman. 2011. Ascl1a/Dkk/beta-catenin signaling pathway is necessary and glycogen synthase kinase-3beta inhibition is sufficient for zebrafish retina regeneration. *Proc Natl Acad Sci U S A*. 108:15858-15863.
- Randall, R.M., Y.Y. Shao, L. Wang, and R.T. Ballock. 2012. Activation of Wnt Planar cell polarity (PCP) signaling promotes growth plate column formation in vitro. *J Orthopaed Res*. 30:1906-1914.
- Regard, J.B., Z. Zhong, B.O. Williams, and Y. Yang. 2012. Wnt signaling in bone development and disease: making stronger bone with Wnts. *Cold Spring Harbor perspectives in biology*. 4.
- Reinecke, M., B.T. Bjornsson, W.W. Dickhoff, S.D. McCormick, I. Navarro, D.M. Power, and J. Gutierrez. 2005. Growth hormone and insulin-like growth factors in fish: Where we are and where to go. *General and comparative endocrinology*. 142:20-24.
- Renn, J., C. Winkler, M. Scharlt, R. Fischer, and R. Goerlich. 2006. Zebrafish and medaka as models for bone research including implications regarding space-related issues. *Protoplasma*. 229:209-214.
- Reverdin, J.-L., and A. Reverdin. 1883. Note sur vingt-deux opérations de goître. Accidents et résultats. *Revue Médicale de La Suisse Romande* 3.
- Reznik, S.E., and L.D. Fricker. 2001. Carboxypeptidases from A to Z: implications in embryonic development and Wnt binding. *Cell Mol Life Sci*. 58:1790-1804.
- Rotllant, J., D. Liu, Y.L. Yan, J.H. Postlethwait, M. Westerfield, and S.J. Du. 2008. Sparc (Osteonectin) functions in morphogenesis of the pharyngeal skeleton and inner ear. *Matrix Biology*. 27:561-572.
- Rozen, S., and H. Skaletsky. 2000. Primer3 on the WWW for general users and for biologist programmers. *Methods in molecular biology*. 132:365-386.

- Rulifson, E.J., C.H. Wu, and R. Nusse. 2000. Pathway specificity by the bifunctional receptor frizzled is determined by affinity for wingless. *Mol Cell*. 6:117-126.
- Sanders, L.H., and K.E. Whitlock. 2003. Phenotype of the zebrafish masterblind (mb1) mutant is dependent on genetic background. *Dev Dynam*. 227:291-300.
- Sandler, B., P. Webb, J.W. Apriletti, B.R. Huber, M. Togashi, S.T.C. Lima, S. Juric, S. Nilsson, R. Wagner, R.J. Fletterick, and J.D. Baxter. 2004. Thyroxine-thyroid hormone receptor interactions. *Journal of Biological Chemistry*. 279:55801-55808.
- Santaolalla-Montoya, F., A. Martinez-Ibarguen, J.M. Sanchez-Fernandez, and A. Sanchez-del-Rey. 2012. Principles of cranial base ossification in humans and rats. *Acta Oto-Laryngol*. 132:349-354.
- Santos-Ruiz, L., J.A. Santamaria, and J. Becerra. 2001. Differential expression of FGF receptors during zebrafish fin regeneration. *Int J Dev Biol*. 45:S131-S132.
- Sawada, H., N. Inoue, and M. Iwano. 2014. Sexual reproduction in animals and plants. SpringerOpen, Tokyo ; New York. xii, 480 pages pp.
- Schipani, E., K. Kruse, and H. Juppner. 1995. A constitutively active mutant PTH-PTHrP receptor in Jansen-type metaphyseal chondrodysplasia. *Science*. 268:98-100.
- Schreiweis, M.A., J.P. Butler, N.H. Kulkarni, M.D. Knierman, R.E. Higgs, D.L. Halladay, J.E. Onyia, and J.E. Hale. 2007. A proteomic analysis of adult rat bone reveals the presence of cartilage/chondrocyte markers. *J Cell Biochem*. 101:466-476.
- Schroeder, A.C., and M.L. Privalsky. 2014. Thyroid hormones, t3 and t4, in the brain. *Frontiers in endocrinology*. 5:40.
- Schulte-Merker, S. 2002. Looking at embryos. In Zebrafish - A practical approach. 39-58.
- Schwanhauser, B., D. Busse, N. Li, G. Dittmar, J. Schuchhardt, J. Wolf, W. Chen, and M. Selbach. 2011. Global quantification of mammalian gene expression control. *Nature*. 473:337-342.
- Segni, M., E. Leonardi, B. Mazzone, I. Pucarelli, and A.M. Pasquino. 1999. Special features of Graves' disease in early childhood. *Thyroid : official journal of the American Thyroid Association*. 9:871-877.
- Sepich, D.S., D.C. Myers, R. Short, J. Topczewski, F. Marlow, and L. Solnica-Krezel. 2000. Role of the zebrafish trilobite locus in gastrulation movements of convergence and extension. *Genesis*. 27:159-173.
- Shkil, F.N., D.V. Kapitanova, V.B. Borisov, B. Abdissa, and S.V. Smirnov. 2012. Thyroid hormone in skeletal development of cyprinids: effects and morphological consequences. *J Appl Ichthyol*. 28:398-405.
- Simo-Costa, M., and M.E. Bronner. 2013. Insights into neural crest development and evolution from genomic analysis. *Genome Res*. 23:1069-1080.
- Singh, S.K., M.G. Lakshmi, S. Saxena, C.V. Swamy, and M.M. Idris. 2011. Proteome profile of zebrafish caudal fin based on one-dimensional gel electrophoresis LCMS/MS and two-dimensional gel electrophoresis MALDI MS/MS analysis. *Journal of separation science*. 34:225-232.
- Sintuu, C., S.S. Murray, K. Behnam, R. Simon, J. Jawien, J.D. Silva, M.E. Duarte, and E.J. Brochmann. 2008. Full-length bovine spp24 [spp24 (24-203)] inhibits BMP-2 induced bone formation. *J Orthopaed Res*. 26:753-758.
- Slusarski, D.C., V.G. Corces, and R.T. Moon. 1997a. Interaction of Wnt and a Frizzled homologue triggers G-protein-linked phosphatidylinositol signalling. *Nature*. 390:410-413.
- Slusarski, D.C., J. Yang-Snyder, W.B. Busa, and R.T. Moon. 1997b. Modulation of embryonic intracellular Ca²⁺ signaling by Wnt-5A. *Developmental biology*. 182:114-120.

- Smith, A., J. Zhang, D. Guay, E. Quint, A. Johnson, and M.A. Akimenko. 2008. Gene expression analysis on sections of zebrafish regenerating fins reveals limitations in the whole-mount in situ hybridization method. *Developmental dynamics : an official publication of the American Association of Anatomists*. 237:417-425.
- Song, L.X., and L.D. Fricker. 1997. Cloning and expression of human carboxypeptidase Z, a novel metallocarboxypeptidase. *Journal of Biological Chemistry*. 272:10543-10550.
- Sophia Fox, A.J., A. Bedi, and S.A. Rodeo. 2009. The basic science of articular cartilage: structure, composition, and function. *Sports health*. 1:461-468.
- Soto, A.M., H. Justicia, J.W. Wray, and C. Sonnenschein. 1991. p-Nonyl-phenol: an estrogenic xenobiotic released from "modified" polystyrene. *Environmental health perspectives*. 92:167-173.
- Spemann, H. 1938. Embryonic development and induction. Yale University Press; H. Milford, Oxford University Press, New Haven, London,. xii, 401 p. pp.
- Spence, R., G. Gerlach, C. Lawrence, and C. Smith. 2008. The behaviour and ecology of the zebrafish, *Danio rerio*. *Biological reviews of the Cambridge Philosophical Society*. 83:13-34.
- Spoorendonk, K.M., C.L. Hammond, L.F.A. Huitema, J. Vanoevelen, and S. Schulte-Merker. 2010. Zebrafish as a unique model system in bone research: the power of genetics and in vivo imaging. *J Appl Ichthyol*. 26:219-224.
- Spoorendonk, K.M., J. Peterson-Maduro, J. Renn, T. Trowe, S. Kranenbarg, C. Winkler, and S. Schulte-Merker. 2008. Retinoic acid and Cyp26b1 are critical regulators of osteogenesis in the axial skeleton. *Development*. 135:3765-3774.
- Sprague, J., D. Clements, T. Conlin, P. Edwards, K. Frazer, K. Schaper, E. Segerdell, P.R. Song, B. Sprunger, and M. Westerfield. 2003. The Zebrafish Information Network (ZFIN): the zebrafish model organism database. *Nucleic Acids Res*. 31:241-243.
- St-Jacques, B., M. Hammerschmidt, and A.P. McMahon. 1999. Indian hedgehog signaling regulates proliferation and differentiation of chondrocytes and is essential for bone formation. *Genes Dev*. 13:2072-2086.
- St Johnston, D. 2002. The art and design of genetic screens: *Drosophila melanogaster*. *Nat Rev Genet*. 3:176-188.
- Stevens, D.A., C.B. Harvey, A.J. Scott, P.J. O'Shea, J.C. Barnard, A.J. Williams, G. Brady, J. Samarut, O. Chassande, and G.R. Williams. 2003. Thyroid hormone activates fibroblast growth factor receptor-1 in bone. *Mol Endocrinol*. 17:1751-1766.
- Stevens, D.A., R.P. Hasserjian, H. Robson, T. Siebler, S.M. Shalet, and G.R. Williams. 2000. Thyroid hormones regulate hypertrophic chondrocyte differentiation and expression of parathyroid hormone-related peptide and its receptor during endochondral bone formation. *J Bone Miner Res*. 15:2431-2442.
- Stickens, D., D.J. Behonick, N. Ortega, B. Heyer, B. Hartenstein, Y. Yu, A.J. Fosang, M. Schorpp-Kistner, P. Angel, and Z. Werb. 2004. Altered endochondral bone development in matrix metalloproteinase 13-deficient mice. *Development*. 131:5883-5895.
- Strochlic, L., J. Falk, E. Goillot, S. Sigoillot, F. Bourgeois, P. Delers, J. Rouviere, A. Swain, V. Castellani, L. Schaeffer, and C. Legay. 2012. Wnt4 Participates in the Formation of Vertebrate Neuromuscular Junction. *PLoS one*. 7.
- Su, N., X. Du, and L. Chen. 2008. FGF signaling: its role in bone development and human skeleton diseases. *Front Biosci*. 13:2842-2865.
- Tahimic, C.G., Y. Wang, and D.D. Bikle. 2013. Anabolic effects of IGF-1 signaling on the skeleton. *Frontiers in endocrinology*. 4:6.
- Takahashi, S., S.V. Reddy, J.M. Chirgwin, R. Devlin, C. Haipek, J. Anderson, and G.D. Roodman. 1994.

- Cloning and Identification of Annexin-II as an Autocrine/Paracrine Factor That Increases Osteoclast Formation and Bone-Resorption. *Journal of Biological Chemistry*. 269:28696-28701.
- Tay, L.X., C.K. Lim, A. Mansor, and T. Kamarul. 2014. Differential Protein Expression between Chondrogenic Differentiated MSCs, Undifferentiated MSCs and Adult Chondrocytes Derived from *Oryctolagus cuniculus* in vitro. *Int J Med Sci*. 11:24-33.
- Tay, T.L., Q.S. Lin, T.K. Seow, K.H. Tan, C.L. Hew, and Z.Y. Gong. 2006. Proteomic analysis of protein profiles during early development of the zebrafish, *Danio rerio*. *Proteomics*. 6:3176-3188.
- Thompson, Z., T. Miclau, D. Hu, and J.A. Helms. 2002. A model for intramembranous ossification during fracture healing. *Journal of orthopaedic research : official publication of the Orthopaedic Research Society*. 20:1091-1098.
- Thorngren, K.G., and L.I. Hansson. 1973. Effect of thyroxine and growth hormone on longitudinal bone growth in the hypophysectomized rat. *Acta endocrinologica*. 74:24-40.
- Thummel, R., C.T. Burket, J.L. Brewer, M.P. Sarra, L. Li, M. Perry, J.P. McDermott, B. Sauer, D.R. Hyde, and A.R. Godwin. 2005. Cre-mediated site-specific recombination in zebrafish embryos. *Dev Dynam*. 233:1366-1377.
- Tiaden, A.N., M. Breiden, A. Mirsaidi, F.A. Weber, G. Bahrenberg, S. Glanz, P. Cinelli, M. Ehrmann, and P.J. Richards. 2012. Human Serine Protease HTRA1 Positively Regulates Osteogenesis of Human Bone Marrow-derived Mesenchymal Stem Cells and Mineralization of Differentiating Bone-forming Cells Through the Modulation of Extracellular Matrix Protein. *Stem Cells*. 30:2271-2282.
- Timpl, R., T. Sasaki, G. Kostka, and M.L. Chu. 2003. Fibulins: A versatile family of extracellular matrix proteins. *Nat Rev Mol Cell Bio*. 4:479-489.
- Tocharus, J., A. Tsuchiya, M. Kajikawa, Y. Ueta, C. Oka, and M. Kawaichi. 2004. Developmentally regulated expression of mouse HtrA3 and its role as an inhibitor of TGF-beta signaling. *Dev Growth Differ*. 46:257-274.
- Topczewski, J., D.S. Sepich, D.C. Myers, C. Walker, A. Amores, Z. Lele, M. Hammerschmidt, J. Postlethwait, and L. Solnica-Krezel. 2001. The zebrafish glypican knypek controls cell polarity during gastrulation movements of convergent extension. *Dev Cell*. 1:251-264.
- Triffitt, J.T., U. Gebauer, B.A. Ashton, M.E. Owen, and J.J. Reynolds. 1976. Origin of Plasma Alpha-2 Hs-Glycoprotein and Its Accumulation in Bone. *Nature*. 262:226-227.
- Trokovic, N., R. Trokovic, P. Mai, and J. Partanen. 2003. Fgfr1 regulates patterning of the pharyngeal region. *Gene Dev*. 17:141-153.
- Tsuchiya, A., M. Yano, J. Tocharus, H. Kojima, M. Fukumoto, M. Kawaichi, and C. Oka. 2005. Expression of mouse HtrA1 serine protease in normal bone and cartilage and its upregulation in joint cartilage damaged by experimental arthritis. *Bone*. 37:323-336.
- Ungar, A.R., G.M. Kelly, and R.T. Moon. 1995. Wnt4 Affects Morphogenesis When Misexpressed in the Zebrafish Embryo. *Mechanisms of development*. 52:153-164.
- Urano, T. 2006. [Wnt-beta-catenin signaling in bone metabolism]. *Clinical calcium*. 16:54-60.
- van der Meulen, T., S. Kranenbarg, H. Schipper, J. Samallo, J.L. van Leeuwen, and H. Franssen. 2005. Identification and characterisation of two runx2 homologues in zebrafish with different expression patterns. *Biochimica et biophysica acta*. 1729:105-117.
- van Gool, S.A., J.A.M. Emons, J.C.H. Leijten, E. Decker, C. Sticht, J.C. van Houwelingen, J.J. Goeman, C. Kleijburg, S.A. Scherjon, N. Gretz, J.M. Wit, G. Rappold, J.N. Post, and M. Karperien. 2012. Fetal Mesenchymal Stromal Cells Differentiating towards Chondrocytes Acquire a Gene Expression Profile Resembling Human Growth Plate Cartilage. *PLoS one*. 7.

- van Impel, A., Z.H. Zhao, D.M.A. Hermkens, M.G. Roukens, J.C. Fischer, J. Peterson-Maduro, H. Duckers, E.A. Ober, P.W. Ingham, and S. Schulte-Merker. 2014. Divergence of zebrafish and mouse lymphatic cell fate specification pathways. *Development*. 141:1228-U1101.
- Veeman, M.T., D.C. Slusarski, A. Kaykas, S.H. Louie, and R.T. Moon. 2003. Zebrafish prickles, a modulator of noncanonical Wnt/Fz signaling, regulates gastrulation movements. *Curr Biol*. 13:680-685.
- Veien, E.S., M.J. Grierson, R.S. Saund, and R.I. Dorsky. 2005. Expression pattern of zebrafish *tcf7* suggests unexplored domains of Wnt/beta-catenin activity. *Dev Dynam*. 233:233-239.
- Viguet-Carrin, S., P. Garnero, and P.D. Delmas. 2006. The role of collagen in bone strength. *Osteoporosis Int*. 17:319-336.
- Vortkamp, A., K. Lee, B. Lanske, G.V. Segre, H.M. Kronenberg, and C.J. Tabin. 1996. Regulation of rate of cartilage differentiation by Indian hedgehog and PTH-related protein. *Science*. 273:613-622.
- Wakahara, T., N. Kusu, H. Yamauchi, I. Kimura, M. Konishi, A. Miyake, and N. Itoh. 2007. *fibin*, a novel secreted lateral plate mesoderm signal, is essential for pectoral fin bud initiation in zebrafish. *Developmental biology*. 303:527-535.
- Walker, M.B., and C.B. Kimmel. 2007. A two-color acid-free cartilage and bone stain for zebrafish larvae. *Biotechnic & Histochemistry*. 82:23-28.
- Wallingford, J.B., A.J. Ewald, R.M. Harland, and S.E. Fraser. 2001. Calcium signaling during convergent extension in *Xenopus*. *Curr Biol*. 11:652-661.
- Wang, B., T. Sinha, K. Jiao, R. Serra, and J. Wang. 2011. Disruption of PCP signaling causes limb morphogenesis and skeletal defects and may underlie Robinow syndrome and brachydactyly type B. *Hum Mol Genet*. 20:271-285.
- Wang, F.S., C.L. Lin, Y.J. Chen, C.J. Wang, K.D. Yang, Y.T. Huang, Y.C. Sun, and H.C. Huang. 2005a. Secreted frizzled-related protein 1 modulates glucocorticoid attenuation of osteogenic activities and bone mass. *Endocrinology*. 146:2415-2423.
- Wang, L., Y.Y. Shao, and R.T. Ballock. 2009. Carboxypeptidase Z (CPZ) links thyroid hormone and Wnt signaling pathways in growth plate chondrocytes. *J Bone Miner Res*. 24:265-273.
- Wang, L., Y.Y. Shao, and R.T. Ballock. 2010. Thyroid Hormone-Mediated Growth and Differentiation of Growth Plate Chondrocytes Involves IGF-1 Modulation of beta-Catenin Signaling. *J Bone Miner Res*. 25:1138-1146.
- Wang, Y., and J. Nathans. 2007. Tissue/planar cell polarity in vertebrates: new insights and new questions. *Development*. 134:647-658.
- Wang, Y., and H. Steinbeisser. 2009. Molecular basis of morphogenesis during vertebrate gastrulation. *Cell Mol Life Sci*. 66:2263-2273.
- Wang, Y., and S. Zhang. 2011. Expression and regulation by thyroid hormone (TH) of zebrafish IGF-I gene and amphioxus IGF-I gene with implication of the origin of TH/IGF signaling pathway. *Comparative biochemistry and physiology. Part A, Molecular & integrative physiology*. 160:474-479.
- Wang, Y.L., R. Xiao, F. Yang, B.O. Karim, A.J. Iacovelli, J.L. Cai, C.P. Lerner, J.T. Richtsmeier, J.M. Leszl, C.A. Hill, K. Yu, D.M. Ornitz, J. Elisseeff, D.L. Huso, and E.W. Jabs. 2005b. Abnormalities in cartilage and bone development in the Apert syndrome FGFR2(+/-S252W) mouse. *Development*. 132:3537-3548.
- Wasinger, V.C., M. Zeng, and Y. Yau. 2013. Current status and advances in quantitative proteomic mass spectrometry. *International journal of proteomics*. 2013:180605.
- Webb, S.E., K.W. Lee, E. Karplus, and A.L. Miller. 1997. Localized calcium transients accompany furrow

- positioning, propagation, and deepening during the early cleavage period of zebrafish embryos. *Developmental biology*. 192:78-92.
- Wehner, D., W. Cizelsky, M.D. Vasudevaro, G. Ozhan, C. Haase, B. Kagermeier-Schenk, A. Roder, R.I. Dorsky, E. Moro, F. Argenton, M. Kuhl, and G. Weidinger. 2014. Wnt/beta-Catenin Signaling Defines Organizing Centers that Orchestrate Growth and Differentiation of the Regenerating Zebrafish Caudal Fin. *Cell Rep*. 6:467-481.
- Weiner, S., and H.D. Wagner. 1998. The material bone: Structure mechanical function relations. *Annu Rev Mater Sci*. 28:271-298.
- Weiss, R.E., and S. Refetoff. 1996. Effect of thyroid hormone on growth. Lessons from the syndrome of resistance to thyroid hormone. *Endocrinology and metabolism clinics of North America*. 25:719-730.
- Westfall, T.A., R. Brimeyer, J. Twedt, J. Gladon, A. Olberding, M. Furutani-Seiki, and D.C. Slusarski. 2003. Wnt-5/pipetail functions in vertebrate axis formation as a negative regulator of Wnt/beta-catenin activity. *J Cell Biol*. 162:889-898.
- Wheatley, D.N., A.M. Wang, and G.E. Stragnell. 1996. Expression of primary cilia in mammalian cells. *Cell Biol Int*. 20:73-81.
- Williams, G.R. 2003. Thyroid hormone actions in bone and cartilage. *J Bone Miner Res*. 18:1357-1357.
- Wilson, P.A., and A. Hemmati-Brivanlou. 1997. Vertebrate neural induction: inducers, inhibitors, and a new synthesis. *Neuron*. 18:699-710.
- Wilson, R., E.L. Norris, B. Brachvogel, C. Angelucci, S. Zivkovic, L. Gordon, B.C. Bernardo, J. Stermann, K. Sekiguchi, J.J. Gorman, and J.F. Bateman. 2012. Changes in the Chondrocyte and Extracellular Matrix Proteome during Post-natal Mouse Cartilage Development. *Mol Cell Proteomics*. 11.
- Wisniewski, J.R., and M. Mann. 2009. Spin filter-based sample preparation for shotgun proteomics Reply. *Nat Methods*. 6:785-786.
- Wodarz, A., and R. Nusse. 1998. Mechanisms of Wnt signaling in development. *Annual review of cell and developmental biology*. 14:59-88.
- Wojcicka, A., J.H. Bassett, and G.R. Williams. 2013. Mechanisms of action of thyroid hormones in the skeleton. *Biochimica et biophysica acta*. 1830:3979-3986.
- Xin, X., R. Day, W. Dong, Y. Lei, and L.D. Fricker. 1998. Cloning, sequence analysis, and distribution of rat metallocarboxypeptidase Z. *DNA and cell biology*. 17:311-319.
- Xing, W.R., K.E. Govoni, L.R. Donahue, C. Kesavan, J. Wergedal, C.L. Long, J.H.D. Bassett, A. Gogakos, A. Wojcicka, G.R. Williams, and S. Mohan. 2012. Genetic evidence that thyroid hormone is indispensable for prepubertal insulin-like growth factor-I expression and bone acquisition in mice. *J Bone Miner Res*. 27:1067-1079.
- Xu, Q., Y. Wang, A. Dabdoub, P.M. Smallwood, J. Williams, C. Woods, M.W. Kelley, L. Jiang, W. Tasman, K. Zhang, and J. Nathans. 2004. Vascular development in the retina and inner ear: control by Norrin and Frizzled-4, a high-affinity ligand-receptor pair. *Cell*. 116:883-895.
- Yamada, Y., F. Ando, N. Niino, T. Miki, and H. Shimokata. 2003. Association of polymorphisms of paraoxonase 1 and 2 genes, alone or in combination, with bone mineral density in community-dwelling Japanese. *J Hum Genet*. 48:469-475.
- Yamamoto, S., O. Nishimura, K. Misaki, M. Nishita, Y. Minami, S. Yonemura, H. Tarui, and H. Sasaki. 2008. Cthrc1 selectively activates the planar cell polarity pathway of Wnt signaling by stabilizing the Wnt-receptor complex. *Dev Cell*. 15:23-36.
- Yan, Y.L., P. Bhattacharya, X.J. He, B. Ponugoti, B. Marquardt, J. Layman, M. Grunloh, J.H. Postlethwait, and D.A. Rubin. 2012. Duplicated zebrafish co-orthologs of parathyroid hormone-related

- peptide (PTHrP, Pthlh) play different roles in craniofacial skeletogenesis. *The Journal of endocrinology*. 214:421-435.
- Yan, Y.L., J. Willoughby, D. Liu, J.G. Crump, C. Wilson, C.T. Miller, A. Singer, C. Kimmel, M. Westerfield, and J.H. Postlethwait. 2005. A pair of Sox: distinct and overlapping functions of zebrafish sox9 co-orthologs in craniofacial and pectoral fin development. *Development*. 132:1069-1083.
- Yang, D.C., C.C. Tsai, Y.F. Liao, H.C. Fu, H.J. Tsay, T.F. Huang, Y.H. Chen, and S.C. Hung. 2011. Twist Controls Skeletal Development and Dorsoventral Patterning by Regulating Runx2 in Zebrafish. *PLoS one*. 6.
- Yin, C., M. Kiskowski, P.A. Pouille, E. Farge, and L. Solnica-Krezel. 2008. Cooperation of polarized cell intercalations drives convergence and extension of presomitic mesoderm during zebrafish gastrulation. *J Cell Biol*. 180:221-232.
- Zancan, I., S. Bellesso, R. Costa, M. Salvalaio, M. Stroppiano, C. Hammond, F. Argenton, M. Filocamo, and E. Moro. 2015. Glucocerebrosidase deficiency in zebrafish affects primary bone ossification through increased oxidative stress and reduced Wnt/beta-catenin signaling. *Hum Mol Genet*. 24:1280-1294.
- Zhang, G., B.F. Eames, and M.J. Cohn. 2009. Chapter 2. Evolution of vertebrate cartilage development. *Current topics in developmental biology*. 86:15-42.
- Zhang, H., K.W. Marshall, H. Tang, D.M. Hwang, M. Lee, and C.C. Liew. 2003. Profiling genes expressed in human fetal cartilage using 13,155 expressed sequence tags. *Osteoarthritis Cartilage*. 11:309-319.
- Zhang, M., S.H. Xuan, M.L. Bouxsein, D. von Stechow, N. Akeno, M.C. Faugere, H. Malluche, G.S. Zhao, C.J. Rosen, A. Efstratiadis, and T.L. Clemens. 2002. Osteoblast-specific knockout of the insulin-like growth factor (IGF) receptor gene reveals an essential role of IGF signaling in bone matrix mineralization. *Journal of Biological Chemistry*. 277:44005-44012.
- Zhu, W.H., J.W. Smith, and C.M. Huang. 2010. Mass Spectrometry-Based Label-Free Quantitative Proteomics. *J Biomed Biotechnol*.
- Zien, A., P.M. Gebhard, K. Fundel, and T. Aigner. 2007. Phenotyping of chondrocytes in vivo and in vitro using cDNA array technology. *Clin Orthop Relat Res*. 460:226-233.
- Zoeller, R.T. 2004. Editorial: Local control of the timing of thyroid hormone action in the developing human brain. *J Clin Endocr Metab*. 89:3114-3116.
- Zorn, A.M., and J.M. Wells. 2009. Vertebrate endoderm development and organ formation. *Annual review of cell and developmental biology*. 25:221-251.

Summary

Historically the skeleton, in particular bone, was depicted as a rigid, inflexible, lifeless structure that readily breaks upon bending. We now know that bones in living organisms are complex, dynamic organs that combine toughness with flexibility. Astonishing is the fact that after their initial formation, bone structures are continuously remodeled (recycled and renewed), adapting to environmental demands at such a speed that in active healthy humans the distal part of the femur is completely replaced every six to twelve months. The zebrafish is a relatively new model organism in the field of skeletal development and primarily used as a powerful model for the identification of novel gene functions during skeletogenesis. At the molecular level, the biological similarity between zebrafish and humans is striking (Spoorendonk et al., 2010), but the actual skeletal composition of the zebrafish remained largely unknown.

The mechanical properties of the skeleton are largely dependent on the composition of proteins that are secreted into the extracellular matrix (ECM). In order to increase our understanding of normal skeletal development, it is necessary to identify and characterize changes in skeletal composition. The aim of this thesis was to analyze the composition of the extracellular matrix in zebrafish, in order to enable the identification of potential key regulatory proteins. By determination of the protein content in the zebrafish skeletal ECM with major changes in protein abundance during development we were able to identify various components of signaling pathways implicated in skeletogenesis. This first proteomic analysis of the zebrafish skeleton revealed the homology between the zebrafish and the skeleton of other vertebrate species including mammals. Our study provides a solid foundation for future studies on the composition and the regulation of the morphogenesis of the vertebrate skeleton.

After the identification of potential regulatory proteins in the developing zebrafish skeleton during the MS-based approach, the protein carboxypeptidase Z (Cpz) was selected for further analysis. This peptidase has previously been implicated in the Wnt signaling pathway, an elaborate pathway that regulates crucial aspects of development (Nusse and Varmus, 2012). Previous studies implicated a regulatory role for this peptidase through the processing of Wnt (Moeller et al., 2003; Wang et al., 2009). An analysis of the role of this peptidase in zebrafish was still lacking and therefore we mapped the spatio-temporal expression of *cpz*. We showed that expression of *cpz* is localized in and around juvenile zebrafish ossified structures. A more thorough analysis showed a complex expression pattern during early developmental stages that partially overlaps with that observed in other species. Furthermore, we provide a comparative view of *cpz* expression and the expression of its proposed ligand, Wnt4 (zebrafish Wnt4a and Wnt4b). Partial overlap with *wnt4* expression provided the first evidence for a potential complementary function in the Wnt signaling pathway as observed in mammalian species.

In order to explore the role of *cpz* in zebrafish development, a loss-of-function mutant for zebrafish *cpz* was generated via TALEN-mediated mutagenesis. We show that mutant embryos display a variety of phenotypes during early development, most of which were similar to described defects in the Wnt/Calcium signaling pathway. These morphological phenotypes provide the first evidence for a connection between *Cpz* and regulation of the β -catenin independent Wnt signaling pathways which places the function of *Cpz* in a completely new perspective.

As a complement to these genetic studies an alternative approach was employed to examine the role of another pathway, the thyroid hormone system, in skeletogenesis. Thyroid hormones are required for skeletal development (Kim and Mohan, 2013), but to what extent thyroid hormone affects early bone development in zebrafish remained unclear. By exposing zebrafish embryos to the thyroid hormone triiodothyronine (T3) we showed that exposure accelerates ossification of craniofacial elements including the opercle and ceratohyal in a dose-dependent manner. This provides the first histological evidence of increased ossification in zebrafish due to thyroid hormone exposure which can be used as a starting point to explore the mechanism of thyroid hormone on skeletal development at a greater depth.

The zebrafish skeleton displays remarkable resemblance to that of other vertebrate species with regards to composition, regulatory components and hormonal response. The use of zebrafish as a model in future research will undoubtedly increase our understanding of vertebrate skeletal development and disease. In this thesis we provide a first insight in the extracellular protein content of the zebrafish skeleton, identify a role for the *Cpz* protein in β -catenin independent (non-canonical) Wnt signaling during development and shows the effect of thyroid hormone on ossification during early zebrafish development.

Samenvatting

Het skelet, en dan met name bot, werd vroeger gezien als een harde levenloze structuur die gemakkelijk bezweek onder belasting. Tegenwoordig weten we echter dat botten in levende organismen complexe dynamische structuren zijn die stevigheid combineren met flexibiliteit. Het is dan ook verbazingwekkend dat deze botstructuren – nadat ze gevormd zijn – continue vernieuwd worden om zo aan de vereisten te voldoen die aan deze structuren gesteld worden. Dit gebeurt met een zodanige snelheid dat in actieve, gezonde mensen bijvoorbeeld het distale gedeelte van het dijbeen elke 6 tot 12 maanden volledig vervangen wordt. De zebravis is een veel gebruikt modelorganisme in onderzoek, echter relatief nieuw op het gebied van skeletontwikkeling. Hierin wordt de zebravis voornamelijk ingezet als een model voor de identificatie van nieuwe genen die een rol spelen bij de vorming van het skelet. Er is een grote overlap in de genen die betrokken zijn bij skeletvorming in de zebravis en andere vertebraten (gewervelden), waaronder de mens (Spoorendonk et al., 2010). Of dit ook geldt voor de samenstelling van het skelet zelf (bot en kraakbeen) is echter onbekend, voornamelijk doordat deze nog niet eerder onderzocht is in de zebravis.

De eigenschappen van het skelet zijn grotendeels afhankelijk van de samenstelling (eiwitten en mineralen). Eiwitten worden tijdens de vorming van het skelet uitgescheiden in de extracellulaire matrix, alwaar ze hun functie uitoefenen. Om een goed beeld te krijgen van de ontwikkeling van het skelet is het noodzakelijk deze samenstelling, en veranderingen hierin gedurende de ontwikkeling, te karakteriseren. Dit onderzoek begon met het analyseren van deze eiwitsamenstelling in het skelet van de zebravis gedurende de ontwikkeling. Daarbij werd de mogelijkheid benut om eiwitten met een regulerende functie te identificeren. Deze eerste eiwitanalyse van het zebravisskelet leverde het bewijs dat het zebravisskelet een vergelijkbare samenstelling heeft met dat van andere gewervelden, waaronder mensen. Deze studie biedt dan ook een solide basis voor toekomstige studies die de samenstelling of de ontwikkeling van het skelet willen bestuderen.

Naast de analyse van de samenstelling werd deze data gebruikt voor het identificeren van eiwitten met een potentiële regulatoire rol in skeletvorming. Een van de geïdentificeerde eiwitten, carboxypeptidase Z (Cpz), is eerder gevonden in andere vertebraten waarin het een belangrijke rol leek te spelen in de Wnt signalering. Wnt signalering is een complex netwerk van signalen dat cruciale aspecten van de ontwikkeling aanstuurt (Nusse en Vermus, 2012). Aangezien het daadwerkelijke mechanisme waarop CPZ zijn functie uitoefent nog ontbrak, en dit eiwit niet eerder bestudeerd was in de zebravis, werd dit eiwit geselecteerd voor verdere analyse. Hierbij werd eerst gekeken naar de genexpressie van *cpz* in de stadia gebruikt voor eiwitanalyse. Hieruit bleek dat dit eiwit gemaakt werd in en rondom gemineraliseerde structuren van jong adulte zebravissen. Een uitgebreidere analyse toonde een complex expressiepatroon gedurende de vroege ontwikkeling, hetgeen gedeeltelijk overlapt met de eerdere waarnemingen in andere vertebraten. Dit verkregen expressiepatroon werd vergeleken met dat van *wnt4* (in zebravis *wnt4a* en *wnt4b*), het vermoedde substraat van CPZ in andere vertebraten. De gedeeltelijke overlap die werd

gevonden bevestigt de mogelijke rol van Cpz in zebravis Wnt signalering.

Om een beter idee te krijgen van de rol van Cpz in de ontwikkeling van de zebravis werd het *cpz* gen uitgeschakeld door middel van een mutatie (via TALEN-gemedieerde mutagenese). Nakomelingen van deze mutanten werden geanalyseerd en lieten een verscheidenheid aan afwijkende fenotypes zien gedurende de vroege ontwikkeling. Sinds vergelijkbare afwijkende fenotypes zijn beschreven als gevolg van defecten in Wnt /calcium signalering, is dit het eerste bewijs van een verband tussen Cpz en de regulatie van de β -catenine-onafhankelijke Wnt-sigtaalroutes. Daarmee plaatsen deze resultaten de functie van CPZ in een geheel nieuw perspectief.

Naast deze genetische studies hebben we het zebravisskelet op een alternatieve wijze bestudeerd door de rol van het schildklierhormoon te kijken. Schildklierhormonen spelen een belangrijke rol in de ontwikkeling van het skelet (Kim en Mohan, 2013), maar in welke mate het de botontwikkeling in de zebravis beïnvloedt was echter nog onduidelijk. Door zebravis embryo's bloot te stellen aan het schildklierhormoon triiodothyronine (T3), hebben we kunnen aantonen dat de vorming van bepaalde botstructuren versneld wordt op een dosis-afhankelijke wijze. Dit verschaft het eerste histologische bewijs dat schildklierhormoon botvorming in de zebravis versnelt. Deze resultaten kunnen gebruikt worden als een startpunt om het mechanisme achter het effect van schildklierhormoon op skeletontwikkeling beter te begrijpen.

Het zebravisskelet toont een opmerkelijke gelijkenis met dat van andere vertebraten met betrekking tot samenstelling, regulerende elementen en hormonale respons. Een toename in het gebruik van de zebravis als een alternatief model zal in de toekomst ongetwijfeld bijdragen aan ons groeiende begrip van de ontwikkeling van het skelet en het ontstaan van ziekten. In dit proefschrift geven we inzicht in de eiwitcompositie van het zebravisskelet, identificeren een rol voor het Cpz eiwit in β -catenine-onafhankelijke Wnt-signalering tijdens de ontwikkeling en presenteren het effect van het schildklierhormoon op botvorming tijdens de vroege ontwikkeling van de zebravis.

Acknowledgements

Dankwoord

"The difference between try and triumph is just a little umph!" – Johnsen's Jottings

The past years have been... moving. And the sentence 'there can be no peaks without valleys' is one that fits both the professional and personal experiences of my time spent on this thesis. Here I would like to express my gratitude to all those who were there to contribute and support me during this period, and highlight some.

I would like to start by expressing my gratitude to **Sacco, Johan** and **Stefan**. I would like to thank you for giving me the opportunity to perform this PhD project at the chair groups of Biochemistry and Experimental Zoology. Sacco and Johan, I am greatly indebted to the two of you, handling all my questions, doubts, problems and sometimes the somewhat too enthusiastic ideas. Sacco, your help and input during writing was indispensable. Our weekly meetings helped me to push through the rough parts and finish this thesis. I wish you all the best in future endeavors and your department a great start in the new Helix building. Johan, despite your busy schedule you always checked up on me and gave advice when necessary. Your scientific view on topics helped me a lot, especially during the final months and during the formation of the propositions. Your passion for your work is admirable, and often you were there in the weekends to help your PhD students or work on your own 'side-projects' such as imaging mosses. For you and EZO, I also wish nothing but the best in the future. Stefan, after a zebrafish exchange during my master thesis in Stockholm, you were the person that linked me to Wageningen and this PhD project. Your advice over the years has been extremely important to me as well as the project, and your critical view on this thesis is greatly appreciated. The support from your group members at the Hubrecht Institute was imperative to this project. Thank you for everything you have done for me. I wish you all the best with your newly appointed professorship in Münster.

Sander, I am very grateful for your guidance, great feedback and your ability to respond to my (most often) spontaneous visits and questions. Your door was always open for me and even when I came with problems and questions that were outside your 'scientific comfort zone', you were able to reason towards a satisfactory solution. Based on those qualities I think it's a shame you don't continue to supervise PhD students (their loss), though your great didactic skills will be most welcome to the students you now advise and will be educating in the future. I hope you, Ellen and your girls will be very happy in your new home and wish all of you a great, happy and healthy future.

Karen, you were my savior in the lab. You helped me so much with cloning, cell culture, in situs (for which I also have to thank **Taslima** for all her hard work), etc. Every time I overlooked the

amount of work in embryo staging, embryo selecting or whatever, you stepped in and saved me. I apologize for all the crazy cloning ideas which made you order primer upon primer set, changing cloning strategies so often that it became a full-time job to keep up. Also thank you for your (and Henk's) patience in the lab. My lab space conquering skills often resulted in a game of stratego, by working at those spots closest to my own position at a specific moment made the underpopulated lab still a bit untidy. Thinking back, you have had so much patience with me, trying to keep the lab workable. Thank you for everything.

The next person is no one less than **Henk**. You were the miracle worker that helped with many of the imaging (including the cover) challenges. You were always reachable and those few questions you didn't know the answer to by heart were resolved on the spot. During the years we all learned about your amazing eye for external features combined with your ability to grant them a number ;) **LOL**. A lot of interns were supervised by you over the years, and I always saw them having a great time (I think). There were no dull moments, only unexpected moves, like the time your lab journal was mysteriously misplaced on the ceiling... Thank you for all your help, advice and the fun way of presenting it (and wet clothing during the last lab outing).

Another major contributor to this thesis is **Sjef**. Your help, guidance and input were indispensable. Your skills on the mass-spec and knowledge on protein-related experiments are of great value. I learned over the years that, next to me, a lot of researchers in and outside of Wageningen appreciate your skills. I am very happy that I had the chance to work with you and learn from you.

For my experiments at the Hubrecht Institute, I would like to give my special thanks to **Leonie**. Leonie, thank you for the help with the FACS protocol and not to forget, creating the basis of this PhD project. And now I mentioned FACS sorting, **Jan Bergervoet**, thank you for all your help! You took it on you to help me out with sorting, and kept that promise even after the sorter died beyond repair. Your effort resulted in fixing an arrangement that allowed us to use the FACS sorter at the NIOO. Thank you for all your time and effort in this pursuit. I also would like to use this opportunity for acknowledging **Ivonne** and **Barae** for the pleasant collaboration with the Toxicology group in Wageningen for their, as well as that of **Azath**, major contribution to the Thyroid-related chapter in this thesis.

Another important role in this thesis was fulfilled by **Menno**, **Truus**, **Wian** and **Sander** (as well as **Sietze** and **Aart** during my first years). Thank you for taking care of the zebrafish, supporting and helping out in any way you could (planning, feeding, setting up fish, maintaining the different lines). And of course I also have to mention the well-organized yearly Glühwein event. Regarding the experiments with zebrafish, I would like to thank **Rob Steenmans** for his help applying for the DEC proposals. It was very nice to have personal contact and quick feedback on these proposals.

Annemarie and **Laura**, without your support I would have gotten lost in translation. You both helped me with all the paperwork and political hassle that comes with a PhD project. Thank you so much. Laura, I did not spend much time at the Biochemistry department but the (in the end) weekly conversations were very welcome. Annemarie, people joked about it but at EZO you really are a second mother to us (PhD students). Thank you for all the help and the times you defended us against hilarious claims that stated we did not clean out the dishwasher etc. Also thank you for opening your home to us for the now traditional winter bbq's and Christmas dinners. We always felt very welcome at your place despite the extremely large chickens that guard it. Apologies that we almost burned Geert with one of the fire pits (vuurkorf) ;)

Then, I want to express my gratitude towards my other colleagues. At EZO, **Sander G, Florian, Bart, Martin and Kees S**, thank you for the fun times during coffee breaks and the lively discussions. **Remco**, thank you for all the help with disassembling and assembling the eventually never used flow tunnel, and of course for the great Christmas meals that were mostly arranged and prepared (even the year you were not there in person) by you. Also you and **Marcel** were the force behind the amazing puzzle day which despite of the whiskey was a great experience. Thank you guys. The same goes for the colleagues working at CBI and HMI, in particular **Peter van Baarlen, Ellen, Nico, Anja, Ellen and Maria**. Thank you for your help with small and more difficult problems. In addition, I would like to thank all my colleagues working at the Biochemistry department. After initially dividing time by working at both departments, working closer to the zebrafish eventually took the upper hand. Therefore, I did not spend much time at Biochemistry but I still would like to thank you for the discussions and all the help. I would like to highlight **Cathy, Walter and Lisette**, thank you for the pleasant conversations every time I did come in, **Christina** and **Stefania** for the great experience of planning and executing the lab outing at Biochemistry, and **Wilma** and **Christoph** for the pleasant talks in between work.

Then my brothers and sisters in arms/crime, the PhD students of EZO (**Ansa, Sebastian, Kees, Remco, Elsa, Mike, Uros, Julian and Peter**), CBI (**Joeri, Lieke, Christine, Carmen, Esther, Eva, Marloes, Adriaan, Jules, Olaf and Annemiek**), and HMI (**Bruno, Edo, Marcella, Linda, Sam, Nadya, Agnieszka, Rogier and Nirupama**). Over the years we had so many good and fun times that I have no idea what to highlight. The long working days were made feasible by the '*micro-pauzes*', a good laugh, an interesting plot, some handmade coffee or a game of Uno, jungle speed or croquet. The PhD weekends relaxing, skiing or climbing (with the off-road skiing Stiene and robo-Kees), the laser gaming, paint ball (with rabbit Kint), winter BBQs, pool party at the forum, as well as the '*who is the mole*' (of course Edo) weekend (with our blind-folded 'rowing' Mike) were so much fun. The CBI-ladies (Lieke, Christine, Carmen, Marloes) which initiated many of the activities including the forum run in un-runnable minion costumes (together with a few sexy strawberries), '*formal Friday*', '*tokki Thursday*', and the widely discussed but never considered appropriate enough to indeed do it '*transgender Tuesday*'. I would like to highlight, hopefully without breaking doctor-patient privilege, Lieke, thank you for the mental sessions which saved me a lot of money for a psychiatrist ;) My roomies; Ansa, you were the zebrafish expert when I started. Thank you for the help, talks over (of course) tea and the fun times. Mike and Elsita, we had some great times with intentional awful or just great music, with problems of too many or just too big office fish, and the never ending battle against algae. Elsa, thank you for all the Spanish lessons from which some unforgettable words arose ('*pollo mas grande*'). And Mike, I think it is still ashamed that the '*Ai Caramba*' air cleaner conspiracy did not work out.

Then a very special thanks for my paranymphs, Sebastian and Kees. Sebas, what can I say... what didn't we do. Your '*beautiful mind*' made us swim in a hole in the ice in midwinter, pull your car out of a ditch, got Joeri's room in a lot of trouble (sorry for that Joeri) and started the tradition of the winter bbq. I can't remember a dull moment. Thank you for your friendship, your brutal honesty, and all the times spent on crazy fail compilations. You also were the person that together with Marcel introduced the (delicious!!) Bicky burger to the E-wing. We had some great laughs. And, not to forget, you, Joeri and I were partners in crime in the best lab outing ever!! Kees, I think you are the most originally dressed person in the building. Always wearing the most original shirts. Your vocabulary led to a lot of crazy new words, and I don't think it will take long before you will get your own dictionary containing words like '*flerpje*' and '*loedeltje*'. Your amazing lab skills will

be talked about for years and years to come (especially your autoclave skills). And your extensive knowledge of biological processes, especially concerning endoplasmic reticula, made my choice to pick you as my paranymp very easy.

My non-work-related friends, the guys I have known since we were just boys (**Ruurd, Remy, Ronald, Egbert, Roderik, Rob, Tom, Stefan, Sander, Steven, Alwin, Rob, Niek** and of course **Tim** (nog...?!)), as well as all your better halves. The past few years I did not see you guys as much as I had wanted. But the times we did meet were as memorable as they always were. Schoolfeest, sailing trips, the yearly dinners and new year's parties were a big a mess as always ;). Never a boring moment. Thank you for your understanding and help during the lesser period in my life a few years ago, it means the world to me. The same goes for the partially overlapping Nijmegen gang (Groepje 10 +) (**Wally** (*maxi and mini*), **Sanne, Ronald, Karijn, Remy, Anneke, Rebecka, Jeroen, Karlijn, Roel, Jose, Martijn** and **Rozanne**). We had, and hopefully will have loads of fun during the yearly weekends (*except 2013*), the '4-daagse feesten' and all other gatherings. Serious conversations and often the not so serious conversations were ideal to put life into perspective. Thank you for all the good times!!

Henk en Tonny, dank jullie voor alle interesse en de gezellige middagen en avonden in Bathmen. Hetzelfde geldt natuurlijk ook voor **Jantina** en de rest van de familie. **Koen en Sjoerd**, waar we vroeger nog wel eens onenigheden hadden ;) zijn we nu drie handen op één buik met (wat mam soms minder leuk vindt) precies dezelfde humor. Koen, binnenkort je eigen tandarts praktijk en Sjoerd (onze personal) fysiotherapeut. Ik ben erg trots op jullie... en hoop dat jullie samen met jullie betere helften, **Nienke** en **Jelleke**, een goede, gelukkige en gezonde toekomst tegemoet gaan. Bedankt voor de afleiding en het relativeren van het PhD leven. Dan **Loppis**, bedankt voor alle enthousiaste onthalen bij thuiskomst en de rustgevende wandelingen. Het kost altijd wel een half uur om je bij aankomst gedag te zeggen, maar dat is toch één van de hoogtepunten van thuis thuis komen.

Pap en mam, ik wil jullie ontzettend bedanken voor alles dat jullie voor mij gedaan hebben en voor jullie eindeloze steun. Jullie hebben altijd voor ons/mij klaar gestaan voor... eigenlijk alles. Zonder jullie twee was ik nooit gekomen waar ik nu ben. Jullie hebben ons altijd gestimuleerd ons hart te volgen en te doen wat je leuk vindt. Het fijne gevoel van thuis thuis komen dat gedurende de studenten tijd ontstond is over de jaren eigenlijk nooit veranderd. Bedankt voor alle hulp die meestal al aangeboden werd voor er om gevraagd kon worden. Dank voor jullie steun, hulp en liefde de afgelopen jaren.

Lieve **Carla**, de afgelopen jaren waren niet altijd even gemakkelijk voor jou. Toch was je er altijd voor me ondanks de meest onmogelijke werktijden. Sorry dat ik je ieder jaar weer mee sleurde in het creëren van de meest onmogelijke (maar uiteindelijk erg mooie) verjaardagstraktaties ;) Bedankt voor alle steun de afgelopen jaren, zonder welke dit boekje er zeker niet zou liggen.

Personalia

CURRICULUM VITAE

Een curriculum vitae is veelal alleen maar een (indrukwekkende) opsomming van allerlei activiteiten, welke ter bevordering van kennis, IQ en bekwaamheden uitgevoerd werden. Nu Maurijn mij gevraagd heeft zijn CV te schrijven, maak ik van de gelegenheid gebruik om een iets breder beeld te schetsen van deze jongeman! En benoem ik ook de EQ-aspecten.

Onverstoorbaarheid en flegma zijn karaktertrekken. Ook in het karakter van Maurijn zijn deze vertegenwoordigd, hetgeen hem overigens niet euvel te duiden is, gezien de noemenswaardige aftrap van zijn leven:

1982 Je start als zygote in Noorwegen, om als embryo terug te vliegen naar Iseyin (Yorouba gebied in West Nigeria) – vervolgens reis je in de hoedanigheid van ongeboren kind opnieuw weer naar Nederland, waar je op 14 maart 1983 geboren wordt. Dan breng je als jonggeborene het eerste jaar in de tropen door... Met recht een warm en turbulent begin van je leven! Een start die je ook je Yorouba naam oplevert: Ori Yomi, hetgeen zoveel betekend als "geboren in gevaar" [een keizersnede was in die tijd en omstandigheid in Afrika toch een risicovolle activiteit, red.].

1986 In je derde levensjaar verhuis je met je ouders naar de plek waar je tot je adolescentie woont en opgroeit: een oude verwaarloosde boerderij op het platteland in Twente. Daar help je enthousiast mee aan het opknappen van huis en tuin, maar vooral ben je veel buiten: een jongetje die zich erg interesseert in de natuur, de vogels, de dieren. Hierin van harte gestimuleerd door je (groot)moeder. Als **dierenvriend** redt je eens het leven van een gevangen muis, die je vervolgens als dank in je vinger bijt... Wat een verontwaardiging!

1989 Redelijk opgewekt doorloop je de peuterspeelzaal, lagere school, MAVO en HAVO (per ongeluk met dubbel profiel). Tot het moment daar is dat er een beroeps/studiekeuze gemaakt moet worden... je wist het even niet. Terwijl je opvoeders dachten aan allerlei scholingen met veel natuur of dier, viel je keus op het laatste nippertje op het vak dat je (klaarblijkelijk) leuk of bijzonder vond in de eindexamenklas: Scheikunde. Op het Saxion kreeg dat een "opgeleukte" benaming van "Life Science and Technology".

2001 Tijdens deze studie stak je met name veel energie in het onderdeel "Life": veel leuke dingen **organiseren** in het studentenleven... Zodanig dat dit aspect bij je diploma uitreiking als bijzondere additionele vaardigheid door je mentor benoemd werd! Halverwege de HBO opleiding moest er een keus gemaakt worden en gezien de "stand der techniek van dat moment" en na een stage in Groningen, kreeg je het idee te kiezen voor de research richting, "iets met DNA gaan doen, want dat wordt de toekomst..."

2006 Medio 2006 rond je de HBO studie af en verhuis je naar Nijmegen om daar de master Medische Biologie op te pakken. Dat levert afwisselende research stages in Nijmegen en Stockholm, en Carla – je partner – op. Het lezen van de aldaar gebruikte technieken roept vast ook bij u als lezer het gevoel op dat we eigenlijk maar magertjes onderlegd zijn... Wat voorbeelden: micro-injection Zebrafish, morpholino-mediated knockdown, cDNA synthesis, qPCR analysis, in situ hybridization including cloning and RNA probe generation...

2010 Eind 2009 woon je **gelukkig** samen en ben je medisch bioloog. Je solliciteert op de vacature voor een promotie onderzoek bij professor Dr Schulte-Merker. Je wordt via hem aangenomen in Wageningen en start begin 2010 met je onderzoek. Evenals in Stockholm, spelen ook nu weer de zebravissen een hoofdrol. Voor ons buitenstaanders is de grote lijn van het onderzoek maar korte tijd duidelijk: het gaat om het identificeren van een/meerdere eiwitten die een belangrijke rol spelen in de botvorming van je visjes. Spoedig zijn we echter de draad kwijt, en hopen dan ook van harte op een Jip en Janneke samenvatting in dit boekwerk, opdat ook de gemiddelde medemens snapt waar je die 5 jaar mee bezig geweest bent.

2015 Je collega's, studenten en professoren, hebben naast je dagelijkse werkzaamheden, nog veel plezier beleefd aan alle randactiviteiten die je in de vrije tijd organiseerde. Ze zullen je missen!

En dan nu op zoek naar een "echte" baan, succes!

F.J.M. Kessels

OVERVIEW OF COMPLETED TRAINING ACTIVITIES

Discipline specific activities

Comparative Proteomics	2010
Course on Laboratory Animal Science	2010
Proteomics	2011
Advanced visualization, integration and biological interpretation of ~omics data	2011
Interdisciplinary Approaches in Fish Skeletal Biology, (IAFSB), Tavira, Portugal (poster)	2011
Training and execution of TALEN-mediated mutagenesis, Hubrecht Institute, Utrecht	2013
Bioinformatics – A User’s Approach	2013

General Courses

VLAG PhD week	2010
High-Impact Writing in Science	2012
Ethics and Philosophy in Life Sciences	2013
Basic Statistics	2013
Techniques for Writing and Presenting a Scientific Paper	2013

Optional activities

Preparing PhD proposal	2010
EZO weekly lab meetings	2010-2014
EZO weekly journal club	2010-2014

Cover design: Henk Schipper and Maurijn Y. Kessels
Layout: Maurijn Y. Kessels

This thesis was printed by Gildeprint, Enschede
Financial support from the departments of Biochemistry and Experimental Zoology for
printing this thesis is gratefully acknowledged.